Analysis of Homeodomain interacting protein kinase 2 in glioblastoma multiforme

Inauguraldissertation

zur Erlangung des Grades eines Doktors der Medizin
des Fachbereichs Medizin
der Justus-Liebig-Universität Gießen

Vorgelegt von Darici, Dogus
aus Kars

Gießen (2018)

Aus dem Biochemischen Institut,
unter Leitung von Prof. Dr. Lienhard Schmitz,
des Fachbereichs Medizin
der Justus-Liebig-Universität Gießen

Gutachter: Prof. Dr. Lienhard Schmitz

Gutachter: Frau PD Dr. Schänzer

Tag der Disputation: 15.10.2018

Erklärung zur Dissertation

“Hiermit erkläre ich, dass ich die vorliegende Arbeit selbständig und ohne unzulässige Hilfe oder Benutzung anderer als der angegebenen Hilfsmittel angefertigt habe. Alle Textstellen, die wörtlich oder sinngemäß aus veröffentlichten oder nichtveröffentlichten Schriften entnommen sind, und alle Angaben, die auf mündlichen Auskünften beruhen, sind als solche kenntlich gemacht. Bei den von mir durchgeführten und in der Dissertation erwähnten Untersuchungen habe ich die Grundsätze guter wissenschaftlicher Praxis, wie sie in der „Satzung der Justus-Liebig-Universität Gießen zur Sicherung guter wissenschaftlicher Praxis“ niedergelegt sind, eingehalten sowie ethische, datenschutzrechtliche und tierschutzrechtliche Grundsätze befolgt. Ich versichere, dass Dritte von mir weder unmittelbar noch mittelbar geldwerte Leistungen für Arbeiten erhalten haben, die im Zusammenhang mit dem Inhalt der vorgelegten Dissertation stehen, oder habe diese nachstehend spezifiziert. Die vorgelegte Arbeit wurde weder im Inland noch im Ausland in gleicher oder ähnlicher Form einer anderen Prüfungsbehörde zum Zweck einer Promotion oder eines anderen Prüfungsverfahrens vorgelegt. Alles aus anderen Quellen und von anderen Personen übernommene Material, das in der Arbeit verwendet wurde oder auf das direkt Bezug genommen wird, wurde als solches kenntlich gemacht. Insbesondere wurden alle Personen genannt, die direkt und indirekt an der Entstehung der vorliegenden Arbeit beteiligt waren. Mit der Überprüfung meiner Arbeit durch eine Plagiatserkennungssoftware bzw. ein internetbasiertes Softwareprogramm erkläre ich mich einverstanden“

_____ _____

Ort, Datum Unterschrift

Table of contents

Introduction

1.1 Glioblastoma multiforme (GBM)

1.1.1 History

All intrinsic brain tumours stemming from non-neural glial tissues are called *glioma*. Glia cells naturally surround neurons and exhibit various supportive functions such as holding them in place (Glia is a Greek word, which means glue). Genetic alterations may lead to their dedifferentiation and malignant transformation [5].

In 1867 Rudolf Virchow conceived the idea of the intestinal origin of brain tumours [6]. The first reported intracranial surgery for cerebral glioma was published in 1884 by Bennett and Godlee [7]. The patient did well initially, but eventually postoperative herniation and meningitis resulted in death. Further ineffective approaches included decompression of the brain by a subtemporal resection of the bone [8] and preoperative trial of potassium iodide [9]. The first breakthrough in understanding brain tumours was achieved by a systematic histological classification of gliomas, which was published in 1926 by Bailey and Cushing [10]. They found correlations between the histology of the tumour, the operative procedure, and the overall survival rate of the patients. The most frequently occurring subtype of glioma with a mixed morphology and the poorest prognosis has been named glioblastoma multiforme.

In the following years GBM was further classified into two groups: primary and secondary GBM [11, 12]. Over 90% of the fast-growing primary GBM cases develop de novo in elderly patients, while younger patients in the range of 30–50 years tend to have a less malignant type of GBM with different genetic and epigenetic profiles. This type, known as secondary GBM develop from more benign tumours such as low-grade diffuse astrocytoma or anaplastic astrocytoma [13].

A newer attempt to classify GBM in subtypes according to distinct molecular characteristics is revealed by genome-wide expression studies. Four subtypes have been distinguished: classical, mesenchymal, proneural, and neural GBM [14].

Although the number of scientific publications concerning GBM exploded during the last 10 years (2004 ~700 publications, 2014 ~2300 publications), there have been only marginal benefits for the patients. GBM is still exceedingly lethal with a bad prognosis.

1.1.2 WHO classification

An international working group of 25 pathologists and geneticists convened at the German Cancer Research Center in Heidelberg in November 2006 to form the fourth edition of the WHO classification of tumours of the central nervous system. Underlying a histological malignancy scheme, these tumours were graded into four groups (WHO Grades I–IV). Since Grades I and II subsume benign tumours with a good prognosis, Grades III and IV are reserved for lesions with histological malignancy. The most frequently occurring histological types of gliomas include astrocytoma (Grades I–IV), oligodendroglioma (Grades II–III), and oligoastrocytoma (Grades II–III) [15]. Glioblastoma multiforme is classified as Grade IV astrocytoma, which is marked by rapid disease evolution and fatal outcomes [16].

1.1.3 Epidemiology

The incidence of GBM increases with age: the peak is reached by people belonging to the age group between 75–84 years [17]. Since elderly patients are less likely to have a histological diagnosis, the incidence of GBM in this group might be underestimated. The age-adjusted incidence of GBM ranges from 0.59 (Korea 2005), 3.19 (USA 2006–2010) to 3.69 (Greece 2005–2007) per 100,000 persons [15]. These incidence rates have been stable over the periods assessed [18]. In the USA all gliomas are much more common in non-Hispanic white people than other entities [19]. The fact that the incidence of glioma is 50% greater in adult men than in women and that there is a higher risk for postmenopausal women leads to the hypothesis of a protective influence of sexual hormones on the pathogenesis of GBM [17, 20]. Only 0.05% to 4.7% of patients with GBM have survived over the past five years' diagnosis [19].

1.1.4 Etiology

Even though GBM is the most common brain tumour in adults, less is known about the etiology of such tumours. Epidemiological data from A-bomb studies suggest a linear dose-dependent association between ionizing radiation and all kinds of malignant brain tumours [21]. While the risk for gliomas is doubling, meningioma and acoustic neuroma risk is even higher [22]. According to these results, several studies tried to find an association between CT scans and the risk of getting a brain tumour [23-25]. They show that the risk significantly increases at a minimum dose of ~ 10-50 mSv. In comparison, the X-ray dose of one single CT scan is estimated as ~ 4 mSv on average [25]. Taken together, radiation-induced malignant gliomas pose an evident, but relatively rare, iatrogen complication.

Since epidemiological data showed an inverse correlation between allergic hypersensitivity reactions and risk of glioma, several groups investigate a potential immunological etiology [26-28]. A meta-analysis in published in 2007 showed that allergic dispositions reduce glioma risk by nearly 40% [29]. Newer results indicate a protective influence of varicella-zoster [30] and human cytomegalovirus [31] in the pathogenesis of human brain tumours.

Only 1% of all glioma cases are caused by dominant monogenetic disorders including neurofibromatosis type 1 and type 2 (NF1, NF2), tuberous sclerosis (TSC), Lynch syndrome (HNPCC), Li-Fraumeni syndrome, Melanoma-neural system tumour syndrome, and Maffucci syndrome. The carriers of HNPCC and Li-Fraumeni syndrome are predisposed for GBM [32]. Besides monogenetic predispositions, DNA single nucleotide polymorphisms (SNPs) are found to significantly correlate with glioma risks. Some candidate genes are: TERT (5p15.33), two SNPs in EGFR (7p11.2), CCDC26 (8q24.21), CDKN2B (9p213), PHLDB1 (11q23.3), TP53 (17p13.1), and RTEL1 (20q13.33) [33].

A possible relationship between radiofrequency fields of cellular phones and glioma incidence was suggested by the International Agency for Research on Cancer (IARC) in 2011 [34]. Further epidemiological studies find no sudden increase in glioma rates, indicating inadequate evidence for this hypothesis [18, 35].

1.1.5 Molecular features of GBM

During the last few decades, intense molecular research has discovered a confusing amount of genetic alterations and pathway aberrations concerning GBM (Fig. 1.1). A prognostic and predictive clinical value of some of these alterations has already been confirmed—e.g., O^6-alkylguanine DNA alkyltransferase (MGMT)-methylation status and Isocitrate dehydrogenase 1 (IDH1) mutation. GBM has hyperdiploid and complex karyotypes [36]. Since they are “multiforme”, these biomolecular results are important in a process where a deeper understanding might help to individualize tumour therapy. This chapter focuses on the main results and is not exhaustive.

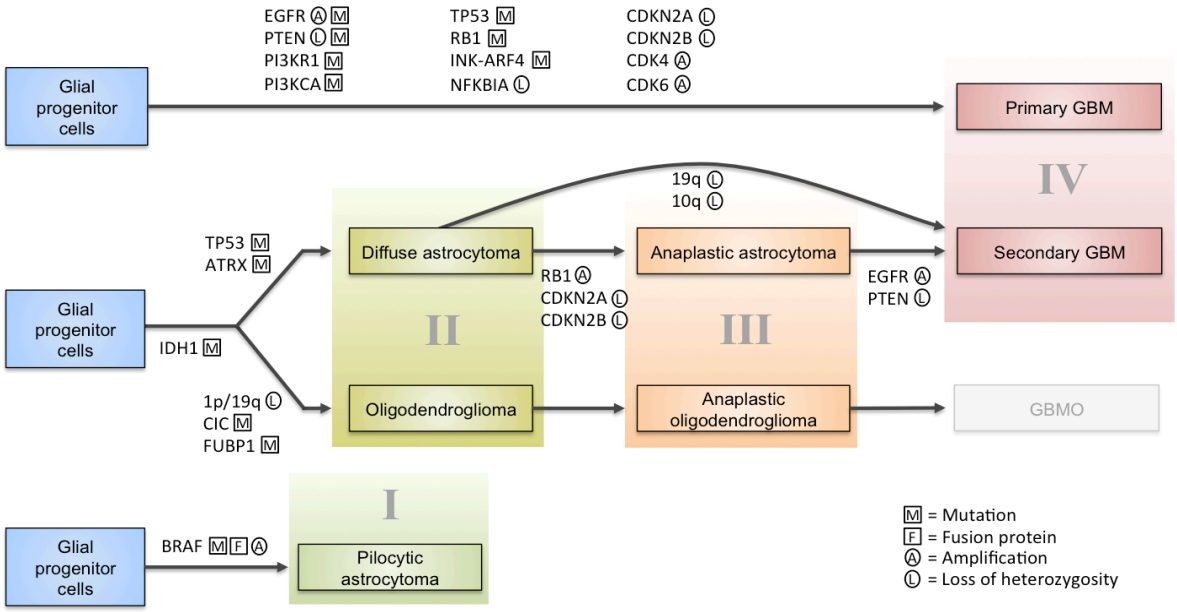

Figure 1.1: Overview of genetic alterations in the development of primary and secondary GBM: Various amplifications, deletions, and mutations can lead to malignant transformation. The genetic profile differs between primary and secondary GBM. Primary GBM develops de novo from glial progenitor cells, whereas secondary GBM grows from lower-grade tumours, such as diffuse astrocytoma or oligodendroglioma.

1.1.5.1 Isocitrate dehydrogenase 1 (IDH1)

IDH1 is an enzyme of the citric acid cycle and very frequently mutated in younger patients with low-grade glioma and secondary GBM (>80%), but rarely in primary GBM (<5%) [37]. Since 2008, when IDH1 mutations were discovered first [38], many studies have confirmed its role as a genetic marker to reliably distinguish primary from secondary GBM [14, 37, 39]. Molecular research on IDH1 mutation is still going on: it has been shown that the IDH1 mutation on the active site (R132H) dominantly inhibits endogenous IDH1 activity, which decreases α-ketogluterate and increases cellular HIF-1α protein levels [40]. This mutation leads to increased conversion of 2-hydroxygluterate, instead of α-ketogluterate [41]. Newer results show an influence of the oncometabolite 2-hydroxygluterate on epigenetic events and tumourigenesis [42]. Besides its positive prognostic value, further research is still needed to show the impact of IDH1 mutations in tumour biology.

1.1.5.2 Epidermal growth factor receptor (EGFR) pathway alterations

EGFR, as a member of the ERBB family, is a receptor tyrosine kinase on the cell surface where it physiologically initiates cell proliferation, differentiation, and survival when activated by specific ligands (Fig. 1.2). The binding of the EGF ligand to EGFR activates the RTK/RAS/PI3K pathways. Besides a common aberrant amplification of 7p11

- EGFR (~70%), GBM may exhibit a functional and permanently activated mutant EGFRvIII (~50%), resulting from the deletion of exons 2–7 [43]. Since EGFRvIII is phosphorylized by EGFR, both EGFR amplification and EGFRvIII mutation are mostly coexpressed and result in a EGFRvIII-STAT3 nuclear complex formation, leading to increased tumour proliferation [44]. However, the prognostic value of EGFR and EGFRvIII alterations seems to be less evident [45, 46].

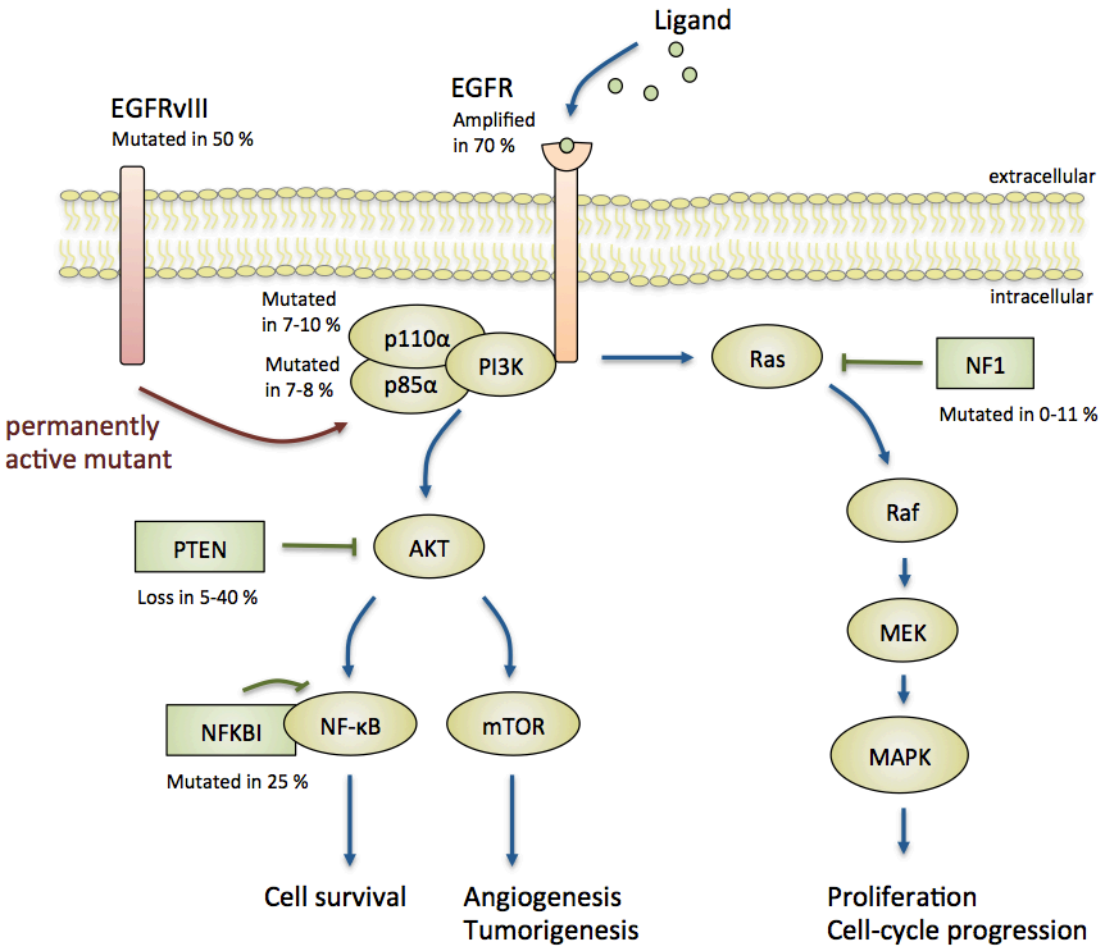

Figure 1.2: EGFR pathway in GBM. Ligand binding to EGFR surface receptors leads to activation of PI3K/AKT and Ras/Raf/MEK/MAPK pathways, inducing growth advantage for the cells. PI3K encompasses two subunits, the catalytic subunit p110α and the regulatory subunit p85α. EGFRvIII is a mutant form of EGFR in GBM with oncogenic potential through permanently active EGFR-signalling. PTEN acts as a tumour suppressor by inhibiting AKT, and NFKBI negatively regulates NF-κB by binding it. NF1 is able to increase the GTPase activity of Ras and thereby stops MAPK signalling.

Having a closer look at the downstream signalling processes of the EGFR-pathway, more alterations can be found in GBM:

The phosphatase and tensin homolog (PTEN) is a tumour suppressor, which physiologically dephosphorylates PIP3 to PIP2 and therefore negatively regulates the

PI3K/Akt pathway. Loss of PTEN expression due to deletion, mutation, or methylation affects 5–40% of all GBM cases [47, 48], and leads to accumulation of PIP3 and activation of the oncogenic Akt/mTOR pathway. Since the prognostic relevance of PTEN mutation in GBM is not clear, it is shown to be a negative prognostic factor in anaplastic astrocytoma (WHO III) [49].

Beyond that, mutations of the subunits of PI3K can be found in GBM. The catalytic subunit p110α, encoded by PIK3CA, is affected in 7–10 %, while the regulatory subunit p85α, encoded by PIK3R1, is affected in 7–8 % of the cases [50].

The protein complex NF-κB is included in the transcription of immune modulating genes and has an oncogenic impact on tumour cells, when permanently activated. Besides an EGFR-triggered increase in NF-κB activity, the constitutive activation of NF-κB through deletion of the inhibitor NFKBIA might play an important role in GBM pathogenesis [51]. The downregulation of NFKBIA, especially with a recently identified polymorphism [52], is associated with lower survival, behaviour, and response to chemotherapeutic drugs, especially Temozolomid [51].

The GTP-binding oncogene Ras is a molecular switch, which, when activated, leads to increased cellular proliferation. Even though many malignant tumours exhibit a permanently active Ras-mutant, mutations of Ras in GBM is a rarely seen alteration [53]. Nevertheless, deletions in NF1, which terminates Ras signalling by inducing its GTPase activity, have been observed [14]. *In vitro* experiments indicate the influence of YKL-40 protein in activating Akt and MAPK pathways [54, 55].

1.1.5.3 P53 and Rb pathway alterations

Because of this important protective function, the powerful tumour suppressor protein p53 is also called the “guardian of the genome”. Upon DNA damage, p53 activates several protective pathways associated with cell cycle arrest or induction of apoptosis under severe damage. HIPK2 is also involved in this pathway by phosphorylating p53 at Ser46 [56]. The expression of mutant p53 is common in cancer; it leads to increased resistance to radio and chemotherapy. In GBM, amplification of MDM2 (13%) [57] and deletion of CDKN2A (49%) [58, 59] result in downregulation of the p53-pathway. MDM2 amplification might be associated with a shorter survival time [57]. Additionally, TP53 is often found to be silenced in GBM by mutations (31–38%) and hypermethylation events [50, 60]. The prognostic impact has still remained controversial [57, 61].

Rb signalling is decreased through deletion of CDKN2, amplification of CDK4 (18%), CDK6 (1%) and CCND2 (2%), as well as mutation or deletion of Rb1 (11%) [62]. In

addition, a loss of the tumour suppressors INK4A/ARF in primary GBM leads to downregulation of Rb and p53 activities [63].

1.1.5.4 microRNAs

Newer results indicate that non-protein-coding short microRNAs (miR) molecules are included in the pathogenesis of GBM concerning proliferation, invasion, stem cell behaviour and angiogenesis. Especially the oncogenic miR-21 is highly expressed in cancer and targets PTEN and other tumour suppressors (TIMP3, PDCD4) [64]. Experimental evidence shows that downregulation of miR-21 leads to decreased glioma proliferation in vivo through PDCD4 upregulation [65]. Another promising candidate is miR-7, which inhibits EGFR by binding to its 3'-UTR. Independent of its EGFR inhibition, miR-7 can also inhibit the downstream Akt pathway [66]. Moreover, microRNAs are used to get the expression profiles of GBM subtypes and thus have prognostic relevance [67].

1.1.5.5 O-6-methylguanine-DNA methyltransferase (MGMT)

MGMT is an enzyme which usually repairs DNA in response to alkylating stress [39, 68]. In about 40% of primary GBM and over 70% of secondary GBM, MGMT is epigenetically hypermethylated [69]. This eventually inactivates the enzyme and increases the vulnerability to Temozolomide (TMZ), the most common chemotherapeutic substance in GBM therapy. When spontaneously activated, the prodrug TMZ is able to damage the DNA at guanine on the position O-6 by alkylation [70]. Alkylated O^6-methyl-guanine results in DNA strand breaks and eventually leads to cell-cycle arrest and cell death. All in all, GBM patients with MGMT promoter hypermethylation exhibit a better prognosis via an improved response to TMZ [68].

1.1.6 Clinical signs

GBM is a fast-growing tumour with a low metastatic potential [71]. Clinical signs depend on the localization in the brain, edema, blood supply of the tumour, and resistance or limited response to therapy. Initial symptoms are not specific; they are caused by intracranial hypertension related to the amount of edema and lead to headache, nausea and vomiting. These symptoms can easily be misinterpreted as infections or circulatory and inflammatory diseases [72]. Newly appeared seizures are always suspicious for brain tumours [73]. Depending on tumour location (infra or supratentorial) and migration behaviour, 30-40% of brain tumour patients develop neurological symptoms such as hemiparesis, speech and memory problems, nystagmus, visual changes, and other dysfunctions related to brain damage and cranial nerve inju-

ries. The most favourable location for GBM is the white matter of the frontal lobe (40%), and temporal (29%), parietal (14%), and occipital lobes (3%) [74]. In particular, a tumour in the frontal lobe bears the risk of personality change, disinhibited behaviour, and a deficient mood. Unusual localization in the spinal cord and infratentorial edema shows a severe risk of lower brain herniation of the brainstem and upper cervical spinal cord, which are responsible for important vital functions such as respiration, cardiac function, and vomiting [75]. Patients undergoing chemotherapy may develop nausea and vomiting due to unspecific cytotoxicity of the drugs.

1.1.7 Treatment options

The treatment of GBM concentrates on surgery, radiation, and chemotherapy in order to regress the tumour and provide a longer survival with less symptoms. Unfortunately, there is no possible cure at present. Preoperative intracranial hypertension can be controlled with high doses of corticosteroids. The decision to perform an elective operation for a suspicious brain tumour depends on the diagnosis, age of the patient, and localization. There is evidence that intraoperative use of 5-ALA and MRT, which is used to help localize the tumour, increases the success of the operation [76]. Since GBM infiltrates the brain, there is no chance of achieving a complete resection of all malignant cells. The intention is to resect as much as possible without damaging the functional brain matter. Radiotherapy helps to control the remaining local tumour mass. The best results are obtained with 54–60 Gy, while doses over 60 Gy show high side-effects for the patient [77].

Besides surgery and radiotherapy, the patient is treated with Temozolomide (TMZ), an alkylating agent. The Cochrane meta-analysis shows that during TMZ treatment the overall survival and the progression-free survival of a defined cohort significantly increase in the primarily diagnosed, but not in recurrent, GBM [78]. Also, the MGMT promoter methylation status is an independent favourable prognostic factor, which increases the median survival from 15.3 to 21.7 months upon TMZ treatment [79]. Another alkylating drug for local intra-cavity treatment of GBM is carmustine, which is implanted into the resection bed during surgery. A positive effect on survival is shown for primary diseases [80]. Cilengitide, an inhibitor of the integrins, shows no benefit for the patients [81]. Since they increase the median progression-free survival from 6.2 to 10.6 months, therapies with the monoclonal antibody Bevacizumab, a VEGF inhibitor, are evident for the treatment of GBM [82, 83]. Newer approaches focus on the altered pathways in GBM. Rindopepimut is an EGFRvIII-targeting vaccine, which already shows an improved overall survival in Phase II studies [84]. Dacomitinib is an EGFR tyrosine kinase inhibitor. Early studies indicate its positive effect on EGFR amplified

cells with and without EGFRvIII mutation [85]. Since virus infections seem to play a role in GBM pathogenesis, anti-viral treatments are also in focus [31]. Recent studies have identified tumour stem cell markers (e.g., CD133+ and L1CAM), but their therapeutic relevance is still unclear [86]. A deeper understanding of the biomolecular pathways might help to find new ways to treat patients suffering from GBM.

Table 1: Overview of current pharmacological approaches of GBM treatment

Pharmacodrug	Mechanism	Reference
Temozolomid	DNA alkylation	[70, 78, 79]
Carmustine	DNA alkylation	[80]
Cilengitide	Integrin inhibitor	[81]
Bevacizumab	VEGF inhibitor	[82, 83]
Rindopepimut	EGFRvIII-targeting vaccine	[84]
Dacomitinib	EGFR inhibitor	[85]

Table 1: Overview of pharmacological approaches of GBM treatment. Besides the widely used DNA-alkylating Temozolomid, many other drugs for GBM therapy are still under investigation. Some of them have different targets, such as integrin, VEGF, and EGFR inhibitors, as well as the specific mutant EGFRvIII, which seems to be a reasonable target for pharmacological treatment.

1.2 Homeodomain-interacting protein kinase 2 (HIPK2)

1.2.1 What is HIPK2?

HIPK2 is serine/threonine kinase and belongs to the HIPK family/DYRK subfamily, together with HIPK1, HIPK3, and HIPK4. In 1998 a yeast two-hybrid screen discovered HIPK1-3 as a novel family of co-repressors for homeodomain transcription factors [87]. Since then, many publications have shown that especially HIPK2 holds a larger number of cellular functions such as regulation of the transcription including cell death, development, differentiation, and segmental identity. HIPK1-3 shows > 90% homology, where HIPK4 remains a relative with only 50% structural resemblance [88]. The fact that HIPKs are evolutionarily conserved among vertebrates leads to the supposition that mutations may lead to a non-viable form. Since HIPK2$^{-/-}$ mice show no morphological deficiencies, double knockout mice HIPK1$^{-/-}$ and HIPK2$^{-/-}$ exhibit severe neurological problems probably due to defective proliferation in the neural fold. Such experimental data suggests that HIPK1 is able to take over several functions of HIPK2 [89]. The impact of HIPK2 on the central nervous system can further be observed in the deficient survival of midbrain dopamine neurons upon HIPK2 knockout. HIPK2$^{-/-}$ mutants show psychomotor abnormalities due to decreased TGF-β signalling [90]. HIPK2 mRNA is expressed in most human adult tissues [91], particularly in retina, muscle, and neural tissues [92]. An increased expression of HIPK2 and its interaction partner, CtBP2 is also detectable after traumatic brain injuries in the peritrauma brain cortex [93]. Newer results could show a phosphorylation of H2B by HIPK2 at the midbody, which is shown to be required for a faithful cytokinesis. Loss of HIPK2 by RNA interference results in cytokinesis failure and tetraploidization, indicating a role in tumourigenicity [94].

1.2.2 Structure and localization of HIPK2

The human form of HIPK2 has 1,198 amino acids. Its protein kinase domain is located at the N-terminus, which is followed by an interaction domain for transcription factors. The protein can be SUMOylated at lysine 25, exhibits a SUMO-binding motif (SIM) and nuclear localization signals (NLS1 and NLS2) as well as two PEST domains that are rich in proline, glutamic acid, serine, and threonine. The C-terminus is characterized by S, Q, and A repeats and an auto-inhibitory domain which is cleaved by caspase-6 upon early induced p53-activation [95]. The gene encoding HIPK2 is located in chromosome 7q32-q34 [96].

Most of the HIPK1-3 proteins are localized in nuclear speckles in HIPK domains [97]. They, however, show an overlap with Pc2 in polycomb nuclear bodies and PML nucle-

ar bodies. Upon DNA-damage, an auto-regulatory feedback loop between HIPK2 and its E3 ligase Pc2 is established, thereby leading to transcriptional activity [98]. Even though architecturally independent, PML is still required for the kinase activity of HIPK2 [97]. Kinase defective K221A mutants lose their ability to localize in nuclear speckles and therefore spread throughout the whole nucleoplasm. Also, two nuclear localization signals (NLS1, NLS2) and the SIM region are essential for the nuclear localization of HIPK2 [99]. Despite the fact that most of HIPK2 are in the nucleus, small fractions can also be found in cytoplasms [100]. Their functions, however, remain unclear.

1.2.3 Role of HIPK2 in DNA damage response and cell death

Upon DNA damage, HIPK2 is involved in programmed cell death through p53-dependent and p53-independent pathways.

1.2.3.1 HIPK2-mediated p53-dependent pathways upon DNA damage

The tumour suppressor p53 can promote either cell cycle arrest or apoptosis, depending on the severity of the DNA damage (Fig. 1.3). In unstressed cells a complex between p53 and its E3 ubiquitin ligase MDM2 leads to nuclear export and proteasomal degradation of p53 [57]. Upon severe DNA damage, stabilized HIPK2 is able to bind p53 through the C-terminal domain of p53. PML additionally facilitates the p53-HIPK2 complex formation in nuclear bodies by recruiting various enzymes [97, 101]. This protein-binding leads to phosphorylation of p53 at Ser46, which results in the CBP-mediated acetylation of p53 at Lys382 [56, 102, 103]. Activation of apoptotic factors, such as PIG3, p53AIP, BAX, NOXA and PUMA, is a consequence of the p53 transcriptional activity [56]. The phospho-specific isomerase PIN1 is also involved in p53 accumulation and activation, since it binds to phosphorylated Ser46p53 and mediates conformational changes [104, 105]. PIN1 modulates Siah1-HIPK2 interaction and hence, stabilization of HIPK2 [104, 105]: Upon DNA-damage HIPK2 is able to autophosphorylate at Thr880/Ser882 and it was shown that this autointeraction has an impact on p53 phosphorylation and thus DNA-damage induced apoptosis *in cellulo* [104]. In detail, the autophosphorylation enables PIN1 to bind HIPK2 and this interaction prevents HIPK2 from polyubiquitination and thus degradation. Additionally, HIPK2 decreases MDM2 levels and thus antagonizes nuclear export and ubiquitination of p53 [106]. Cofactors of the HIPK2-mediated p53Ser46 phosphorylation are Axin, Daxx, p53DINP1/TP53INP1, and Sp100 [107]. Caspase-6, a p53-induced protein, binds to the autoinhibitory domain of HIPK2, which initially potentiates p53Ser46 phosphorylation and induction of the apoptotic machinery. Later, C-terminally truncated HIPK2 is eliminated by proteasomal

degradation [95]. Upon non-severe DNA damage, the inhibitor p21 is activated through the HIPK2/PCAF-mediated acetylation of p53, which leads to cell cycle arrest [108].

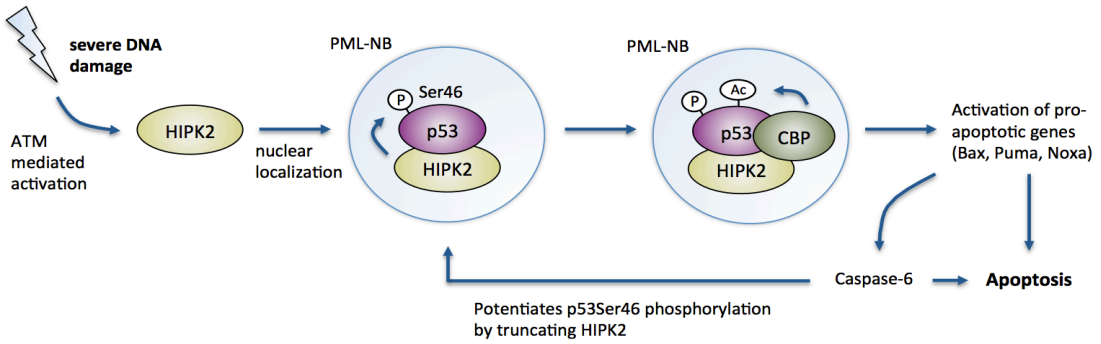

Figure 1.3: HIPK2-mediated p53-dependent pathway upon severe DNA damage. Severe damage stabilizes HIPK2, which phosphorylates p53 at Ser46 in PML nuclear bodies. Subsequent CBP-mediated p53 acetylation fully activates p53 and its pro-apoptotic genes, leading to apoptosis. Caspase-6 can truncate HIPK2 at its C-terminus, thereby potentiating its kinase activity.

1.2.3.2 HIPK2-mediated p53-independent pathways upon DNA damage

Besides p53Ser46 phosphorylation, HIPK2 has other mechanisms to induce apoptosis and promote its work as a tumour suppressor. The phosphorylation of the anti-apoptotic CtBP at Ser422 by HIPK2 leads to its proteasomal degradation and thus increases the transcription of pro-apoptotic genes such as BAX and NOXA [109]. Further, HIPK2 is able to phosphorylate and activate NLK upon Wnt signalling, which results in multiple c-Myb phosphorylations, proteasomal degradation and G1 arrest [110]. It has been shown that apoptosis is induced upon TGF-β stimulation, leading to HIPK2-mediated activation of JNK by using DAXX, MAPKK4, and MAPKK7 [111]. In addition, the phosphorylation of the anti-apoptotic isoform ΔNp63α by HIPK2 has been observed to contribute to its degradation [112].

1.2.4 HIPK2 alterations in cancer

Since HIPK2 is a key protein in the responses to DNA damage, apoptosis, hypoxia, and cytokinesis, it is not surprising that its alteration might be a driver for proliferative diseases.

1.2.4.1 Downregulation of HIPK2 in cancer

Various analyses could show that the expression of HIPK2 is downregulated in neoplastic thyroid carcinoma and breast carcinoma [92], and in well-differentiated thyroid carcinomas through galectin-3 overexpression [113].

Also, the stabilization of HIPK2 upon DNA damage through MYCN activation increases the susceptibility of neuroblastoma to apoptosis [114].

A correlation between HIPK2 expression and the survival of 80 patients with primary colorectal carcinoma has been suggested. Patients with decreased HIPK2 expression exhibited a lower outcome through growth advantages of the tumour cells [115]. Wild-type HIPK2 leads to p53-mediated depletion of β4-Integrin, where the depletion of HIPK2 strongly results in β4 Integrin upregulation as well as phosphorylation of MAPK and Akt, which are both involved in invasion and metastasis [116]. Metastasis and resistance to chemotherapy in bladder cancer are also promoted by downregulation of HIPK2 [117, 118]. Further, a HIF-mediated chemoresistance of hepatocellular carcinoma cells through upregulation of WSB-1 and accordingly degradation of HIPK2 have been observed [119].

It has been reported that carcinogenesis treatment of wild-type, $HIPK2^{+/-}$ and $HIPK2^{-/-}$ mutants results in more skin cancer formations in HIPK2-depleted mice [120]. Pathophysiological mechanisms of skin cancer development can further be explained by the upregulation of the β-Catenin/LEF1-pathway upon HIPK2 depletion. The consequence is a more rapid G1-S transition in cell cycle, epidermal stem cell expansion [120], and VEGF upregulation [121] to promote carcinogenesis. In addition, there is an influence of the viral oncogene HPV23 E6, which acts as a cofactor and targets HIPK2 upon massive UVB-radiation, thereby preventing p53Ser46 phosphorylation [122].

Another example shows the impact of HIPK2 mislocalization in the context of leukemogenesis: RUNX1/PEBP2-β phosphorylation during hematopoiesis is normally mediated by HIPK2 in the nucleus. The oncogenic protein PEBP2-β-SMMHC disrupts RUNX1 phosphorylation by passing over HIPK2 to cytoplasmatic filaments [123]. Incidentally, two missense mutations (R868W and N958) in the SRS domain have been shown to be mutated in acute myeloid leukemia (AML) and myelodysplastic syndrome (MDS), which affects MDM2 and RUNX1-mediated transcription as well as their subcellular localization in speckles [124]. Moreover, a loss of heterozygosity (LOH) has been found in radiation-induced lymphoma, which indicates a function of HIPK2 as a haploinsufficient suppressor gene [125].

1.2.4.2 Upregulation of HIPK2 in cancer

A couple of studies focus on the amplification of HIPK2 in cancer and its loss of tumour suppressor function. Two independent high-resolution genome-wide array platform analyses could identify an amplification of the BRAF and HIPK2 encoding locus at 7q34 in WHO Grade I pilocytic astrocytoma (PAs) [126]. Even though BRAF amplifica-

tions and rearrangements (KIAA1549-BRAF fusion gene) represent the most common alterations in PAs, an examination of 42 tumours with BRAF alterations showed that 22 out of 42 also featured HIPK2 amplifications [127]. Additionally, clonogenic assays with U87 GBM cells demonstrated that HIPK2 overexpression lead to increased cell growth in vitro [126].

Also, HIPK2 mRNA and protein levels increase in cervical cancer in comparison with normal cervical tissues, indicating a role in the development of the tumour. However, after the knockdown of HIPK2 in cervical cancer, tumour cells started to proliferate [128].

1.2.5 Role of HIPK2 in non-tumourigenic diseases

Recent findings indicate a role of HIPK2 in non-tumourigenic diseases: kidney injury, kidney fibrosis, human immunodeficiency virus associated nephropathy, focal segmental glomerulosclerosis, diabetic nephropathy and IgA nephropathy. HIPK2 has been shown to be a key regulator of kidney fibrosis and upregulated in all of these kidney diseases. Depletion of HIPK2 in transgenic mice model improves their renal function [129, 130].

Besides kidney fibrosis, there is evidence that HIPK2 influences the pathogenesis of human idiopathic pulmonary fibrosis (IPF). Fibroblasts of patients suffering from IPF exhibit low HIPK2 levels due to the HIPK2 loss of heterozygosity at locus 7q34 [131].

Since the conformational state of p53 is related to Alzheimer's disease (AD), a connection with its activator HIPK2 has been proposed. The deposition of beta-amyloid peptides is the result of an amyloidogenic pathway in AD, and there is evidence that soluble beta-amyloid peptides can induce HIPK2 degradation [132, 133].

1.2.6 Mechanisms regulating HIPK2

HIPK2 activity can be regulated by its cellular localization. In unstressed cells HIPK2 resides mainly in nucleoplasm. Upon severe DNA damage due to drugs (Cisplatin, Etoposide, Adriamycin), radiation (UV, IR) or replicative stress HIPK2 is recruited to PML nuclear bodies, where it colocalizes with p53 and phosphorylates p53 at Ser46, thereby regulating its acetylation [99].

Apart from cellular mislocalization, HIPK2 is permanently degraded by different ubiquitin E3 ligases such as Siah-1, Siah-2, WSB1, MDM2, and SCF^{Fbx3} in order to restrict its abundance [106, 134-137]. Upon DNA damage, HIPK2 is activated by the checkpoint kinase ATM and ATR through inhibition of Siah-1, resulting in disruptions of HIPK2 and Siah-1, which, in turn, leads to stabilization of HIPK2 [135]. The HIPK2 pro-apoptotic

activity is also downregulated through a negative feedback loop, where p53 activates MDM2 and eventually degrades HIPK2 in case of non-lethal DNA damage [106].

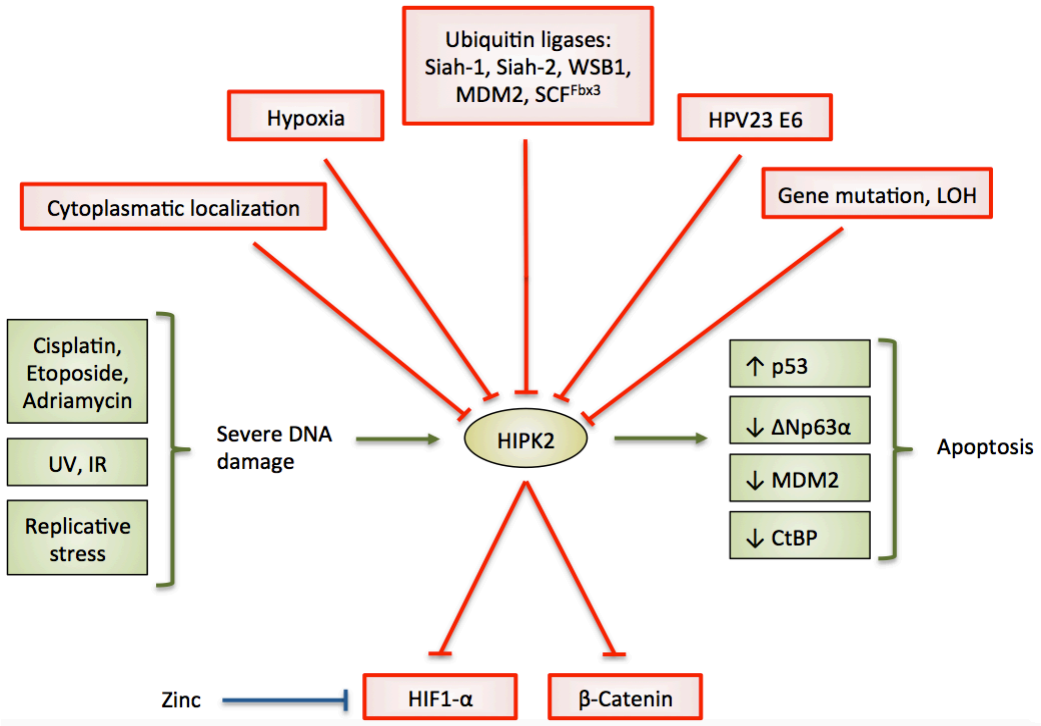

Figure 1.4: Regulation mechanisms of HIPK2. Chemotherapeutic drugs, radiation, or replicative stress can lead to severe DNA damage and activation of HIPK2, which activates p53-dependent and independent pathways in order to induce apoptosis. In unstressed cells HIPK2 is permanently degraded by its Ubiquitin-E3 ligases and also inactivated by its cytoplasmatic localization. Moreover, hypoxic conditions, viral proteins, such as HPV23 E6, or genetic aberrations can be the reason for altered HIPK2 stability or activity. Since Zinc downregulates HIF1-α, it is able to rescue the downregulated HIPK2.

Hypoxic stress activates Siah-2, which in turn leads to proteasomal degradation of HIPK2. Since HIPK2 inhibits HIF-1α, the loss of HIPK2 results in HIF-1α stabilization and the expression of a hypoxic phenotype [137]. One way to restore the hypoxia-inhibited HIPK2 pathway is zinc treatment, which promotes the proteasomal degradation of HIF1α [138].

Recently, an autoinhibitory loop has been identified, where the ATM/AMPKα2 pathway is activated upon ionic radiation, which leads to inhibition of HIPK2 and consequently a disinhibition leading to activation of WIP1. The stabilization of WIP1 eventually terminates the double-strand break signalling cascades by inhibiting ATM [139].

1.3 Aim of this study

Glioblastoma multiforme is still the most common and lethal brain tumour in adults. Although alterations of HIPK2 were already described in pilocytic astrocytoma, less is

known about changes in GBM. The aim of this study was to determine HIPK2 protein and mRNA expression, HIPK2 stability and the mRNA exon structures. Moreover SNP experiments were planned to identify amplifications of the HIPK2 locus and knockdown experiments in order to examine the role of HIPK2 in tumour proliferation. Since multi-dimensional and comprehensive characterization studies revealed several mutations of HIPK2 in GBM, the idea came up to investigate its effects on phosphorylation, enzymatic activity, SUMO1- and PIN1 binding abilities and subcellular localization. A deeper understanding of the molecular mechanisms of HIPK2 in GBM should provide the basis for better tools in diagnosis or therapy of GBM.

2 Materials

2.1 Cells

2.1.1 Human glioblastoma cell lines

Name	Description (p53-status, 7q34-Amplification)
A172 ♂	wt-p53 or Mut-p53 (Cys242Phe)* [1]
U343	wt-p53 [2]
U87 ♂	wt-p53 [1], 7q34+ [3]
U118 ♂	Mut-p53 (Arg213Gln)* [1, 3]
U251MG ♂	Mut-p53 (Arg273His)* [1]
SNB19	Mut-p53 (Arg273His)* [1]
Ln229 ♀	Mut-p53 (Lys164Glu)* [1]
U373MG (Upsala)	Mut-p53 (Arg273His)* [4], 7q34+ [3]
A764	not known
A271	not known
G55	not known

* cell lines with missense or small frameshift mutations

2.1.2 Human non-glioblastoma cell lines

Name	Description
HeLa ♀	Cervix carcinoma
HEK-293T	Embryonic kidney cells with large T antigen of SV40 virus
U2OS ♀	Osteosarcoma

2.1.3 Competent E.coli strains

Name	Genotype	Source
TOP10	F-mcrA∆(mrr-hsdRMS-mcrBC)φ80lacZ∆M15 ∆lacX74 recA1 araD139 ∆(araleu) 7697 galU galK rpsL (StrR) endA1 nupG	Invitrogen

2.2 Buffers

Nonidet P40 lysis buffer (NP40):

20 mM Tris/HCl (pH 7.5)

1% (v/v) NP40

10% (v/v) Glycerol

150 mM NaCl

prior to use:

2 mM Na Vanadate

40 mM NaF

a drop PMSF

5x SDS loading buffer:

312.5 mM Tris/HCl (pH 6.8)

50% Glycerol

10% (w/v) SDS

25% (v/v) β-mercaptoethanol

0.01% (w/v) bromphenol blue

4x Separating gel buffer (lower):

1.5 M Tris/HCl (pH 8.8)

0,4% (w/v) SDS

4x Stacking gel buffer (upper):

0.5 M Tris/HCl (pH 6.8)

0,4% (w/v) SDS

The preparation of the SDS gels is described in 3.2.2

50x Tris-acetate-EDTA buffer (TAE):

0.05 M EDTA

2 M Tris (pH 8.3)

1 M Acetic acid

10x SDS running buffer:

250 mM Tris

2 M Glycine

1% (w/v) SDS

Transfer buffer:

50 mM Tris/HCl

40 mM Glycine

20% (v/v) Methanol

0.038% (w/v) SDS

Washing buffer (10x TBS-T):

250 mM Tris

1.37 mM NaCl

50 mM KCl

7 mM $CaCl_2$

1 mM $MgCl_2$

0.1% (v/v) Tween 20

pH = 7.4

Phosphate buffer saline (1x PBS):

137 mM NaCl

8.1 mM Na_2HPO_4

2.7 mM KCl

1.5 mM KH_2PO_4

pH = 7.4

Mini preparation buffer 1 (P1):

50 mM Tris

81 mM Na_2EDTA

10% RNase

pH = 8.0

Mini preparation buffer 2 (P2):

200 mM NaOH

20% 173 mM SDS (w/v)

Mini preparation buffer 3 (P3):

3 M Potassium acetate

pH = 5.5 (with glacial acetic acid)

GSH elution buffer:

100 mM Tris

15 mM glutathione

pH = 8.0

Dialysis buffer:

20 mM Tris

pH = 7.5

2.2.1 Stock solutions

Name	Description
Dulbecco's Modified Eagle Medium (DMEM)	From Gibco® by Life technologies
Luria Bertani Medium (LB)	1% (w/v) Tryptone 0.5% (w/v) yeast extract 1% (w/v) NaCl If needed, appropriate antibiotics were added.
Luria Bertani Agar Plates	1% (w/v) Tryptone 0.5 % (w/v) yeast extract 1% (w/v) NaCl 1.6% (w/v) Agar Appropriate antibiotics were added.

2.2.2 Medium compositions

Name	Composition
Complete Medium	DMEM containing 2 mM Glutamine, 10% (v/v) FCS and 1% (v/v) Penicillin/Streptomycin
Transfection Medium 1	DMEM containing 2 mM Glutamine
Transfection Medium 2	DMEM containing 2 mM Glutamine and 10% (v/v) FCS
Freezing Medium	FCS containing 10% (v/v) DMSO

2.3 Chemicals

2.3.1 Enzymes

Name	Source
DNase I	Qiagen
GoTaq®-Polymerase	Promega
Lysozyme	Sigma
Pfu Ultra DNA Polymerase	Stratagene
Restriction endonucleases	Thermo Scientific
Super Script II reverse transcriptase	Invitrogen
Trypsin-EDTA	Gibco® by Life technologies

2.3.2 Inhibitors

Name	Targets	Source
Aprotinin	Serine proteases	Sigma
Leupeptine	Serine and cysteine proteases	Sigma
Phenylmethylesulfonyl fluoride (PMSF)	Proteases	Sigma
RiboLock R1	RNAse	Thermo Scientific
Sodium fluoride (NaF)	Serine- and threonine phosphatases	Roth
Sodium orthovanadate (Na_3VO_4)	Tyrosine- and alkaline phosphatases	Sigma

2.3.3 Antibiotics

Name	Final concentration	Source
Ampicillin	100 µg/ml	Sigma
Cycloheximide	10 µg/ml	Sigma
Penicillin/Streptomycin	10000 U/ml	Gibco
Puromycin	1-2 µg/ml	Invitrogen

2.3.4 Kits

Name	Company
ABsolute qPCR SYBR Green ROX Mix	Thermo Scientific
JETstar Plasmid Purification Maxi Kit	Genomed
Pierce® BCA Protein Assay Kit	Thermo Scientific
QuikChange® Site-Directed Mutagenesis Kit	Agilent
RNeasy® Mini Kit	Qiagen

2.3.5 Other chemicals

Name	Source
(L-)Glutamine	Gibco
1,4-Dithiothreitol (DTT)	Acros Organics
2-Propanole	Roth
2-β-Mercaptoethanol	Roth
5x GoTaq Flexi buffer	Promega
5x Green GoTaq Flexi Buffer	Promega
Acetone	Roth

Agarose	PeqLab
Ammonium persulfate (APS)	Sigma
Bovine serum albumine	Sigma
Buffer RDD DNA Digestion buffer	Qiagen
Desoxyribonucleosidetriphosphates (dNTPs)	Thermo
Dimethylsulfoxide (DMSO)	Sigma
Enhanced chemiluminescence solutions (ECL)	Perkin Elmer
Ethanol	Roth
Ethidiumbromide	Roth
FACS Clean	BD Bioscience
FACS Flow	BD Bioscience
FACS Rinse	BD Bioscience
Fetal Bovine Serum (FCS)	Gibco by Life technologies
Glycin	Roth
Goat serum	Sigma
GST	V. V. Saul
GST-PIN1	M. Milanovic
GST-SUMO	V. V. Saul
Hoechst (33342)	Invitrogen
Hydrogen chloride (HCl)	Roth
IPTG	Roth
Kaiser's Glyceringelatine	Merck
Magnesium chloride ($MgCl_2$)	Promega
Methanol	Roth
Microscope Slides	Thermo Scientific
Milk powder	Merck
NaCl	Roth
Oligo $(dT)_{12\text{-}18}$ Primer	Invitrogen

Polybrene (Hexadimethrin Bromid)	Sigma
Polyethyleneimine (PEI)	Sigma Aldrich
Potassium acetate	Roth
Protein A/G agarose beads	Santa Cruz Biotech
RNase A	Sigma
RNAse-Free Water	Promega
Roti®-Fect	Roth
Sodium azide (NaN_3)	Roth
Sodium dodecyl sulfate (SDS)	Bio Rad
Sodium hydroxide (NaOH)	Roth
Tetramethylethylenediamine (TEMED)	Bio Rad
Tris	Roth
Tween 20	Roth
Water	MilliQ

2.4 Antibodies

2.4.1 Primary Antibodies

Name (clone)	Species	Origin	Source
anti-Flag (M2)	mouse	monoclonal	Sigma
anti-GFP (7.1 and 13.1)	mouse	monoclonal	Roche
anti-HIPK2 (rab)	rabbit	polyclonal	M.L. Schmitz
anti-HIPK2 (C1B3)	rat	monoclonal	M.L. Schmitz
anti-HIPK2 (5C6)	rat	monoclonal	M.L. Schmitz
anti-HIPK2 (N6A10)	rat	monoclonal	M.L. Schmitz
anti-Ubiquitin (P4D1)	mouse	monoclonal	Cell Signaling
anti-β-Actin	rabbit	polyclonal	Abcam

anti-β-Tubulin (Tub2.1)	mouse	monoclonal	Sigma

2.4.2 Secondary Antibodies

Name	Species	Conjugated to	Source
anti-mouse IgG (GAM)	Goat	Horseradish peroxidase	Dianova
anti-mouse-488 IgG (GAM-488)	Goat	Cy3	Dianova
anti-rabbit IgG (GAR)	Goat	Horseradish peroxidase	Dianova
anti-rat IgG (GARat)	Goat	Horseradish peroxidase	Dianova

2.5 Oligonucleotides

All Oligonucleotides were ordered from Sigma.

2.5.1 Oligonucleotides for PCR

Name	Sequence (5' → 3')	Species
HIPK2 Exon1 for	CCCGTGTACGAAGGTATGGC	human
HIPK2 Exon1 rev	TGGCAGTGGCGACAGTGG	human
HIPK2 Exon2 rev	CTGCAAGTAGGTGGAGCACA	human
HIPK2 Exon8 for	TTGTACCTCTAGACGTTCG	human
HIPK2 Exon8 rev	CCTCTAAGCACGCTGGCTA	human
HIPK2 Exon12 for	CGGTCAGCGTCATCACCAT	human
HIPK2 Exon12 rev	AGCACGCTGCTGCACGGAGT	human
HIPK2 Exon14/15 for2	GATGAGGCACGTCGTCGCA	human
HIPK2 Exon14/15 rev3	CAAGTTTCACTGGTGTCCCGA	human

HIPK2 Exon 2 rat rev	TTGCAAGTACGTAGAACAGAC	rat

2.5.2 Oligonucleotides for Real-Time PCR

Name	Sequence (5' → 3')	Species
HIPK2 qRT N-term Primer3 for	CCTACCTTACGAGCAGACCAT	human
HIPK2 qRT N-term Primer3 rev	CTTGCCCGGTGACAGAAGT	human
HIPK2 qRT C-term for	CCATCCACCCGAGTCAGTAT	human
HIPK2 qRT C-term rev	AGGGTACTGGTTGACCTTGG	human

2.5.3 Oligonucleotides for site-directed Mutagenesis

Name	Sequence (5' → 3')
HIPK2 R404W for	TCGGAGTATGATCAGATTTGGTATATTTCACAAACACAGG
HIPK2 R404W rev	GTGTTTGTGAAATATACCAAATCTGATCATACTCCGAAGC
HIPK2 R826C for	CACAGCGATCCAAGTGTGTCAAGGAGAACACACC
HIPK2 R826C rev	GTGTTCTCCTTGACACACTTGGATCGCTGTGGG
HIPK2 E890G for	CACGGACGAGGGGGAGGAACAGAAACACG
HIPK2 E890G rev	GTTTCTGTTCCTCCCCCTCGTCCGTGTC
HIPK2 E891K for	CGACGAGGAGAAGGAACAGAAACACGCC
HIPK2 E891K rev	CGTGTTTCTGTTCCTTCTCCTCGTCCGTG

2.6 Plasmids

Name	Vector	Epitope tag	Source
HIPK2 wt	pcDNA3	Flag	L. de la Vega
HIPK2 Mut1	pcDNA3	Flag	L. de la Vega
HIPK2 Mut2	pcDNA3	Flag	L. de la Vega
HIPK2 ΔSIM	pcDNA3	Flag	L. de la Vega
HIPK2 K221A	pcDNA3	Flag	L. de la Vega
HIPK2 R404W	pcDNA3	Flag	D. Darici
HIPK2 R826C	pcDNA3	Flag	D. Darici
HIPK2 E890G	pcDNA3	Flag	D. Darici
HIPK2 E891K	pcDNA3	Flag	D. Darici
pPAX2	-	-	Addgene
pMD2.G	-	-	Addgene
MEF2D	-	Flag	V.V. Saul
shHIPK2 #5	pLKO.1	-	Sigma
shHIPK2 #4	pLKO.1	-	Sigma
shScramble	pLKO.1	-	Sigma
GFP	pLKO.1	Flag	AG Bindereif
SUMO1	pGEX	GST	V.V. Saul
PIN1	pGEX	GST	M. Milanovic

3 Methods

3.1 Methods in cell biology

3.1.1 Cell culture

3.1.1.1 Harvesting and subcultivation

Adherent cells were grown in complete DMEM Medium in a humidified incubator at 37°C and 5% CO_2. The confluence was determined daily by light microscopy.

When cells reached 80% confluency they were trypsinized by adding Trypsin/EDTA (3 ml at 75 cm flask and 5 ml at 175 cm flask) and incubated for 5 min at 37°C. After adding 3 ml of complete DMEM medium the cells were transferred in a new flask (1:10 or 1:20 dilution – depending on cell growth).

3.1.1.2 Freezing and thawing

For freezing purposes, cells were trypsinized as described in 3.1.1.1 and resuspended in complete DMEM medium. After centrifugation at 400 g for 3 minutes, the supernatant was discarded, the pellet was resuspended with 1 ml freezing medium and the suspension was pipetted in a cryotube. The cryotubes then were carefully cooled down in a plastic rack slowly to -80°C and after two days transferred to a -150°C freezer.

For thawing purposes, the freezing medium - containing cytotoxic DMSO – needs to be discarded. Therefore the cell-suspension was quickly thawed at 37°C, transferred to a falcon containing 10 ml of complete DMEM medium and centrifuged at 400 g for 3 min. After removal of the supernatant, cells were resuspended with complete DMEM medium and put in a new flask.

3.1.2 Transfection

3.1.2.1 Transfection with cationic polymers

This method was used to introduce DNA into HEK-293T cells that are easy to transfect. It is based on the binding of the cationic polymers to the negatively charged DNA and the cellular uptake via endocytosis.

A 6 cm dish with 293T cells was seeded one day before transfection. For each microgram of DNA 2 µl of Polyethylenimine (PEI) volume was used and mixed with

Transfection Medium 1. The transfection mix was incubated for 20 min at room temperature. Meanwhile the complete DMEM medium on the cells was removed and changed to antibiotic-free Transfection Medium 2. The transfection mix was then applied to the cells and incubated at 37°C. After 4-6 h the medium was changed to complete DMEM medium. Cells were analyzed 2 days after transfection.

3.1.2.2 Transfection with lentivirus

Lentiviral transfection was used to introduce DNA into glioblastoma cells, which exhibited low transfection-efficiency, especially for knockdown experiments. This method is divided into two steps. First step is to produce the lentivirus, the second step is to infect the cells with the lentivirus. Due to risk of infection, all steps were performed under biosafety level 2 conditions.

3.1.2.2.1 Production of the lentivirus

In order to produce the lentivirus HEK-293T cells were seeded in 10 cm dishes and transiently transfected the following day with 5 µg of PAX 2,5 µg of pMD2.G and 5 µg of the knockdown vectors using Roti®-Fect. For each microgram of DNA 2 µl of Roti®-Fect was used and mixed with Transfection Medium 1. The transfection mix was incubated for 20 min at room temperature. Meanwhile the complete DMEM medium on the cells was removed and changed to antibiotic-free Transfection Medium 2. After incubating the transfection mix for 4-6 h, 5 ml of complete DMEM was applied to the cells. Two days later the supernatant, containing the virus particles, was extracted. It was centrifuged at 400 g for 2 min and filtered through a 0.45 µm filter to remove remaining HEK-293T cells. If needed lentiviruses were frozen at -80°C for later use.

3.1.2.2.2 Lentiviral infection of the cells

Lentiviral infection of the cells was done by applying a certain amount of infectious lentiviral medium and 10 µg of Polybrene to the cells. The optimum virus titer was determined by infecting U87MG and A172 cells with different volumes of infectious medium over 8 days, where 500 µl turned out to work best. Infection efficiency was checked by lentiviral transfection of a GFP-encoding virus under the fluorescence microscope.

3.1.3 Lysis

3.1.3.1 NP40-Lysis

Lysis with the nonionic detergent NP40- was found to be suitable to extract the endogenous HIPK2 protein. All steps were performed on ice. At first the medium was removed from the cells. Subsequently the cells were washed 2 times with appropriate

volumes of cold PBS to remove remaining medium. Then the cells were scraped off and collected in a tube. Depending on the size of the pellet, different volumes of NP40-Lysis Buffer (premixed with inhibitors) were added and thoroughly resuspended. After 20 minutes lysis on ice – including several vortexing steps intermittently – a centrifugation step for 12 min at 13000 rpm was performed. The supernatant was extracted and either directly used for protein quantification assays or mixed with SDS buffer at final concentration of 1x, followed by a 5 min heating step at 95°C for protein denaturation. If needed, samples were frozen at -80°C for later use.

Prior to use, following protease-inhibitors were freshly added to the lysis buffer:

	Aprotinin	Leupeptin	Na_3Va_4	NaF	PMSF
Final Concentration	10 µg/ml	10 µg/ml	0.5 mM	10 mM	< 1 mM

3.1.3.2 SDS-Lysis

Denaturing SDS-Lysis was performed to solubilize nuclear proteins. All steps were performed on ice. After removing the medium and two washing steps with appropriate volumes of cold PBS the cells were collected in a tube and directly mixed with 1x SDS sample buffer.. The lysate was sonified two times for 20 sec and heated at 95°C for 5 min. If needed, samples were frozen at -80°C for later use.

3.1.4 Immunofluorescence

Immunofluorescence experiments were usually performed with U2OS osteosarcoma cells seeded on glass coverslips in 12-well plates., At a confluence of 80%, cells were transiently transfected with 1 µg of DNA. Two days after transfection cells were fixed on the cover glasses by adding 1 ml of a -20°C cold acetone/methanol-mixture for 1 minute. Unspecific binding-sites were blocked by using 1 ml of a blocking buffer containing 10% goat-serum in PBS for 60 min. Following steps are describing the detection with the antibodies which were diluted in PBS containing 1% (v/v) goat-serum.

The anti-Flag [M2] antibody was diluted (1:4000), whereof 500 µl was applied and incubated at 4°C over night. Because of light sensitivity, following steps were performed under a light-protecting box. Four washing steps with PBS were performed.

The next day, cells were treated with the secondary antibody anti-mouse (dilution 1:5000). After an incubation of 2 h, the cells were washed two times with PBS and

stained with Hoechst (1:10000) dye for 8 min in order to reveal the cell nucleus. The coverslips were mounted up site down on the slide with a drop of mounting solution and incubated at -4°C for 1 h. Finally nail polish was used to secure and prevent the coverslips from moving and drying out.

3.1.5 Proliferation assays with Flow cytometry (FACS)

FACS analysis was used to determine the cell number for proliferation assays upon HIPK2 knockdown. The GBM cells were transduced with lentiviruses to express a HIPK2-specific shRNA.

Since the lentiviral transfection experiment terms were established for 6-well-plates, GBM cells were seeded on two 6-well-plates. The lentiviruses were produced as described in 3.1.2.2.1 with the vectors shHIPK2#5 and shScramble. After the extraction of the virus particles, one plate was infected with lentiviruses containing shHIPK2#5 and the other plate with shScramble (as described in 3.1.2.2.2). Puromycin selection with 4-10 µg (depending on cell line) was performed to eliminate the non-transfected cells. One day after selection, cells were pooled and counted via FACS. 2 * 10^5 cells were seeded on 6 cm plates each, which in pretests seemed to work best. Experiments were done in duplicates over 6 days and cells were counted by FACSCalibur after 2, 4 and 6 days.

The counting of the cells was performed for 120 sec at low flow rate (12 µl/min) under following settings:

Parameter	Detector	Voltage	Amp Gain	Mode
P1	FSC	E00	1,00	lin
P2	SSC	300-400	1,00	lin
P3	FL1	394		log
P4	FL2	340		log
P5	FL3	200		log

3.2 Methods in biochemistry

3.2.1 Bicinchoninic acid (BCA) assay

The BCA assay is a method to quantify the total level of proteins and was used to determine protein amounts after NP40-Lysis (3.1.3.1) so that equal amounts of protein

could be used for SDS-PAGE (3.2.2). Using the Pierce™ BCA Protein Assay Kit, 150 µl of the Working Reagent (50:1, Reagent A:B) was mixed with 10 or 20% of the lysate and incubated for 30 min at 37°C. Absorbance was then measured at 562 nm in a 96-well-plate Spectrophotometer, normalized to water and total protein amount was determined comparing with a BSA-standard curve.

3.2.2 SDS-Polyacrylamid gel electrophoresis (SDS-PAGE)

First step in the detection of proteins is the SDS-PAGE, which separates polypeptides based on their size independently from their charge. For this purpose, SDS-gels have been prepared in different concentrations - depending on the protein size of interest - as follows:

Separating gel [1.5 mm]:

% Acrylamid	6%	8%	10%	12%
30% Acrylamid	1,6 ml	2,1 ml	2,7 ml	3,2 ml
4x Lower Buffer	2 ml	2 ml	2 ml	2 ml
ddH2O	4,4 ml	3,9 ml	3,3 ml	2,8 ml
10% APS	50 µl	50 µl	50 µl	50 µl
TEMED	5 µl	5 µl	5 µl	5 µl

Stacking gel [1.5 mm]:

30% Acrylamid	0,5 ml
4x Lower Buffer	1 ml
ddH2O	2,5 ml
10% APS	50 µl
TEMED	5 µl

If needed, gels were stored in a humidified plastic bag for at least two days in a fridge.

All samples were loaded on the gel with the Hamilton pipette. The protein marker was loaded in the first lane and the lysates beside. Empty lanes were filled up with 1x SDS buffer to avoid bendings. The whole gelelectrophoresis chamber is divided into two disconnected chambers, where the inner chamber, locating the samples, was filled with new fresh Running buffer and the outer chamber with old Running buffer in order to save resources. Migration of the proteins was achieved by applicating voltage from a

power supply. 80 V were supplied until the samples entered the stacking gel. Further electrophoresis was performed with 100 V for about up to 3 h.

3.2.3 Western blot and immune detection

After SDS-Page, the gel was blotted to a PVDF membrane using the method of semi-dry protein transfer. First step was to prewet the PVDF membrane with 100% methanol to reduce its hydrophobicity. Next step was to construct a blotting Sandwich, bottom-up consisting of two layers of soaked Whatman papers, the PVDF membrane, the gel and one layer of Whatman paper on the top. Soaking was performed in Transfer buffer by paying attention, that the chamber is not completely floated. Potential air bubbles were removed by rolling with Falcon. Depending on the protein size, 24 V were applied constantly for at least 1 h. Bigger proteins, such as HIPK2 (~130 kDa) were blotted for 2 h. After the blotting the PVDF membrane was incubated for 30 min in TBS-T with 10% milk powder at room temperature.

Immune detection was performed by incubating the blocked membrane with the protein-specific first antibody over night at 4 °C. The next morning, after five washing steps with TBS-T for 3 min each, the Horseraddish-peroxidase-conjugated second antibody, which is detecting the first antibody, was added and incubated for 1 h at room temperature followed by a second washing procedure. Subsequently the antibody-coupled membrane was soaked with an enhanced chemiluminescence lightning (ECL) system, which is reacting with the Horseraddish peroxidase (HRP) by producing chemiluminescence at 425 nm.

Under light-protective conditions, the chemiluminescence was detected with an X-ray film and visualized with an automated X-ray film developer.

3.2.4 Expression and purification of GST fusion proteins

GST fusion proteins were expressed and purified to perform GST-pulldown experiments (3.2.5). First, competent BL-21 E.coli cells were transformed with GST vectors including GST only as a positive control. 2 colonies of each clone was inoculated in 2 ml of LB-amp. After growing over night at 37°C, 8 ml of warm LB-amp was mixed with the cells and grown for 30 min on the shaker. The cultures were split equally in 2 tubes. 5 µl of IPTG (1 M) was added to one colony in order to induce protein expression. The cells were cultured for 120 min at 30°C and collected by centrifugation (3000 g for 10 min at 4°C). The pellet was washed with 300 µl of cold PBS and the pellet was dissolved. 50 µl of Lysozyme solution (10 mg/ml) was added and incubated for 20 min on ice. The samples were additionally sonified four times for 20 sec and centrifuged for 15

min at 26 000 g at 4°C. The supernatant was transferred to a new Eppendorf tube, 25 µl of equilibrated glutathione (GSH) sepharose beads was added and incubated for 1 h on a spinning wheel. Four washing steps with 10 ml cold PBS were performed. Bound GST fusion proteins were eluted by resuspending the beads in 500 µl GSH elution buffer. Eluates were pooled and dialyzed in 1 L dialysis buffer overnight at 4°C. Finally a SDS-Page was performed to quantify the purified GST fusion proteins.

3.2.5 GST pull-down assay

GST pull-down assay is an in vitro method used to determine physical interaction between proteins. HEK-293T cells were seeded on 10 cm plates and transiently transfected with HIPK2 vectors in order to express and analyze different mutants of the protein. One day after transfection, cells were lyzed using NP40-lysis (3.1.3.1). 5 % of the lysates were used as an input control, whereas the remaining lysates were divided equally and incubated with either 5 µg of the non-fused GST protein or 5 µg of the GST fusion protein together with 50 µg GSH sepharose each for 4 h at 4°C on a rotating wheel. After centrifugation at 2000 g for 1 min, the supernatant was discarded and the pellet was washed three times with NP40-buffer. The elution of the binding proteins was achieved by mixing 100 µl of 2 x SDS sample buffer, heating it for 4 min and analyzing by Western blot (3.2.3).

3.3 Methods in molecular biology

3.3.1 Total RNA extraction

The extraction of total RNA from cell culture tissue was performed with the RNeasy Mini kit using column technology by following the official protocol with few modifications. Because of RNA instability and RNases, work was performed quickly on a cleaned bench. All centrifugation steps were done at 13200 rpm. Cells were harvested (3.1.1.1) preferentially from 10 cm plates to increase the RNA yield. Cells were washed two times with PBS. 1 ml of RLT lysis buffer was premixed with 10 µl β-Mercaptoethanol in order to irreversibly denauture RNases by reducing its disulfide bonds. To homogenize the lysate, cells were passed through a RNase-free syringe for around 3 minutes. 1 ml of 70%-Ethanol was then added to the homogenized lysate. 700 µl of the sample was loaded on a column. Centrifugation was performed for 1 minute and the flow-through was discarded. These steps were repeated until all suspension was lost. Next 350 µl of RWE1 buffer was added to the spin column and centrifugated for 30 sec. Afterwards a DNase-mix, containing 60 µl RDD buffer and 10 µl DNase I, was put on the column and incubated for 15 min.

After DNase-treatment, two independent cleaning steps with 350 µl of RWE1 buffer and 700 µl RPE buffer were performed. Last step included a dilution of total RNA from the column, which was achieved by adding appropriate volumes of RNase-free water – the volume was depending on the yield, which was varying between cell-lines. To avoid subsequent RNA degradation, 1 U of the RNase inhibitor Ribolock was pipetted to the RNA-elution. To measure RNA yield and quality, 1 µl of elution was mixed with 70 µl RNase-free water and photometrically measured. Quality (absorption at 260/280) of the RNA was between 1.8 and 2.0 in average. If needed RNA was frozen at -80°C for later use.

3.3.2 cDNA synthesis

Reverse transcription is the method to transform mRNA into cDNA. One µg of total RNA was mixed with 1 µl of Oligo-dT_{12-18}-Primer and 1 µl of dNTPs which then was adjusted to a total volume of 12 µl with water and heated at 65°C for 5 min. After adding 2 µl of 0,1M DTT and 4 µl of 5x First-strand buffer, the solution was heated again at 42°C for 2 min. Finally 1 µl (200 units) of the reverse transcriptase enzyme (Super-Script II RT) was added, resuspended properly and the reaction mix was incubated for 55 minutes at 42°C and for 15 min at 70°C. If needed, cDNA was frozen at 20°C for later use.

3.3.3 Polymerase chain reaction (PCR)

PCR, as a powerful method to simply amplify specific nucleotide regions of interest, can be performed for many different purposes. Since a couple of primers were used for the reactions, all reactions had to be optimized by pretests.

These pretests were done with varying concentrations of Mg^{2+}, primers and cDNA templates and with different annealing temperatures. For sequencing purposes, the reaction volume was doubled.

	Exon analysis	Sequencing
5x Green Buffer	5 µl	10 µl
dNTPs (10 mM)	0,5 µl	1 µl
Forward Primer (5 µM)	2,5 µl	5 µl
Reverse Primer (5 µM)	2,5 µl	5 µl
$MgCl_2$ (25 mM)	3 µl	6 µl

Taq-Polymerase	0,15 µl	0,3 µl
DMSO (50% in H2O)	2,5 µl	5 µl
cDNA (20 ng)	2,5 µl	5 µl
ddH2O	6,35 µl	12,7 µl
total	25 µl	50 µl

The reagents were mixed properly on an ice rack, whereas the Taq-Polymerase was added right before putting it in the Biorad cycler.

	Temperature	Time	Number of cycles
Initial Denauturation	95°C	3 min	1 cycle
Denauturation	95°C	30 sec	
Annealing	57-67°C	30 sec	35x
Elongation	72°C	1 min/kb	
Final elongation	72°C	5 min	1 cycle
Storage	10°C	infinite hold	

Furthermore the product of the reaction could be either digested with restriction enzymes (3.3.4) visualized by agarose gel electrophoresis (3.3.7), purified for sequencing (3.3.8 and 3.3.9) or frozen at -20°C for later use.

3.3.4 DNA digestion with restriction endonucleases

Bacterial restriction endonucleases are able to cut palindromic DNA sequences at specific restriction sites. They were usually used to control PCR products, after isolation of plasmid DNA (3.3.11) and after site-directed mutagenesis (3.3.5).

The following table illustrates the composition of the reaction mix:

Reagent	Volume
Plasmid DNA (1 µg/µl)	2 µl
10 x restriction buffer	2 µl
Restriction enzyme (10 U/µl)	0,1 µl
ddH2O	10,9 µl

The mix was incubated at 37°C for 2 h and analyzed by agarose gel electrophoresis (3.3.7).

3.3.5 Site-directed mutagenesis

Site-directed mutagenesis is a method to modify the primary DNA code by changing, inserting or deleting bases. Basically several primers, which contain the desired mutation, were constructed.

The mutagenesis reaction was performed using the Quick-Change-Mutagenesis Kit. Following reagents were mixed on an ice rack:

	Volume
Plasmid DNA (100 ng/µl)	1 µl
10x Reaction Buffer	5 µl
dNTP mix (10 mM)	1 µl
Quik Solution	3 µl
Pfu Polymerase (2,5 U/µl)	1 µl
forward primer (10 µM)	1,3 µl
reverse primer (10 µM)	1,3 µl
ddH2O (MilliQ water)	36,4 µl
Total volume	50 µl

Afterwards the following PCR program was used for site-directed mutagenesis.

	Temperature	Time	Number of cycles
Initial Denauturation	95°C	1 min	1 cycle
Denauturation	95°C	50 sec	18 cycles
Annealing	57-60°C	50 sec	
Elongation	68°C	9 min	
Final elongation	68°C	5 min	1 cycle
Storage	10°C	Infinite	

After the PCR finished, DpnI, an enzyme which cleaves the parental methylated bacterial template-DNA, was added and incubated for 2 h at 37°C. Subsequently an Agarose

gel electrophoresis (3.3.7) was performed and the specific band was purified using Agarose gel extraction (3.3.8). The purified Plasmid-DNA was transformed in bacteria (3.3.10) and several clones from the Agar-plate were picked, enriched in mini-preparations (3.3.11) and sequenced (3.3.9) for screening purposes. If a clone was positive for the mutation, a maxi-preparation (3.3.11) was done and the products were test expressed in HEK-293T cells. Correct expression of the mutated protein was ensured by SDS-PAGE (3.2.2) and Western blotting (3.2.3).

3.3.6 Real-Time Quantitative PCR (qPCR)

The RT-PCR enables monitoring of DNA-quality and quantity by measuring the DNA-amount dependent increase of fluorescent-dyes during PCR. This was achieved by adding the DNA binding SYBR green to the PCR reaction. The method was basically used to analyze mRNA expression levels. For that purpose, cells were seeded on 10 cm plates and total RNA was extracted (3.3.1). The mRNA was translated in cDNA (3.2.2). Several dilution-pretests were performed in order to determine the right concentration of the reagents, incuding DNA- and primer-concentration gradients.

The qPCR was started mixing the following reagents on ice:

	Volume
cDNA (10 ng/µl)	2 µl
ABsolute SYBR green ROX mix	5 µl
forward primer (5 µM)	0,4 µl
reverse primer (5 µM)	0,4 µl
ddH2O	2,2 µl
Total volume	10 µl

Accordingly the qPCR was performed in triplicates in an ABI 3000 Real-time PCR cycler (Applied Biosystems), using the following program:

	Temperature	Time	Number of cycles
Initial Denauturation	95°C	15 min	1 cycle
Denauturation	95°C	15 sec	
Annealing	60°C	30 sec	40 cycles
Elongation	72°C	30 sec	

The fluorescence was measured after the Elongation step and an additionally melting curve analysis was performed to evaluate the specificity of the amplified products. After normalizing the ct-values to the housekeeping gene β-actin, the relative expression was calculated using the comparative $2^{-\Delta\Delta ct}$ method by comparing to a predefined reference transcript (expression = 1).

3.3.7 Melting Curve Analysis

Melting curve analysis is a method, which is able to detect dissociation-characteristics of dsDNA. After a Real-Time PCR experiment, a heating step is performed with increasing temperatures by constantly measuring the fluorescence. Since SYBR Green® is sending fluorescence when bound to dsDNA, the dissociation of dsDNA upon heating into ssDNA decreases the signal. The dissociation properties of DNA are depending on the amount of base pairing while G-C rich DNA has a higher melting temperature than DNA with a higher A-T content. Melting Curve Analysis was performed in a Real-time PCR cycler (Applied Biosystems).

3.3.8 Agarose gel electrophoresis

Agarose gelelectrophoresis was mainly used to separate linear DNA, RNA and Plasmids by their size. Depending on the expected size, miscellaneous amounts of agarose was heated with 50 ml TAE buffer in the microwave until the particles completely dissolved. Afterwards 1 µl of Ethidiumbromide, an intercalating dye, was added to the suspension. The gel was poured in a chamber and a comb was inserted. The whole chamber was filled with TAE buffer and electrophoresis was performed at 80 V in the presence of an appropriate DNA marker. After electrophoresis a picture of the gel was taken under UV illumination, where the stained DNA bands appeared as glowing bands.

Agarose gel extraction

Agarose gel extraction is a method to purify DNA fragments from agarose gels. The band of interest was visualized under 70% UV-irradiation in order to limit DNA damage and cutted out with a proper scalpel. The following steps were performed as described in the protocol using the gel extraction kit from JetStar.

3.3.9 Sequencing

Sequencing was used to reveal unknown primary base structures of Plasmid-DNA. For this purpose, samples were prepared as follows:

	final concentration
Plasmid DNA	80 ng/µl
Primer	30 pmol/µl
ddH2O	ad 15 µl

After premixing the substances, the mix was sent to SeqLab (Microsynth Company), who analyzed the samples over night and told the results via e-Mail.

3.3.10 Competent E.coli transformation

Transformation describes the uptake of exogenous DNA material from bacterial cells and is the first step of plasmid amplification. Therefore plasmid DNA was carefully mixed with 50 µl of chemically competent E.coli and incubated for 20 min on ice, following a short heatshock for 90 sec at 42°C in order to allow DNA entering through cell pores. After incubating the bacteria for 5 minutes on ice, 500 µl of antibiotica-free LB medium was added and incubated at 37°C on a shaker for 1 h. Finally, successfully transformed cells were selected through plating on LB agar containing the appropriate antibiotic and incubated at 37°C for at least 12 h.,

3.3.11 Plasmid DNA purification

After transformation (3.3.10), plasmid DNA of interest was purified using the column-based Jetstar 2.0 Plasmid Mini/Midi/Maxi kit according to manufacturer's instructions. The kit uses a modified alkaline/SDS lysis procedure and a column, where the negatively charged plasmid DNA is bound to the positive charges on the resin surface. Once the lysate ran through the column, several washing steps were performed to remove RNA, proteins and carbohydrates. Afterwards RNAse I was added to the column to remove further RNA impurities. The plasmid DNA was eluted and precipitated from the elute with isopropanol and 70% ethanol. A photometrically determined purity of the DNA around 1.80 ($OD_{260/280}$) was achieved.

4 Results

4.1 Analysis of HIPK2 in GBM

4.1.1 Protein levels of HIPK2 in GBM

Several studies described alterations in the serine-threonine kinase HIPK2 in cutaneous tumours [140], leukaemia [124] and other neoplasms [113, 141, 142]. In low-grade pilocytic astrocytoma (WHO I), in particular, there is evidence of a *Hipk2* amplification on gene locus 7q34 [126, 127, 143]. These findings raise the question whether these alterations also occur in high-grade GBM (WHO IV). The first intention of this project was to determine the endogenous HIPK2 expression in 12 GBM cell lines and compare them to HIPK2 levels in other cell lines such as HeLa cells (cervix carcinoma) and HEK-293T cells (human embryonic kidney cells).

To address these questions, semi-quantitative Western Blot experiments should be performed. Before performing the experiment, several pretests had to be conducted. The first point was to test if the antibodies are detecting HIPK2 confidently. Therefor a Western Blot experiment was performed, where endogenous and overexpressed HIPK2 were targeted. The results showed a high specificity of the antibodies for HIPK2 (not shown).

The next step was to check if the antibodies are able to detect small differences in the expression levels of endogenous HIPK2. NP40-lysates of two cell-lines (T98G and U373) were prepared and a BCA assay was employed to determine the protein concentrations. Various amounts of protein (10 µg, 20 µg, 40 µg and 80 µg) were analyzed by Western blotting using antibodies raised against N-terminal and C-terminal epitopes of HIPK2 (Fig. 4.1.1.1). The result of the Western blot shows that endogenous HIPK2 can be detected at high sensitivity with these antibodies.

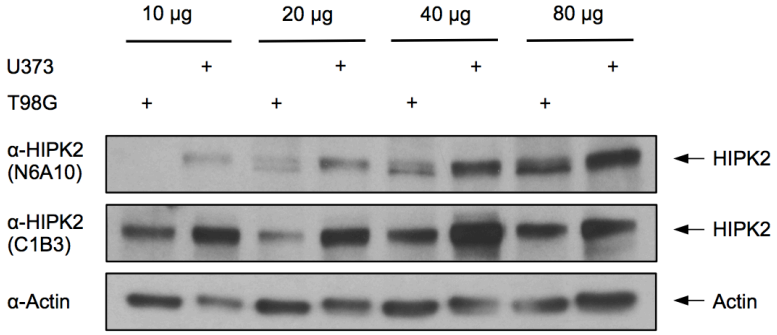

Figure 4.1.1.1: Test expression of endogenous HIPK2 with specific antibodies. Lysates of U373 and T98G cells were analyzed with.BCA assay to determine total protein levels. Different protein amounts of 10-, 20-, 40- and 80 µg from both cell lines were investigated with N-terminal (N6A190) and C-terminal (C1B3) HIPK2 antibodies in Western blot experiments.

After the positive pretests, several cell lines were headed to Western blot (Fig. 4.1.1.2). The polyclonal antibody α-HIPK2 (Rab) showed the best signal and was chosen to compare protein expression. An increased expression of endogenous HIPK2 protein can be assessed in 10 out of 12 GBM cell lines (Ratio > 1), compared to HeLa cells (Ratio = 1). However, there is also a huge difference among the GBM cells themselves. The cell lines U118 and G55 show less HIPK2 protein amounts (Ratio < 1) and stand in contrast to the other GBM cell lines. The U373 cell line overexpresses a remarkable amount of the HIPK2 protein (Ratio > 2). Supporting the test reliability, two C-terminal antibodies (C1B3 and 5C6) show similar results in relation to the fact that they are either not detecting C-terminal HIPK2 in U87, A172 and G55 cells, or only little amounts of it in U118 cells.

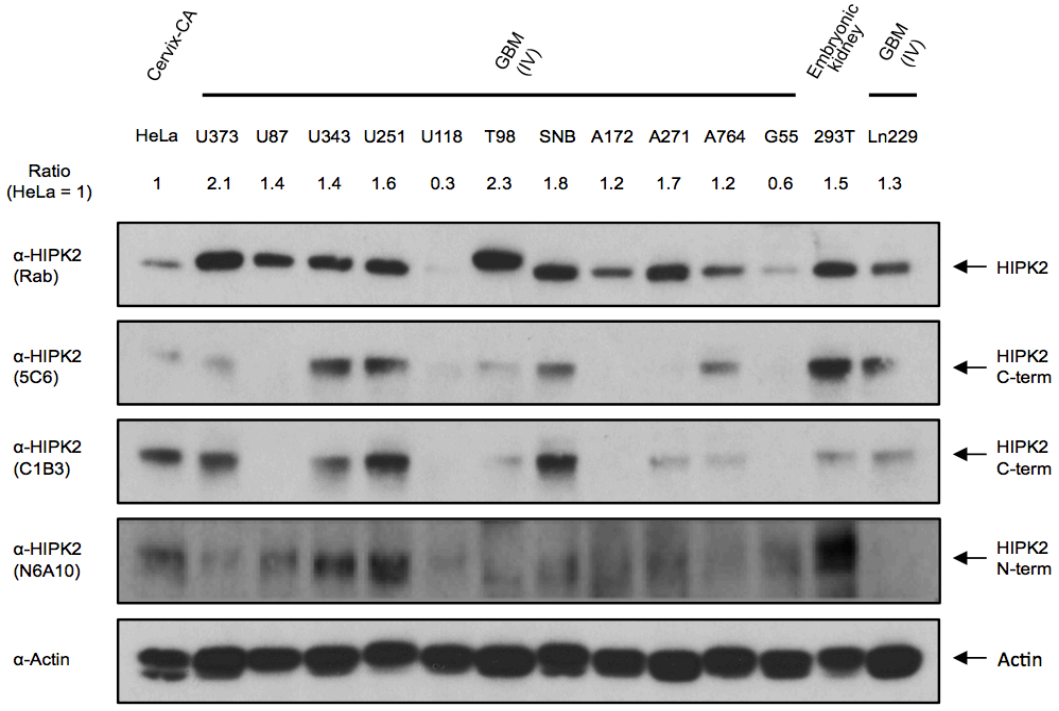

Figure 4.1.1.2: Comparative analysis of HIPK2 protein expression in tumour cell lines. HIPK2 expression of 12 different GBM cell lines, HeLa cells and HEK-293T cells were analyzed. Equal amounts of NP40 lysates (=80 µg) were subjected to Western blot and endogenous HIPK2 was detected with different antibodies. These are either polyclonal rabbit antibodies (Rab) or monoclonal antibodies raised against N-terminal (N6A10) or C-terminal (5C6, C1B3) sequences. HIPK2 expression was quantified by using the software ImageJ®, whereas the α-HIPK2 (Rab) detected expression was used for calculation. The ratio was normalized to expression in HeLa cells. Actin served as a loading control.

Interestingly, the expression of HIPK2 is inconsistent when comparing the different antibodies in U87 and A172 cells. Ln229 cells show no signal when detecting with the N-terminal antibody (N6A10), whereas HEK-293T cells exhibit a strong signal. The limitations of this experiment are that even after changing the experiment settings for the N6A10 antibody, the quality did not get better.

These findings are concluded in two main questions, which will be investigated next: What is the reason for the differences in endogenous HIPK2 expression in GBM and what role does it play in the biology of glioblastoma multiforme?

4.1.2 mRNA levels of HIPK2 in GBM

Since the expression of endogenous HIPK2 protein varies among GBM cell lines (4.1.1), it was interesting to test whether this is also reflected at the mRNA level. After mRNA extraction and cDNA synthesis, the relative mRNA expression of HIPK2 was determined by Real-time PCR. The mRNA expression of U343 cells was used as a reference and set to 1. A negative control was always performed using water.

The mRNA expression of HIPK2 shows either a normal, or a slight overexpression in the cells U87, U343, U251, SNB, A172, A271 and G55, compared to HeLa cells. More interesting is the fact that U373 cells, as well as U118 cells, exhibit four to five times higher HIPK2 mRNA expression than other GBM cell lines. Even though U118 cells express low levels of HIPK2 protein (Fig. 4.1.1.2), they show a quite high HIPK2 mRNA expression (Fig. 4.1.2. (A).

This experiment was repeated with several cell lines and primers, which target the C- and N-terminus of HIPK2. There was no significant difference in the mRNA expression between the C and N-terminal primers in U87, U343, A172 and 293T cells. (Fig. 4.1.2. (B).

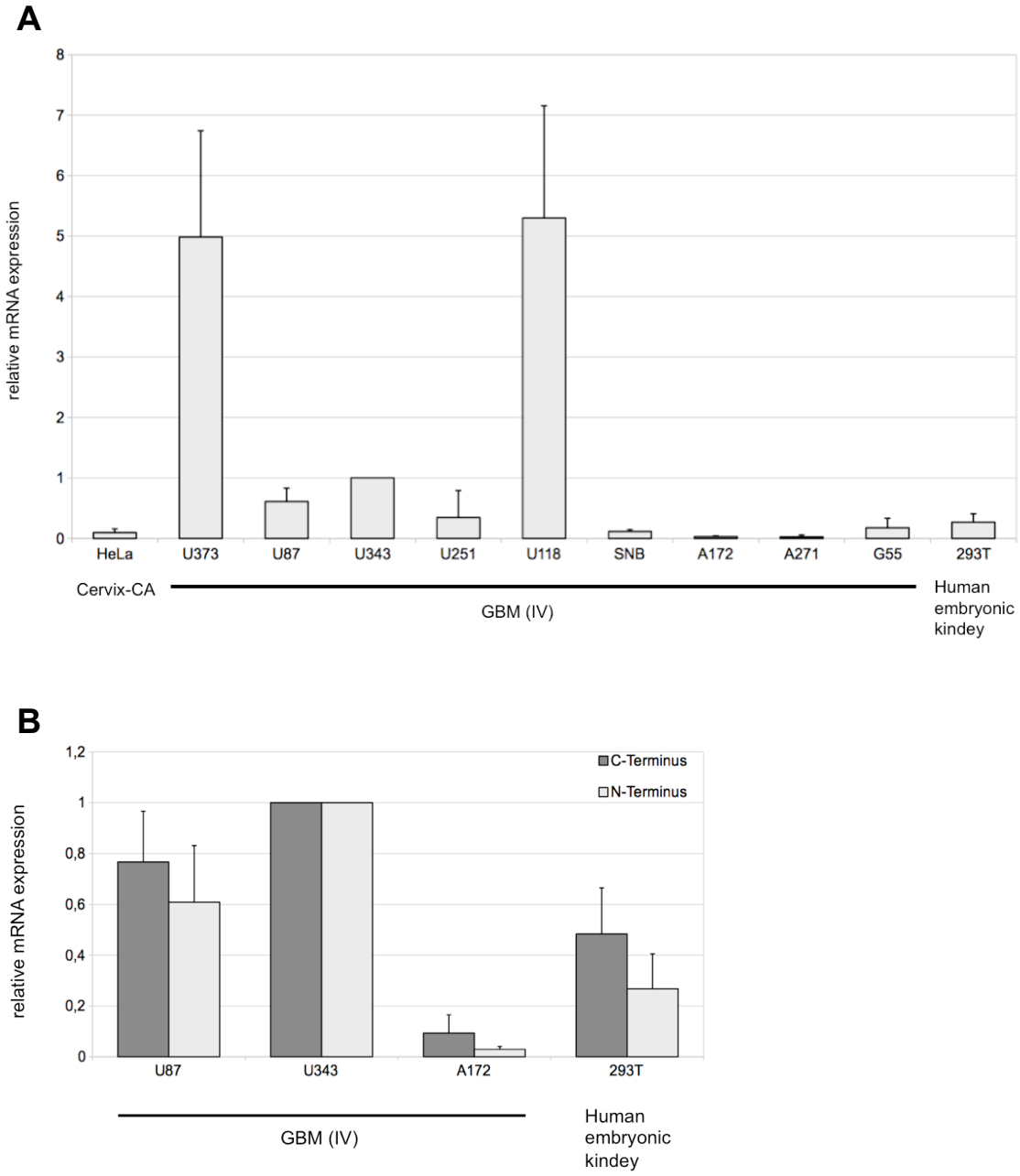

Figure 4.1.2: Analysis of HIPK2 mRNA expression in different GBM cell lines. (A) Total RNA was extracted with the RNeasy Mini kit and transcribed into cDNA using Oligo-(dT) primers. The mRNA expression was quantified by Real-time PCR using specific HIPK2 primers, which are targeting the conserved N-terminus (HIPK2 qRT N-term Primer3 for and rev). Actin was chosen as a housekeeping gene for normalization. In order to facilitate the comparison the expression of HIPK2 mRNA in U343 was arbitrarily set to 1. All measurements were done at least n=3 times in triplicates. The error lines show the standard deviations. **(**B) According to the experimental settings in 4.1.2.A, the C-terminus was additionally investigated in several cell lines with HIPK2 qRT C-term for and rev primer. The results were compared to the mRNA expression of the N-terminal primers.

Differences in protein amounts cannot only be due to different mRNA levels but also to distinct protein stabilities. This was therefore tested in further experiments.

4.1.3 Protein stability of HIPK2 in GBM

Intracellular proteins underlie a continuous proteasomal degradation process. The interplay between the synthesis and degradation determines the amount of the protein in the cell. Since there is a discrepancy between the mRNA expression and protein level of HIPK2 in U118 cells, protein stability experiments using the protein translation inhibitor Cycloheximide (CHX) were performed next.

Different GBM cell lines were seeded and incubated for various periods with CHX (10 µg/ml), followed by Western blot analysis using α-HIPK2 (Rab) antibodies (Fig. 4.1.3.1). The results of the CHX experiments show differences in protein stability in GBM cell lines (Fig. 4.1.3.1). Whereas the cell lines SNB19 and G55 express a constant HIPK2 level over 24 h, Ln229 and U118 cells immediately lose nearly all of their HIPK2 within 4 h. Especially in U118 cells, a significant loss of HIPK2 after only 2 h can be seen, suggesting that the HIPK2 protein is highly instable in these cells.

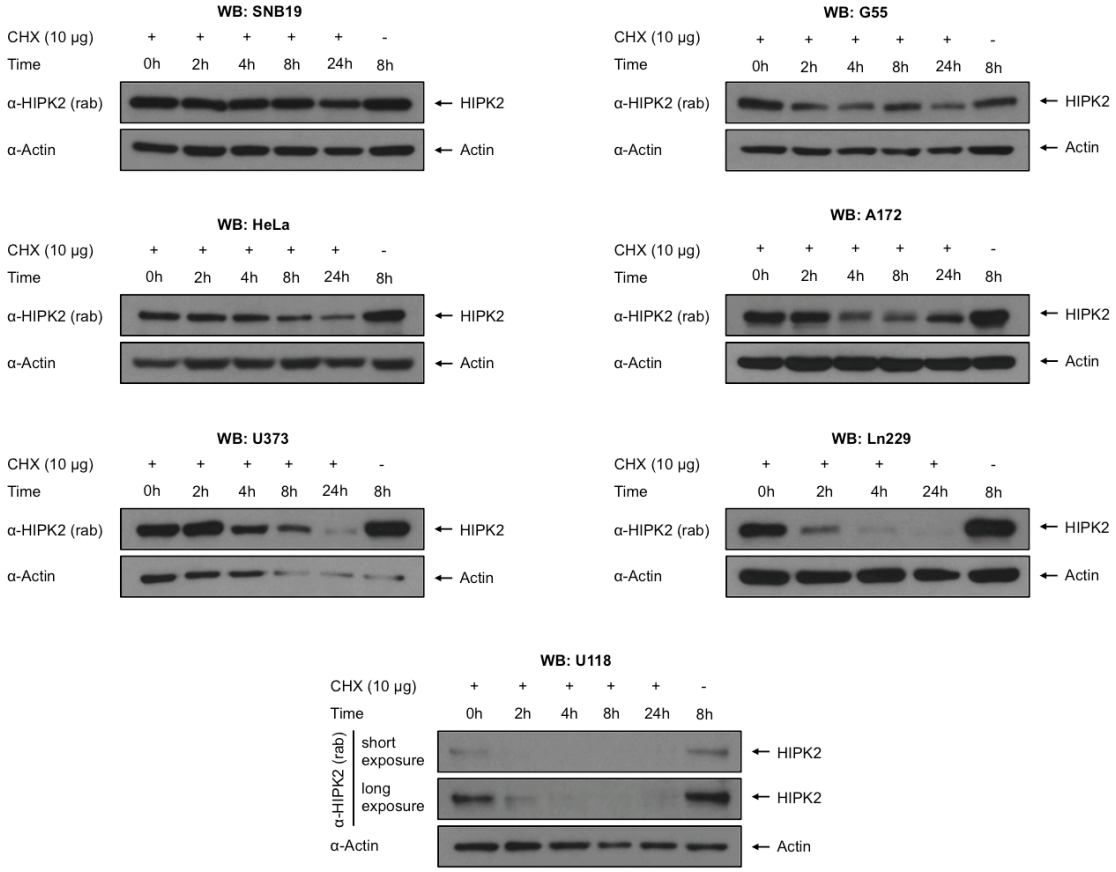

Figure 4.1.3.1: Analysis of HIPK2 protein stability in GBM cell lines. GBM cells were harvested and *de novo* protein synthesis was blocked upon addition of Cycloheximide for various periods. Protein extracts were prepared followed by analysis of HIPK2 protein levels by immunoblotting with the polyclonal α-HIPK2 (Rab) antibody. Actin serves as a loading control. Since U118 cells express low HIPK2 levels, a long time exposure of the WB was additionally performed.

In parallel the effect of CHX treatment on the viability of fast-growing U87 cells was investigated. Since the cells lose the ability of adherence when they die, they can be mostly found in the supernatant medium. The supernatant with the dead cells and the adherent cells were analysed together by WB (Fig. 4.1.3.2).

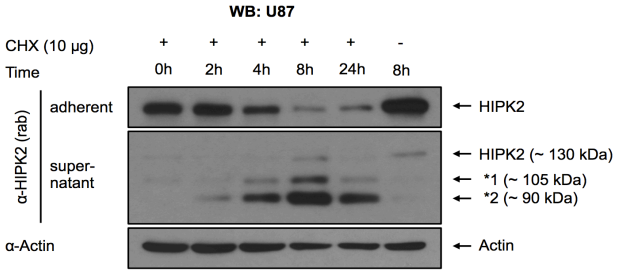

Figure 4.1.3.2: Analysis of degradation fragments of HIPK2 during cycloheximide (CHX) treatment. U87 cells were harvested and treated with CHX for various periods. Both the supernatant and the adherent cells were separately analysed using NP40-lysis and Western blotting with the polyclonal α-HIPK2 (Rab) antibody.

After 8 h of CHX treatment, two products -with molecular weights of around 90 kDa and 105 kDa- clearly appear in the detached cells, indicating ongoing HIPK2 protein processing.

4.1.4 Exon analysis of HIPK2 in GBM

Since HIPK2 was investigated at protein and mRNA levels, the next step was to check the exon structure of the mRNA. Previous experiments in the lab indicate two HIPK2 isoforms in three analysed human cell lines. It was thus interesting to see whether the various GBM cell lines show differences in their exon usage. To address this question, PCR experiments with different primer pairs were performed. First, the cells were harvested and mRNA was extracted. Using a reverse transcriptase, the mRNA was transcribed into cDNA, which was actually used as a template for the PCR experiments.

Figure 4.1.5.A shows the exon structure of HIPK2. Annealing areas of the primers are highlighted with arrows. The results with the cell lines U87, A172, U343, HeLa and 293T show one specific PCR product, with the primer pair 1F/1R and 1F/2R indicating no alteration in these areas (Fig. 4.1.4. (B). However, the primer pair 8F/8R leads to the occurrence of an additional faster migrating PCR product. This second band is less present in 293T cells. A second PCR product can also be detected in G55, U373, U118 and A764 cells, when combining primer 8F/12R (Fig. 4.1.4 (C). This suggests a shorter product of HIPK2 at Exon 8 predominantly in GBM and HeLa cell lines.

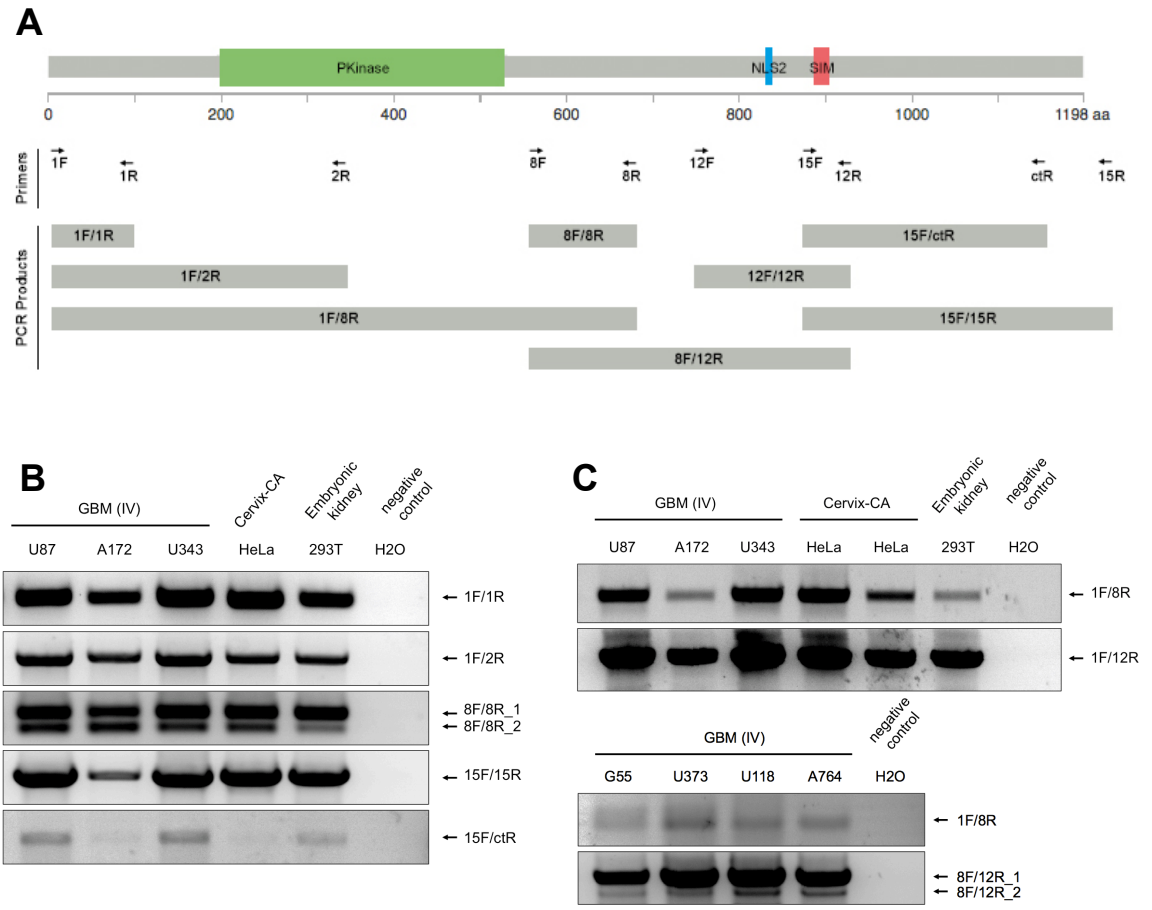

Figure 4.1.4: Analysis of HIPK2 exons in GBM. (A) HIPK2 mRNA exhibits 15 exons of different length. The annealing areas of the used primers are shown. (B) The indicated cells were grown, mRNA was extracted, and translated into cDNA. PCR experiments were performed with the cDNA using the indicated HIPK2 primers. Short PCR products were analyzed by agarose gel electrophoresis, an ethidium bromide-stained agarose gel is shown. (C) Migration of the long-range PCR products is displayed.

4.1.5 Amplification analysis of *Hipk2* in GBM

The previous results showed alterated HIPK2 protein and mRNA expression in GBM cell lines (Fig. 4.1.1 and 4.1.2). As genetic aberrations occur more often in malignant tumour cells, the idea came up that genetic amplifications should be checked, which might explain these alterations. For this purpose, a SNP array was performed in collaboration with the “Institut für Humangenetik” in Gießen. Two GBM cell lines (U373 and U87), which showed high HIPK2 expressions in the previous experiments (Fig. 4.1.1.2), were analysed by SNP arrays (Fig. 4.1.5).

The results indicate a complex chromosomal aberration in chromosome 7 in GBM. The basal rate of log Ratio (red) on chromosome 7 is increased (0.5) and the heterozygous allele cluster has split into two clusters, reflecting allele proportions deviating from 1:1. Besides this alteration, the intensity of the log Ratio is increasing beyond the second half of the long arm of chromosome 7, which indicates that this area is likely amplified. The changes in B allele frequency (blue) and the log ratio indicate an amplification of

the region 7q32-7q35 in U373 cells and 7q31-7q35 in U87 cells. Since the *Hipk2* locus is on 7q34 [96] its amplification in both cases is most likely. The exact copy number changes can be determined with the exact information about the karyotype, which should be further investigated.

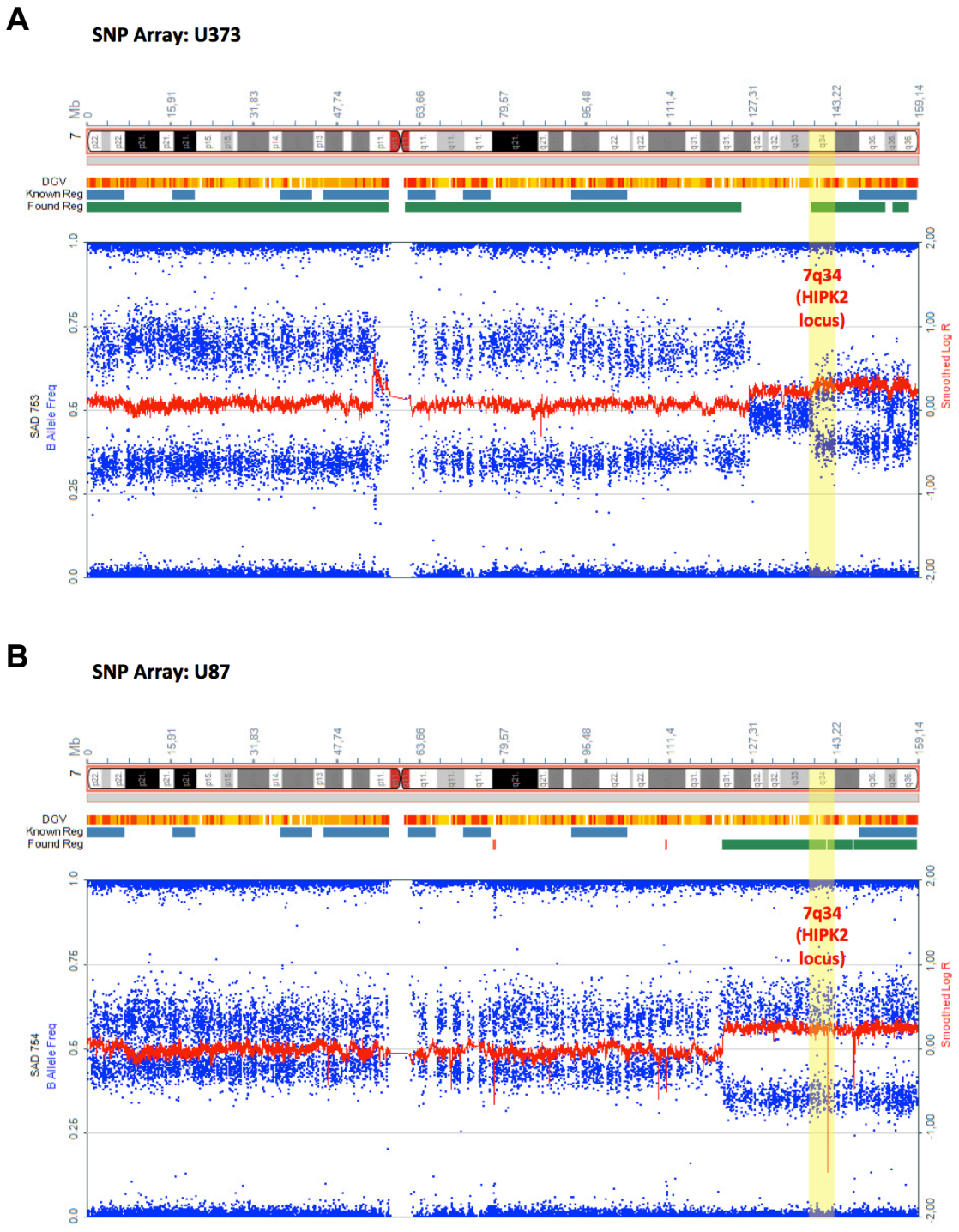

Figure 4.1.5: Amplified regions on 7q in GBM including *Hipk2* locus. Two GBM cell lines U373 and U87 were harvested, DNA was extracted and amplified. A SNP array was then performed and the results were visualized by KaryoStudio from Illumina. The whole chromosome 7 is mapped on the top, whereat the gene locus of *Hipk2* (7q34) is highlighted in yellow. B Allele Frequency is shown as blue dots and log Ratio in red.

4.1.6 The role of HIPK2 for GBM cell proliferation

To investigate the function of HIPK2 for proliferation of GBM cells, knockdown experiments were performed. As GBM cell lines were not transfectable with cationic polymers they were transduced with lentiviruses encoding an shRNA mediating HIPK2 knockdown. The lentiviruses were produced in HEK-293T cells that were transfected with the plasmids (PAX, pMD2.G together with shHIPK2 or shScramble). After production of lentiviruses, which were encoding either a HIPK2-specific shRNA or a scrambled control, GBM cells were infected. In order to achieve valid results, transfection efficiency and knockdown efficiency had to be checked first.

The first step in establishing lentiviral knockdown was to find out working transfection efficiency: A GFP vector was used to control transfection conditions under fluorescence microscope. On adding 500 µl of infectious supernatant, transfection efficiency was regarded as sufficient (Fig. 4.1.6.1).

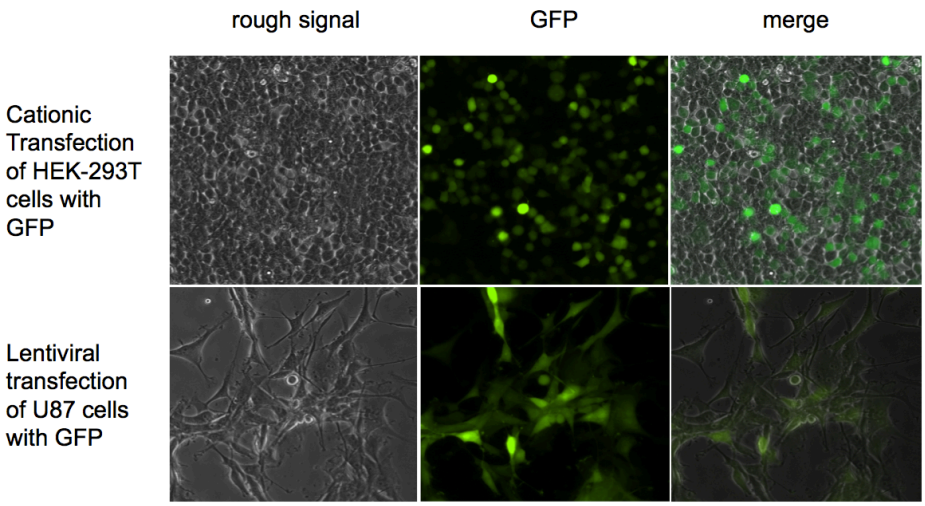

Figure 4.1.6.1: Cationic transfection and lentiviral infection efficiency. HEK-293T cells were transfected with GFP using Rotifect®. After producing lentivirus containing the GFP vector, GBM cells were infected and GFP expression was checked under fluorescence microscope.

After infection of the GBM cells with the shHIPK2 or the shScramble vector, efficiency of the knockdown had to be determined. This can be reliably achieved by checking protein levels after infection. Two GBM cell lines (U87 and A172) were infected and non-infected cells were eliminated by puromycin selection for two or five days. A semi-quantitative Western blot with the polyclonal HIPK2 antibody showed reduced HIPK2 protein amounts 5 days after selection, indicating a successful knockdown (Fig. 4.1.6.2).

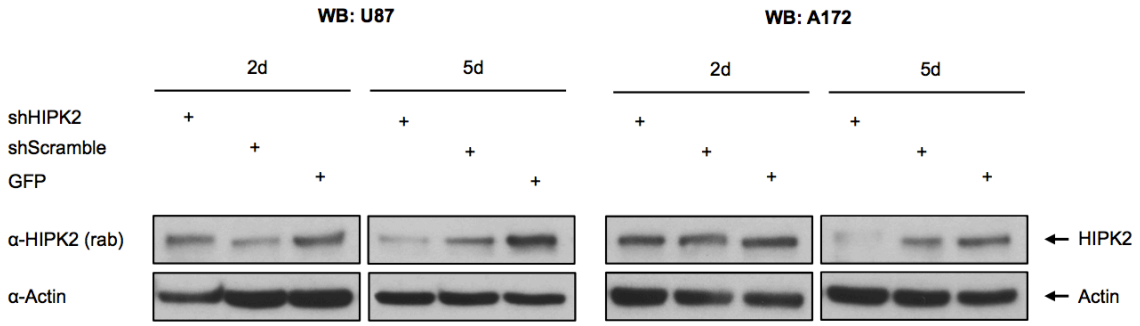

Figure 4.1.6.2: Analysis of HIPK2 knockdown efficiency in GBM cell lines. U87 and A172 cells were transfected with lentivirus encoding shHIPK2, shScramble or GFP. Cells were lyzed and the amount of HIPK2 was measured with Western Blot after 2 days and 5 days of selection.

The next step was to count the cells upon HIPK2 knockdown to observe an effect on cell growth. To approach this question, several GBM cell lines were infected, as described. Starting with 2 * 10^6 cells, the cell numbers were determined after 2, 4 and 6 days of selection using a FACSCalibur. A fraction of the samples was also tested for successful HIPK2 knockdown after 4 days of selection (Fig. 4.1.6.3).

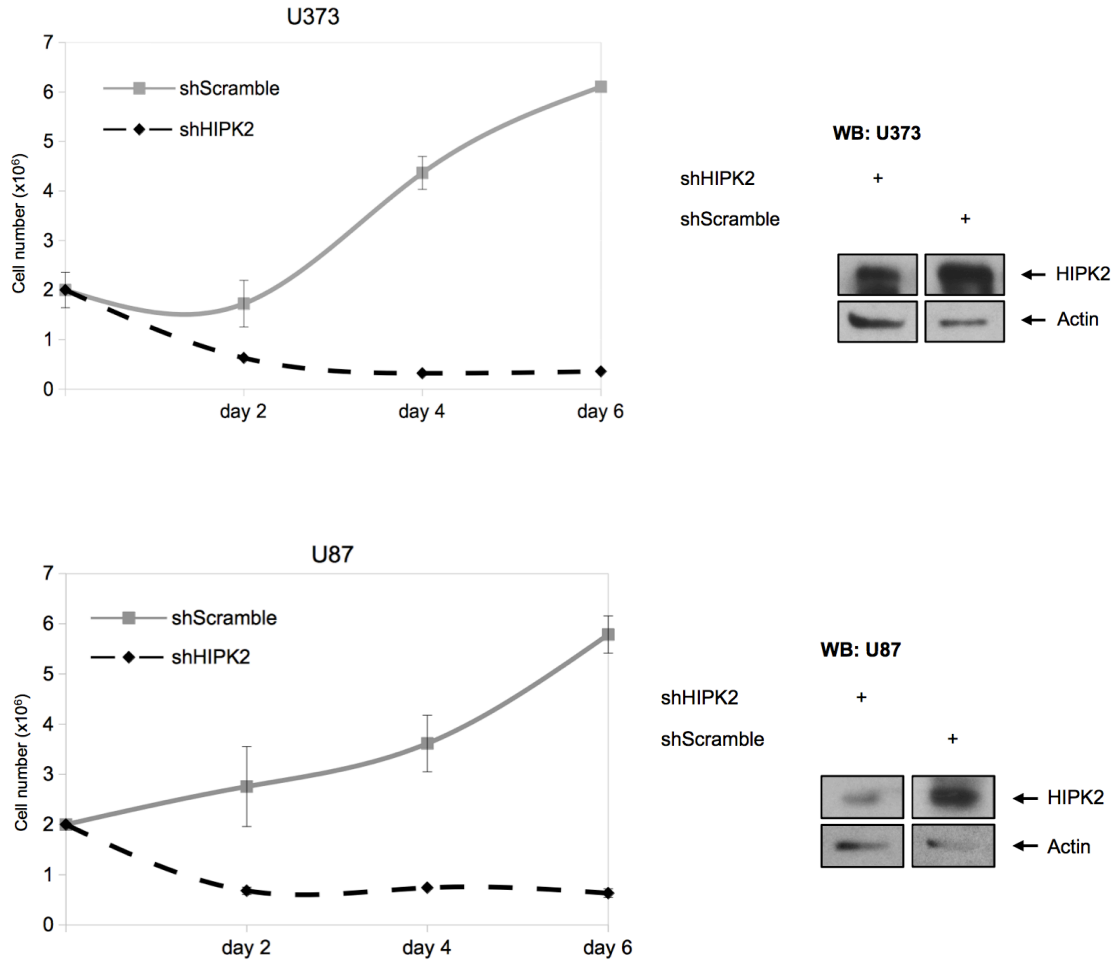

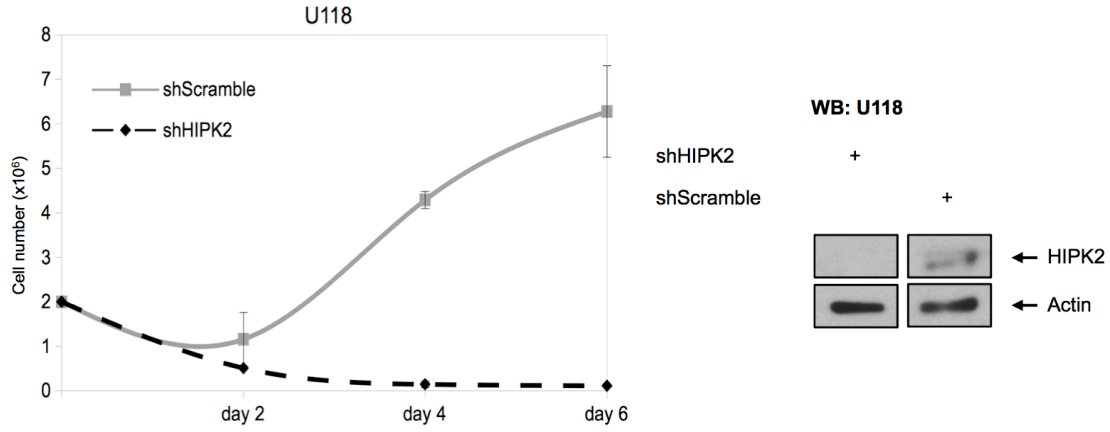

Figure 4.1.6.3: Knockdown of HIPK2 expression inhibits the proliferation of GBM cells. U373, U87 and U118 cells were infected with shHIPK2 and shScramble. Cells were counted at two-day intervals with FACS over 6 days. The black interrupted line represents the cells upon HIPK2 knockdown. The grey solid line shows the negative control upon infection with shScramble. Western Blot analysis during the fourth day was performed to show the knockdown success.

Total knockdown of HIPK2 was only achieved in U118 cells, which already expressed only little amounts of the protein, whereas HIPK2 could be strongly down regulated in U87 cells, but not in U373 cells. Although the HIPK2 levels were down regulated only in two cell lines, the proliferation experiment showed decreased cell numbers in all three GBM cell lines. The drop in shScramble transfected cells after 2 days is most likely due to killing of non-transfected cells.

4.2 Functional analysis of HIPK2 mutants

4.2.1 HIPK2 mutations in cancer

Oncogenic mutations of HIPK2 are rare, but some HIPK2 mutations were described in multi-dimensional and comprehensive characterization studies [144-146]. The analysis of the cbioportal.org showed no mutation hot spot in HIPK2, and a rather distributed occurrence of oncogenic mutations. Four of these mutations are located in regions of potential functional relevance and are displayed in figure 4.2.1.

A

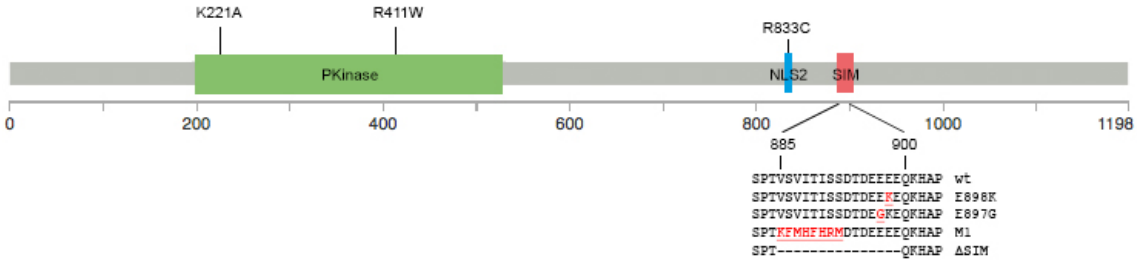

B

Cancer Study	AA change	Region	Cancer type
GBM (TCGA 2013)	R411W	PKinase	Glioblastoma multiforme
GBM (TCGA 2013)	E897G	SIM	Glioblastoma multiforme
ccRCC (TCGA)	E898K	SIM	Kidney renal Clear Cell Carcinoma
CCLE	R833C	NLS2	Breast cancer

Figure 4.2.1: Mutations of HIPK2 in cancer. (A) The distribution of 4 oncogenic mutations chosen for further analysis in HIPK2 is shown. They occur in the kinase domain (HIPK2 R411W), SIM (HIPK2 E897G and E898K), and NLS2 region (HIPK2 R833C). (B) While HIPK2 R411W and E897G mutations were described in GBM, E898K was found in kidney carcinoma and R833C in breast cancer.

Four mutations were focused on in the following experiments. The Cancer Genome Atlas (TCGA) described two interesting mutations: HIPK2- R411W, (PKinase) and E897G (SIM) in GBM [144] and further, an amino acid change of Kidney Carcinoma at HIPK2 E898K (SIM) [146]. The last focus was set on the HIPK2 R833C spot (NLS2) from The Cancer Cell Line Encyclopedia, which was shown to be altered in breast cancer [145]. The mutation spots are illustrated in Figure 4.2.1. (A), including the K221A, ΔSIM and M1 mutant, which were also examined.

4.2.2 Construction of HIPK2 mutants and test expression

Point mutations were introduced in vector encoding the Flag-tagged wild-type HIPK2 protein using the Quickchange kit. The success of the mutagenesis was confirmed by sequencing. The mutation spots are shown in figure 4.2.2. (A). The mutants were also used for test expression in HEK-293T cells.

All mutants were well expressed at the expected molecular weight (Fig. 4.2.2. (B)). These experiments also suggest the intact kinase activity of the oncogenic point mutants, as the autophosphorylation (resulting in a retarded band) was seen for all of the mutants, as opposed to the K221A kinase-dead mutant which migrated faster due to missing autophosphorylation [147].

Figure 4.2.2: Test expression of HIPK2 mutants. (A) Four point mutations of HIPK2 were constructed in order to examine the biological effects of each. The results of the sequencing show the success of the mutagenesis. The bases and amino acids of interest are highlighted in red. (B) The indicated HIPK2 mutants were expressed in 293T cells and analyzed by Western blotting using Flag antibodies. The position of the unphosphorylated and autophosphorylated HIPK2 forms is shown.

4.2.3 Interaction of HIPK2 mutants with SUMO1

The SUMO interaction motif (SIM) of HIPK2 is able to bind SUMO proteins and plays an important role for the localization of HIPK2 in nuclear speckles [99]. It is further relevant in the interaction with PML and Pc2 [148]. Since two mutants—E897G and

E898K—are located in the SIM, it is likely to check the SUMO1 binding ability of the HIPK2 mutants.

To test whether the oncogenic point mutations affect the ability to bind to SUMO1, GST pulldown experiments were performed. First, the GST-SUMO1 fusion protein and the GST control protein were expressed and purified from *E.coli*. Next, the pulldown was performed with the lysates of the Flag-tagged mutants and analyzed by Western blot using a specific Flag antibody. The HIPK2 ΔSIM mutant, who is lacking SIM region, was used as a negative control and wt Flag-HIPK2 was included as a positive control.

The HIPK2 point mutants E897G and E898K retained their ability to interact with SUMO1 (Fig. 4.2.3), although both mutants are located in the SIM region (aa 884-908) of HIPK2. This indicates that single alterations of amino acids in the middle of the SIM region do not affect SUMO1 binding abilities.

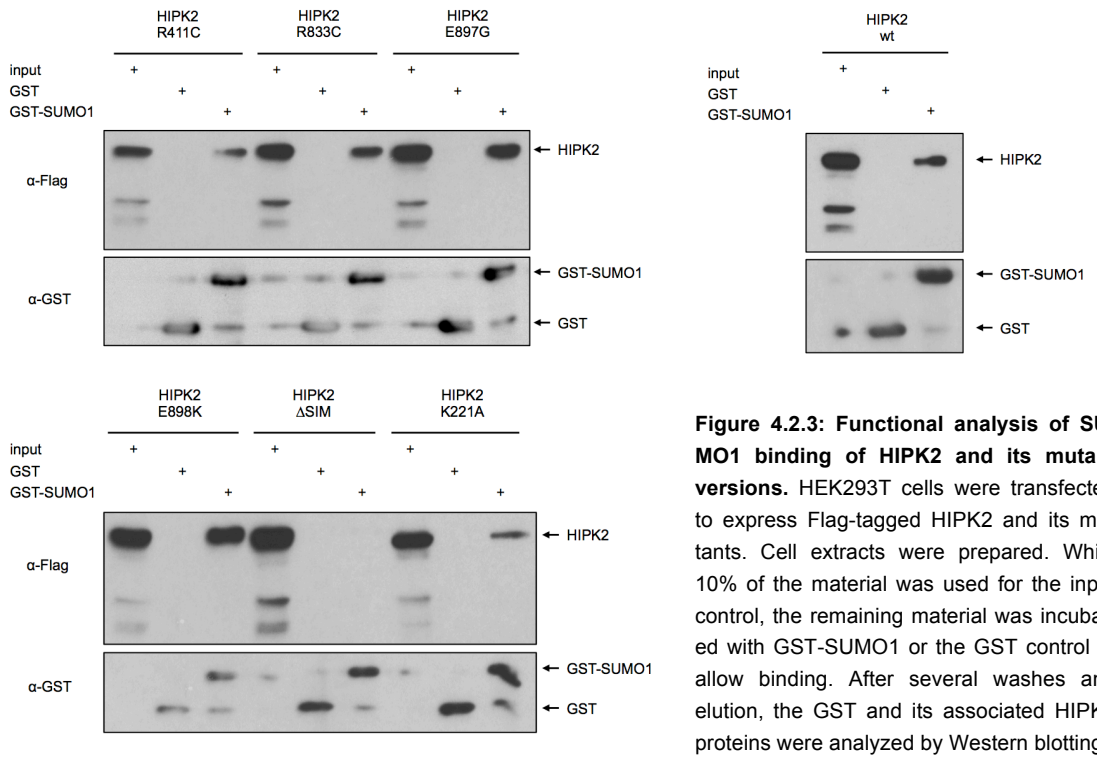

Figure 4.2.3: Functional analysis of SUMO1 binding of HIPK2 and its mutant versions. HEK293T cells were transfected to express Flag-tagged HIPK2 and its mutants. Cell extracts were prepared. While 10% of the material was used for the input control, the remaining material was incubated with GST-SUMO1 or the GST control to allow binding. After several washes and elution, the GST and its associated HIPK2 proteins were analyzed by Western blotting.

4.2.4 Interaction of HIPK2 mutants with PIN1

The phospho-specific isomerase PIN1 is binding to autophosphorylated HIPK2 [149]. It inhibits HIPK2 polyubiquitination and leads to a decrease of proteasomal degradation processes, thus modulating HIPK2 and Siah-1 interaction [104]. In order to investigate whether the mutant R411W in the protein kinase region of HIPK2 affects the interaction with PIN1, a GST-pulldown experiment was performed using GST-PIN1. GST pull-

down experiments showed PIN1 binding by the HIPK2 mutants R826C, E890G, E891K and ΔSIM). In contrast, the HIPK2 K221A negative control showed as expected almost no interaction and the mutant and HIPK2 R411W showed a significantly impaired binding (Fig. 4.2.4). This finding suggests that R411W retains a residual kinase activity, although being less active than the wild-type kinase.

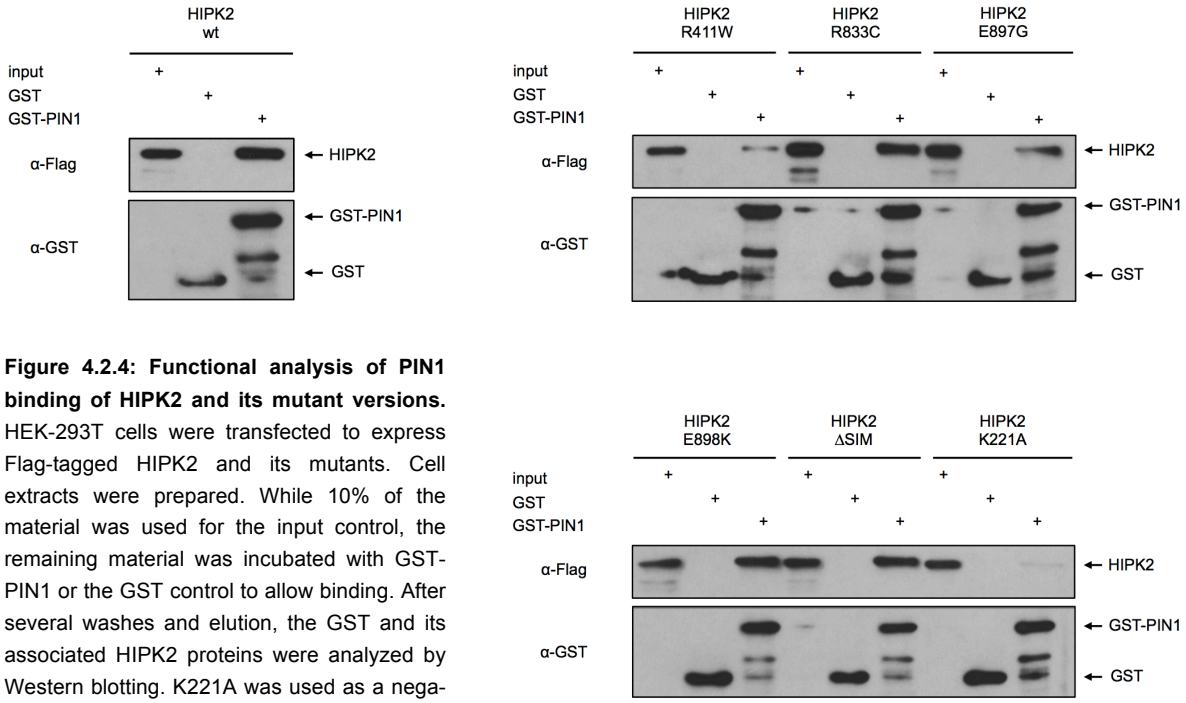

Figure 4.2.4: Functional analysis of PIN1 binding of HIPK2 and its mutant versions. HEK-293T cells were transfected to express Flag-tagged HIPK2 and its mutants. Cell extracts were prepared. While 10% of the material was used for the input control, the remaining material was incubated with GST-PIN1 or the GST control to allow binding. After several washes and elution, the GST and its associated HIPK2 proteins were analyzed by Western blotting. K221A was used as a negative, wild-type (wt) as a positive control.

4.2.5 Enzymatic kinase activity of HIPK2 mutants

To test the kinase activity of the oncogenic HIPK2 mutants, several [87, 150] HIPK2 mutants were co-transfected with Flag tagged version of the HIPK2 substrate protein MEF2D, which is a substrate of HIPK2. Cell lysates were prepared and analyzed by Western blotting. All mutants retained the ability to phosphorylate the substrate protein MEF2D, as visible by the occurrence of a phosphorylated and slower migrating MEF2D band. The results indicate that none of the mutants, including the mutation HIPK2 R411W, affects the enzymatic activity of HIPK2 (Fig. 4.2.5).

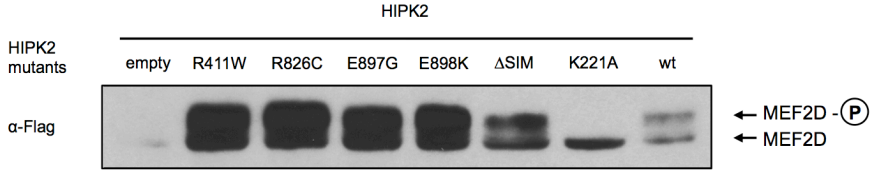

Figure 4.2.5: Enzymatic activity of HIPK2 mutants. After co-transfection of HIPK2 mutants with Flag-MEF2D, cells were lyzed and headed to Western Blot using α-Flag antibody. Kinase dead mutant HIPK2 K221A serves as a negative control and HIPK2 wt as a positive control.

4.2.6 Subcellular localization of HIPK2 mutants

HIPK2 is a protein that is mostly located in subnuclear speckles [99, 101]. Through a SUMO interaction motif (SIM), it is able to bind three isoforms of SUMO (1–3), while only SUMO1 is binding covalently [151-153]. This posttranslational modification and also an intact SIM are required for the localization of HIPK2 in subnuclear speckles [101] [99]. Since two of the mutations are found in the SIM area (HIPK2 E897G, HIPK2 E898K), it was interesting to test their influence on the subcellular localization of HIPK2. In addition, I testes the intracellular localization of the HIPK2 R833C mutant that is found in NLS2. To test the intracellular localization of HIPK2 and its mutants, U2OS osteosarcoma cells were transiently transfected to express several constructs Flag-tagged HIPK2 variants. After two days, cells were analyzed by immunofluorescence using Flag antibodies. 100 transfected cells were randomly chosen for the analysis of the intracellular localization of each mutant. Samples were blinded and localization was categorized as displayed in figure 4.2.6. A. Cells were categorized in four groups: HIPK2 in a) nucleus with speckles, b) nucleus without speckles, c) entire cell with speckles and d) entire cell without speckles. In collaboration with Anita Höland from the statistical institute “Arbeitsgruppe Medizinische Statistik” in Gießen a Chi-square test was performed to determine statistical independency, representative results are shown in figure 4.2.6. B. The results are shown in table 2.

Table 2: Subcellular localization of HIPK2 and its mutants

	Subcellular localization	Significance
HIPK2 wt	39,4 % of P1	p < .001
HIPK2 ΔSIM	34,6 % of P2	p = .036
HIPK2 K221A	67,6 % of P1	p < .001
HIPK2 E897G	45,4 % of P1	p < .001
HIPK2 E898K	49,5 % of P4	p < .001
HIPK2 R833C	52,9 % of P4	p < .001

Table 2: Subcellular localization of HIPK2 mutants. The percental distribution of subcellular localization for HIPK2 and its mutants is shown. Four different possible localizations (P1-P4) are evaluated as according to figure 4.2.6. (A). The distribution was determined with a Chi-square test. The significance is shown as p-value.

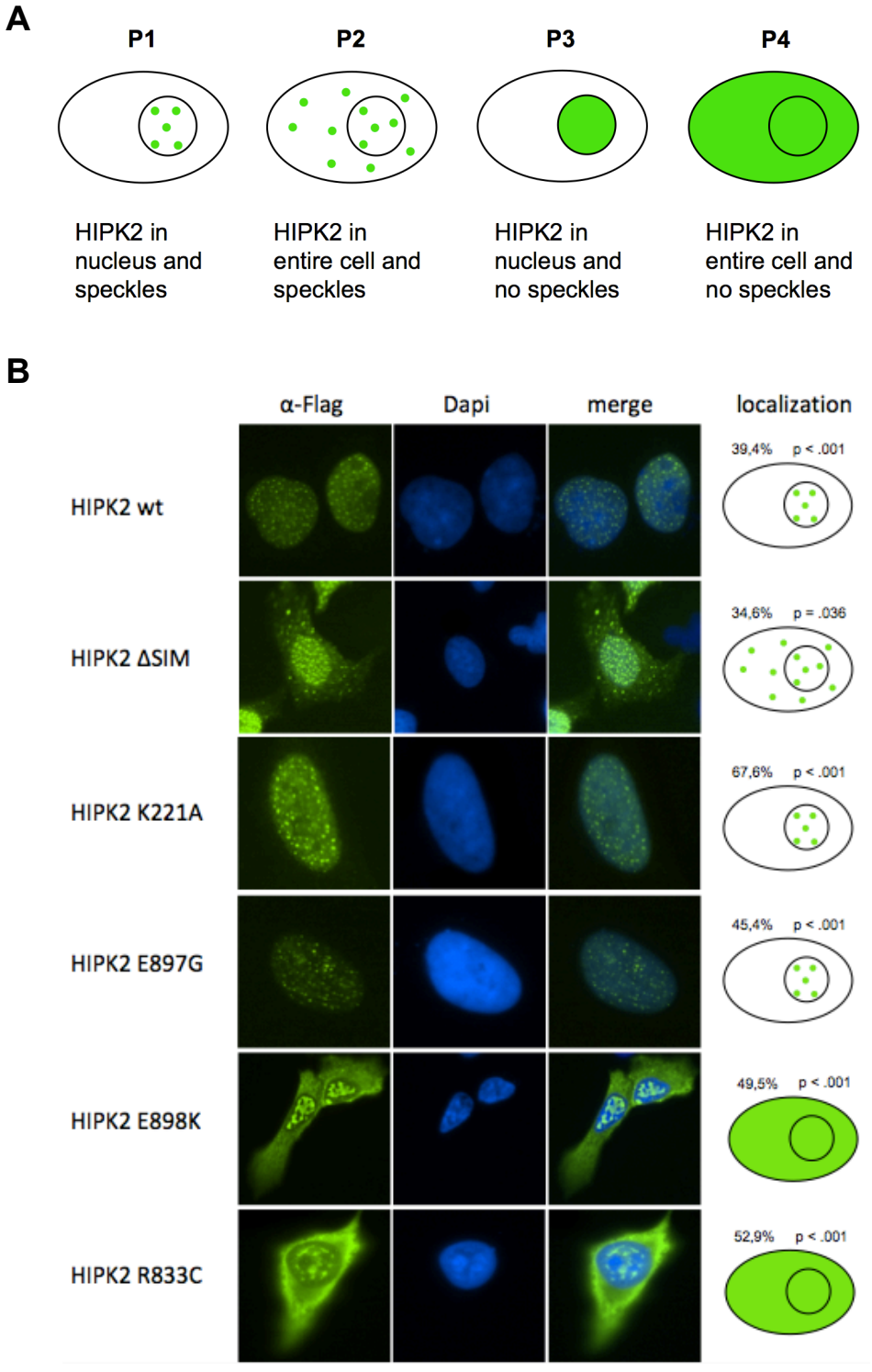

Figure 4.2.6: Subcellular localization of HIPK2 mutants. (A) Schematic representation of four different possible cellular localizations (P1-P4) of HIPK2. (B) U2OS cells were transfected to express the indicated HIPK2 proteins and analyzed by immunofluorescence. Nuclear DNA was stained with Dapi and is shown in blue. Green tags represent Flag-HIPK2. 200 cells were blindly evaluated and the percental distribution was evaluated in which the most common cellular localization is shown on the right. The p-value represents the statistical significance.

5 Discussion

Applied medicine helps people to live much longer than they did in the past. But older organisms have a statistically increased risk to undergoing the inactivation of tumour-suppressors or the activation of proto-oncogenes through genetic and epigenetic mechanisms, resulting in the neoplastic transformation of cells [154]. This development increases the incidence of cancer, which is a new challenge for medical research. The progress in fundamental molecular biological research over the past years has been crucial for a great deal of achievements in tumour therapy. A milestone in this development is the characterization of the oncogenic fusion protein BCR-ABL1 and the construction of its inhibitor, Imatinib. Many patients with chronic myeloid leukemia (CML) and gastrointestinal stromal tumours (GIST) have benefited from this therapy. Modern attempts focus on the construction of monoclonal antibodies, which have been specifically designed to target certain antigens on tumour cells. Some of the examples are: Rituximab targeting CD20 in Non-Hodgkin's lymphoma, Trastuzumab targeting ERBB2 in breast cancer, or Ipilimumab targeting CTLA4 in metastatic melanoma [155]. These developments would not have been possible without the precise characterization of disease-causing molecular events. Even though GBM is the most lethal brain tumour, we do not know much about its intracellular alterations and thus cannot choose the potential candidates for modern drug therapies. In order to identify more factors involved in gliomagenesis, this study focuses on the tumour suppressor HIPK2, which is strongly expressed in the brain and neurons [90] and, which plays an important role in apoptosis, cell cycle regulation and DNA damage responses [156].

5.1 The expression of HIPK2 is dysregulated in GBM

Various studies have shown a dysregulated HIPK2 in neoplastic thyroid carcinoma, breast cancer, and well-differentiated thyroid carcinoma, as well as in pilocytic astrocytoma [127]. My experiments have revealed a highly dynamic HIPK2 expression in various GBM cell lines.

Performing semi-quantitative Western blot experiments, I could show strong variations in HIPK2 protein levels in GBM cell lines. As the cultivation of healthy human astrocytes is difficult, the expression levels were compared with non-GBM cell lines (HeLa and 293T cells). The relative expression of HIPK2 protein was quite variable. In direct comparison to HeLa cells, U118 and G55 cell lines show reduced HIPK2 levels, while most of the GBM cell lines (82 %) exhibit an increased HIPK2 expression (Fig. 4.1.1.2).

This finding corresponds to the finding in Grade I brain tumours (pilocytic astrocytoma), where an overexpression of endogenous HIPK2 was described [126]. Deshmukh et al. (2008) have also performed statistical analysis with primary cells and detected an overexpression of HIPK2 in only 23 % of Grade III (anaplastic astrocytoma) tumours and in 27 % of Grade IV (GBM) tumours [126]. There are three possible explanations for these divergent findings between the results of my study and the results obtained by Deshmukh et al.:

1) Deshmukh et al. have used primary cell lines for their studies. Primary cells can show a different behaviour than that of the cultivated cell lines, which undergo a continuous changing process during subcultivation [157].

2) In contrast to this study, where GBM cells have been compared to HeLa (cervix carcinoma) and 293T (human embryonic kidney) cells, Deshmukh et al. have compared GBM glial cells with non-malignant, healthy brain tissue.

3) Since the sub-classification of GBMs can also be amended by the inclusion of molecular markers [158], I might have investigated different subtypes than those handled by Deshmukh et al. Therefore, the complexity of GBM demands a higher degree of sub-classification. A promising approach can be seen in Verhaak et al. (2010), who have identified clinically relevant subtypes of GBM by including the expression patterns of EGFR, IDH1, NF1, and PDGFRA [10]. However, a confounding factor is the further evolution of subtypes that can change to other subtypes [158]. It would be interesting to see whether HIPK2 expression levels can be helpful in the classification of different GBM subtypes.

In principle, the dynamic HIPK2 expression can be attributed to different mechanisms including genomic changes, such as gene amplification and LOH, as well as to transcriptional, post-transcriptional, translational and post-translational events.

5.2 Mechanisms of HIPK2 dysregulation in GBM

To investigate the molecular mechanisms of the HIPK2 dysregulation in GBM, I explored different steps of protein synthesis.

The first mechanism that I found was an amplification of the HIPK2-encoding locus. The results from SNP array experiments showed an amplification of the *Hipk2* gene in a locus spanning from 7q32-7q35 in U373 cells and 7q31-7q35 in U118 cells including the *Hipk2* locus at 7q34 (Fig. 4.1.5). An additional FISH experiment is further needed to identify the exact karyotype. Since the B-Raf gene is also located in the amplified genomic region at 7q34, it is possible that B-Raf-derived signaling cascades contribute to

the oncogenic transformation of these cell lines [159]. However, this coincidence could be the reason-apart from pilocytic astrocytoma [126, 127] - that the HIPK2 locus was neglected in the past. A copy number gain of *Hipk2* has been described in a study, where 41 out of 63 patients with Grade I tumours (pilocytic astrocytoma) showed *Hipk2* amplifications [126].

The next step in protein synthesis is the transcription of DNA into mRNA and therefore the mRNA expression was investigated with qPCR experiments. The relative mRNA expression in GBM cells showed significantly, around fivefold, increased HIPK2 mRNA levels in two out of nine GBM cell lines (U373 and U118) than in to other GBM and the HeLa and 293T control cell lines (Fig. 4.1.2). Since the *Hipk2* locus was amplified in U373 cells, this could be a reasonable explanation for its increased mRNA levels. Increased *Hipk2* mRNA levels have also been described in low Grade I tumours, and a linear correlation between the *Hipk2* gene amplification and the increased mRNA levels in the same tumour was shown as well [126].

Protein stability experiments have shown that HIPK2 protein is highly unstable in U118 and Ln229 cells, as the protein was absent already two hours after the inhibition of protein translation (Fig. 4.1.3.1). In the course of CHX experiments, I noted two HIPK2-reactive bands in extracts prepared from detached cells (Fig. 4.1.3.2). These products may represent degraded the HIPK2 products of dying or dead cells in the supernatant. The quantity of these two bands is higher after eight hours and diminishes 24 hours after CHX treatment-this reflects the fact that the floating cells are already dead at the late time point.

In brief, dysregulation and a high volatility of HIPK2 levels were found in different GBM cell lines. This study shows that different molecular mechanisms account for the variability in the HIPK2 expression.

To illustrate the “multiform” aspect of glioblastoma multiforme, I will exemplary show the dysregulation of HIPK2 by the two varying GBM cell lines U373 and U118 (Table 3).

- U373 cells exhibit an amplified *Hipk2* locus, increased HIPK2 mRNA, increased HIPK2 protein levels and unaffected protein stability. It is reasonable to suppose that the amplified *Hipk2* locus leads to increased HIPK2 mRNA and thus protein levels.
- U118 cells also show increased HIPK2 mRNA, but relatively low HIPK2 protein levels and increased HIPK2 protein degradation. The *Hipk2* locus was not investigated in U118 cells: however I assume it to be of the wild-type.

Table 3: Dysregulation of HIPK2 in U373 and U118 cells

	U373	U118
Hipk2 locus	7q34+	n.D.
HIPK2 protein amount	↑↑	↓↓
HIPK2 mRNA amount	↑↑	↑↑
HIPK2 protein stability	↔	↓↓

Table 3: Dysregulation of HIPK2 in U373 and U118 cells.

Hipk2 amplified in U373 cells and not determined (n.D.) in U118 cells.

↑↑ = highly upregulated

↓↓ = highly downregulated

↔ = no dysregulation

The increased protein degradation in U118 likely accounts for the reduced levels of the endogenous HIPK2 protein. It will be interesting to investigate whether impaired HIPK2 protein levels would lead to a compensatory induction of *Hipk2* transcription (Fig. 5.1.1). Similarly, the stability of HIPK2 mRNAs could be altered in U118 cells and other GBM cell lines. Further experiments are needed to address these questions.

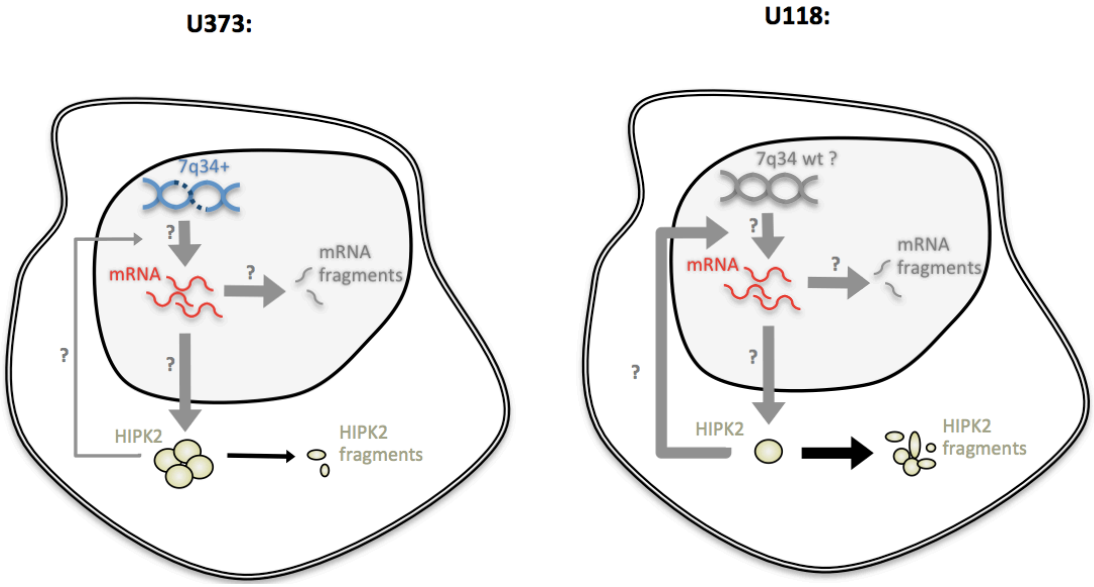

Figure 5.1: Two possible mechanisms leading to HIPK2 dysregulation in U373 and U118 cells. The amplified HIPK2 region in U373 cells might lead to increased mRNA and thus protein levels of HIPK2. In U118 cells however, decrease in protein stability leads to low levels of HIPK2 protein, which might induce the transcription of *Hipk2* and thus could explain the increased mRNA expression.

Another interesting observation is the fact, that the *Hipk2* gene locus is amplified in U87 as well as in U373 cells (Fig. 4.1.5. (B), but only U373 cells seem to express higher HIPK2 mRNA and protein levels when compared to U87 cells (Fig. 4.1.1.2 and Fig. 4.1.2. (A). In the following, I will discuss two explanations for this observation:

1) The p53 status of the cells: The investigated cell line U373 was shown to express mutant p53 (Arg272Gln), whereas U87 cells exhibit the wild-type p53 [1]. It was also shown that expression of the endogenous mutant p53 in SNB19 and U373 GBM cell lines have an impact on cell survival and may lead to increased colony formation [163]. Usually, p53 is an inducible protein that accumulates in the cells after DNA damage [164]. The mutant p53 shows an impaired autoregulation with its negative regulators like Mdm2 and accordingly leads to the accumulation of the mutant p53 even in unstressed cells [165]. Since evidence increasingly indicates an influence of the mutant p53 on the gene expression [166, 167], it would be interesting to investigate whether the transcription of *Hipk2* is affected directly or indirectly from the mutant p53. It is conceivable, that the oncogenic effects of the mutant p53 can be partly mediated through the dysregulation of HIPK2 protein levels or direct protein-protein interactions.
2) As HIPK2 protein levels are controlled by different steps necessary for its synthesis and also decay, so-far unknown and uninvestigated regulatory steps may account for differential protein levels. For example: The dysregulation of proteins that can interact with HIPK2 and influence its stability has already been described in the literature [168]. It would be interesting to investigate further E3-ligases, such as Siah-1 and Siah-2, in the context of HIPK2 dysregulation and GBM.

Taken together, GBM cells seem to have highly divergent levels of the HIPK2 protein. Even though HIPK2 amounts are strongly variable in various cell lines, different mechanisms contribute to the HIPK2 dysregulation in GBM. These results also put a cautionary note on many deep-sequencing and genome-wide association studies [169] that describe only the genomic levels of potential tumour regulators. My results show that high mRNA levels do not necessarily correlate with high protein levels and *vice versa*. Since proteins are responsible for cellular and extracellular functions, it is necessary to investigate changes at the genomic as well proteomic levels. The following figure summarizes the results of my experiments (Fig. 5.1.3).

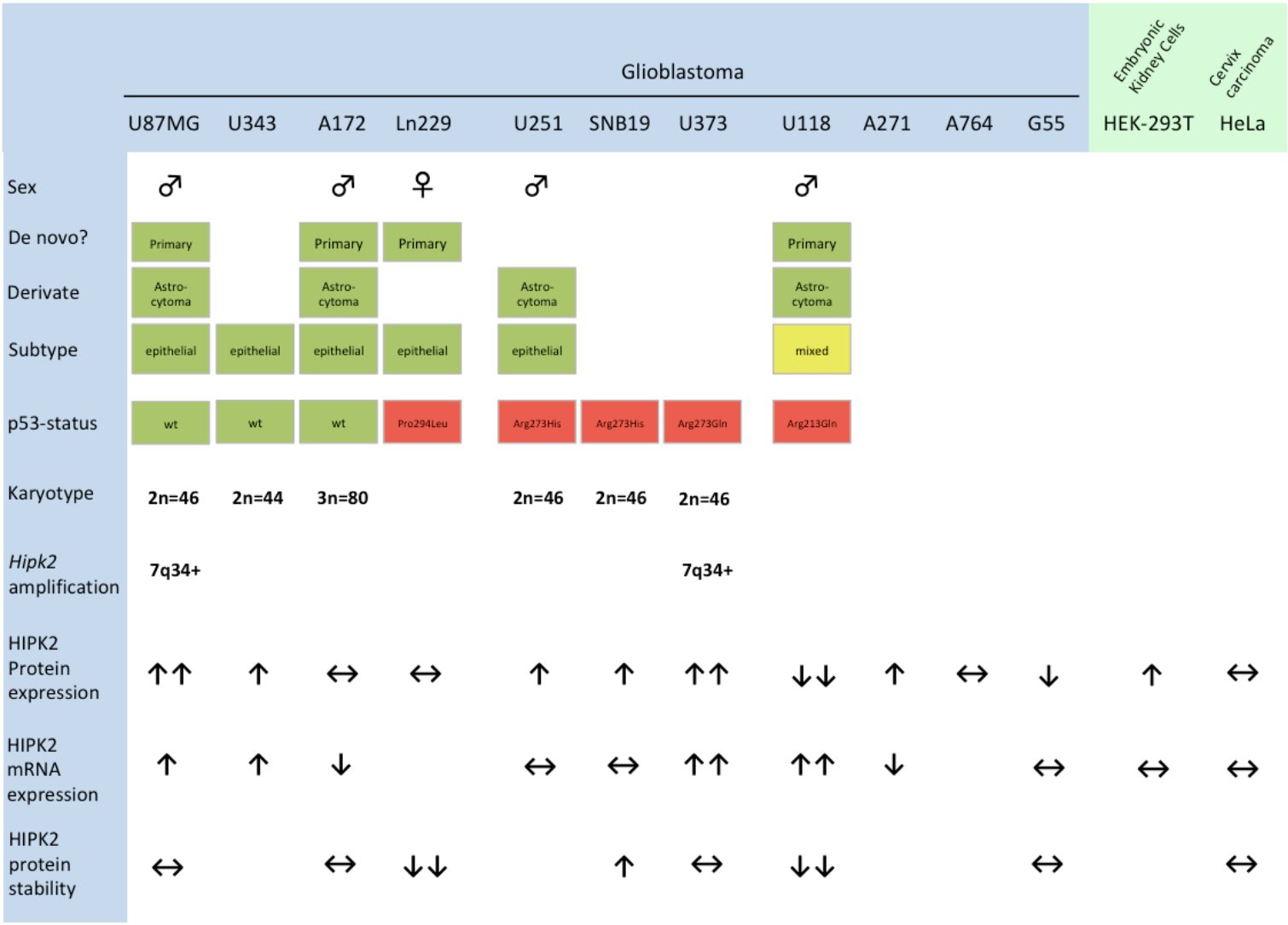

Figure 5.2: Schematic summary of the results. The information concerning sex, primary or secondary GBM, derivate, and subtype were retrieved from ATCC.org. Further information about their p53 status and karyotpe was obtained from different sources [1-4]. This study revealed HIPK2 gene amplifications, protein expression, mRNA expression and protein stability. One Arrow up means upregulated, two arrows up means highly upregulated, arrow down means downregulated and neutral arrow means no dysregulation. HeLa cells were used as reference point for neutral expression patterns.

5.3 The role of HIPK2 in GBM cell proliferation

In the literature, HIPK2 has been postulated as a tumour suppressor [170]. Its knockout in Hipk2$^{-/-}$ mice mutants can lead to cancer development, cancer progression, increased tumour formation, metastatic potential and resistance to chemotherapy[120, 171]. In this study, the functional role of HIPK2 was studied by determining the proliferation of cells after the knockdown of HIPK2. The lentiviral knockdown of HIPK2 in U373, U87 and U118 cell lines led to a massive collapse of cell proliferation (Fig. 4.1.6.2). The impact of HIPK2 deficiency on cell viability occurs already two days after the transfection of the shRNA encoding plasmid. While HIPK2 knockdown abolishes the proliferation of U373 and U118 cell lines, its impact on cell proliferation was less severe in U87 cells: Around 500,000–1 million U87 cells survived the knockdown treatment. These findings show that HIPK2 knockdown has differential effects on the various cell lines tested.

The differential effects of HIPK2 on cell proliferation and viability could be due to several reasons.

Most of the cells in this study could not fully reach HIPK2 knockdown, whereas the knockout mice described by Isono et al completely lack HIPK2 [89]. It is possible that decreased levels of HIPK2 protein might harm the cell and cause apoptosis [97, 101], while the complete lack of HIPK2 is compensated by other members of the HIPK family [89]. Another paper shows that HIPK2 knockdown increases the increased proliferation of mouse embryonic fibroblast (MEF) cells [149]. The discrepancy could be due to the use of different cells from different species or potential off-target effects of the shRNA. Further studies are required to clarify the consequences of HIPK2 knockdown in a systematic manner.

a) Isono et al. (2006) have shown that *Hipk2* deficient mice had no relevant deficits [89]. But a few methodical differences with my study can be found. Isono et al. have performed a knockout and worked with a mouse model. I did a lentiviral knockdown, treated cell lines and focussed on human GBM. So, species-specific differences and differences in the knockout or knockdown response between mice and human cannot be excluded.

b) Furthermore, by considering that some GBM cell lines overexpressed endogenous HIPK2 and amplified *Hipk2*, it could be possible that HIPK2 plays an additionally independent role in GBM tumour-biology. Several studies have also described the amplification of *Hipk2* in low-grade astrocytoma [126, 143, 159]. Further experiments are needed to ascertain if the knockdown specifically affects tumour cells that are addicted to the overexpression of HIPK2 (Fig. 4.1.7).

A reasonable approach could be the complementary use of another method for HIPK2 downregulation. A modern approach is the CRISPR-Cas9 system, which can precisely cleavage at endogenous genomic loci [173]. Also, a negative control with healthy cells should be performed.

Interestingly, U118 cells, which express low basal HIPK2, and U373 and U87 cells expressing high basal levels of HIPK2 failed to survive the treatment with the knockdown vector shHIPK2 (Fig. 4.1.6.3). In contrast, the impact of HIPK2 downregulation on cell survival was only minor in U87 cells, indicating that probably a subset of tumour cells rely on HIPK2-dependent functions.

The differential effects of HIPK2 protein amount variations can be considered with respect to the suggested “optimum model” [174]. This postulated model suggests that a disease can be caused by deviant HIPK2 amounts - either too little or too much. According to this suggestion, only an optimum amount of HIPK2 ensures sufficient function, while higher concentrations of HIPK2 inactivates the protein probably due to misfolding or inactive protein aggregates [174].

5.4 Functional analysis of HIPK2 mutants occurring in tumours

Only a few mutations of HIPK2 have been described. In 2007, two *Hipk2* missense mutations (R868W and N958I) were described in human acute myeloid leukemia cells. These mutants affected their nuclear localization [124]. It is not clear whether mutations in the *Hipk2* gene are relevant for tumourigenesis or a consequence of genomic instability, which is typically observed in tumour cells [175]. Further multidimensional and comprehensive characterization studies of primary GBM cells, kidney renal clear cell carcinoma and breast cancer cells, as summed up on the cancer portal cbioportal.org, were able to find several mutations of HIPK2 [144]. However, these studies have not investigated the effect of the *Hipk2* mutations on the functionality or localization of HIPK2.

In the second part of my work, I investigated the selected *Hipk2* mutations occurring in regions that might affect functional regions including the protein kinase domain, NLS2, and the SIM region. The mutations were reconstructed by mutagenesis, and their functional behaviour was analyzed after the expression in 293T-HEK cells. The results of these experiments can be interpreted in the context of a wild-type control.

The first mutation, which I examined, was HIPK2 R411W. This mutation has been described in GBM and is located in the protein kinase domain [144]. In the following, I will discuss the investigated effects of HIPK2 R411W mutation on a) transphosphorylation and b) autophosphorylation.

a) As the protein kinase domain of HIPK2 is necessary for the phosphorylation of several target proteins, such as p53 or MEF2D, it was interesting to check the transphosphorylation abilities of HIPK2 R411W. This was achieved by the co-transfection of miscellaneous HIPK2 mutants with a Flag-tagged MEF2D. Western blotting showed an upshifted band in HIPK2 R411W, which corresponds to a phosphorylated MEF2D protein (Fig. 4.2.5). So, the HIPK2 R411W mutant seemed to retain its MEF2D transphosphorylation abilities.

b) I also investigated the autophosphorylation abilities of HIPK2 R411W. Since the autophosphorylation of HIPK2 was shown to be crucial for PIN1-binding [149], GST-pulldown experiments with GST-PIN1 and several HIPK2 mutants were performed in order to indirectly measure the HIPK2 autophosphorylation capability. Actually, the results showed an impaired HIPK2 R411W and PIN1 binding when compared to the wild-type HIPK2 (Fig. 4.2.4), a reduced autophosphorylation. The interaction between PIN1 and HIPK2 was also shown to stabilize HIPK2 protein and prevent it from degradation [104]. Since I could show alterations in the HIPK2 degradation in GBM (Fig. 4.1.3.1), the mutation of HIPK2 R411W may play a role in HIPK2 protein stability and should be checked especially in GBM cell lines with increased HIPK2 degradation such as U373, Ln229, and U118 (Fig. 4.1.3.1).

My experiments could show that the PIN1 binding ability was partly affected by the HIPK2 R411W mutation (Fig. 4.2.4), indicating reduced autophosphorylation ability. Since HIPK2 and PIN1 binding depends on the autophosphorylation of HIPK2 [104], it can be assumed that the HIPK2 R411W mutant in the kinase region is less active than the wild-type kinase, even tough it remains a residual kinase activity.

The mutants I investigated next were HIPK2 E897G and E898K, which are located in the C-terminal SIM region of HIPK2. Since both mutations are close to each other and were described in two different cancer studies for GBM (E897G) and kidney carcinoma (E898K) [144, 146], this region seemed to be a promising candidate in terms of functional relevance. The SIM region is important for HIPK2 and serves as a docking motif for SUMO proteins and promotes protein-protein interaction networks [176]. SUMO-binding to HIPK2 also plays a role in the subcellular localization of HIPK2 in nuclear speckles [176]. So, I investigated the mutants HIPK2 E897G and E898K relating to a) SUMO1-binding and b) nuclear localization.

a) The binding abilities of the HIPK2 mutants with SUMO1 were determined with GST-pulldown experiments. A mutant lacking the whole SIM region was used as a control. The results could not show any impact of the mutants HIPK2 E897G and E898K on SUMO-binding (Fig. 4.2.3). It seems that the mutation of

only one amino acid in the SIM region is not sufficient to affect the SUMO-binding capability of HIPK2. Interestingly, the literature shows that HIPK2 mutations of the whole range aa 885-892 and 893-899, impair the SUMO1-binding ability [177].

b) The subcellular localization of HIPK2 mutants was determined with immunofluorescence. Therefore, U2OS osteosarcoma cells were transfected with the mutants HIPK2 E897G and E898K. The results showed that most of the HIPK2 E897G mutants could co-localize their HIPK2 in nuclear speckles. However in contrast, the HIPK2 E898K mutants spread their HIPK2 mostly throughout the entire cell (Fig. 4.2.6). Hence, the HIPK2 mutation E898K might impact the subcellular localization of HIPK2, even though its SUMO-binding ability is not impaired (Fig. 4.2.3). This raises the question as to mechanisms other than the SUMO-binding capability could contribute to a mislocalization of the mutant HIPK2 E898K.

The last mutant I examined was HIPK2 R833C, which was described in breast cancer [145]. This mutant is located in the NLS2 region of HIPK2. The literature shows, that HIPK2 has two NLS sequences, namely NLS1 and NLS2 [177]. Only one mutation of an amino acid in NLS2 is needed for inactivation, while two mutations of residues in NLS1 are required. This indicates that NLS2 is more important for the localization of HIPK2 than NLS1. So I hypothesized that the mutant HIPK2 R833C in NLS2 would affect subcellular localization. According to the literature, most of the mutants failed to localize in the nucleus and could be detected throughout the entire cell in nucleoplasma (Fig. 4.2.6). However, a small fraction still could be seen in the nucleus, probably due to an interaction of the SIM region in nuclear speckles.

In summary, the results from this section show that the HIPK2 variants with the examined mutations retain most of their functions, but they do display some differences concerning their intracellular localization (HIPK2 R833C) or PIN1-binding ability (HIPK2 R411W). However, it can be assumed that the observed mutations are likely due to genomic instability rather than a driver for tumourigenesis.

Summary

Glioblastoma multiforme (GBM) is a primary CNS neoplasm and the most common, aggressive and malignant brain tumour in adults. Even though many studies have been performed on its pathological genetics and molecular pathways, there is currently no possible cure. The aim of this study was to investigate the role of the serine/threonine kinase homeodomain interacting protein kinase 2 (HIPK2) in the pathology of GBM. A variety of experimental approaches revealed strong variations in HIPK2 protein expression levels. My work showed that these expression changes are due to a variety of factors including gene amplification (U373 and U87 cells), mRNA expression and protein stabilities. Further proliferation experiments showed that GBM cell lines (U373, U87 and U118 cells) stop growth upon the lentiviral HIPK2-knockdown. These results suggest that at least some GBMs depend on HIPK2 for their proliferation. In parallel, this study analyzed the functional consequences of HIPK2 mutations that were detected in tumour cells. HIPK2 expression vectors carrying these mutations were generated and tested for their localization, kinase activity and for their ability to interact with the SUMO protein and the prolyl isomerase PIN1. No major differences in all these parameters were observed - this suggests that the functional role of HIPK2 in oncogenesis is due to its relative expression levels.

Zusammenfassung

Glioblastoma multiforme (GBM) ist eine primäre Neoplasie des zentralen Nervensystems und der häufigste, aggressivste und bösartigste Gehirntumor beim Erwachsenen. Trotz zahlreicher genetischer, molekularbiologischer Experimente, sowie klinischer Studien, gibt es zurzeit keine Möglichkeit auf Heilung. Das Ziel dieser Studie war es, die Rolle der Serin-Threonin-Kinase Homeodomain interacting protein kinase 2 (HIPK2) in der Pathogenese des GBM zu untersuchen. Die Experimente zeigten insbesondere eine fehlregulierte HIPK2 Proteinexpression und es gelang mir zu belegen, dass diese Fehlregulierung auf unterschiedliche Faktoren, wie Genamplifikation (U373 und U87 Zellen), mRNA-Expression und Proteinstabilität zurückzuführen sind. Weiterhin zeigten Proliferationsexperimente, dass GBM Zelllinien (U373, U87 und U118 Zellen) während eines lentiviralen Knockdowns von HIPK2 aufhören zu wachsen. Diese Ergebnisse lassen vermuten, dass das GBM Wachstum von HIPK2 abhängig ist. Gleichzeitig untersuchte ich die Auswirkungen von HIPK2 Mutationen, die bei Tumorzellen detektiert wurden. Dafür wurden HIPK2 Vektoren generiert, die diese Mutationen enthalten und die Auswirkungen auf die Lokalisation, Kinase-Aktivität und die Interaktionsfähigkeit mit SUMO Proteinen, sowie der Prolyl-Isomerase PIN1 untersucht. Hierbei zeigten sich keine großen Unterschiede in den beobachteten Parametern, weswegen sich die onkogene Rolle von HIPK2 in der relativen Expression vermuten lässt.

List of abbreviations

% (v/v)	Volume/volume percentage
% (w/v)	Weight/volume percentage
5-ALA	5-aminolevulinic acid
A-bomb	Atomic bomb
aa	Amino acid
AD	Alzheimer's disease
Akt	see PKB
AML	Acute myeloid leukemia
AMPKα	AMP-activated protein kinase alpha
APS	Ammonium persulfate
ATCC	American Type Culture Collection
ATRX	Alpha thalassemia/mental retardation syndrome x-linked
BAX	BCL2-associated X protein
BCA	Bicinchoninic acid assay
BRAF	B-raf proto-oncogene
CA	Carcinoma
CCDC	Coiled-coil domain-containing protein
CDK	Cyclin-dependent kinase
CDKN	Cyclin-dependent kinase inhibitor
CHX	Cycloheximide
CIC	Capicua transctiptional repressor
cRNA	Complementary DNA
CT	Computed tomography
CtBP	C-terminal binding protein
CTLA	Cytotoxic T-lymphcyte-associated protein
Da	Dalton
DAXX	Death-domain associated protein
ddH2O	Double-distilled water
dsDNA	Double-stranded DNA
DMEM	Dulbecco's modified eagle medium
DMSO	Dimethyl sulfoxide
DNA	Deoxyribonucleic acid
dsDNA	Double-stranded DNA
DTT	Threo-1,4-dimercapto-2,3-butanediol

DYRK	Dual-specificity tyrosine-phosphorylation regulated kinase
EGF	Epidermal growth factor
EGFR	Epidermal growth factor receptor
ERBB	Erb-b2 receptor tyrosine kinase 2
et al.	et alii (and others)
FACS	Fluorescence activated cell sorting
FUBP	Far upstream element (FUSE) binding protein
GBM	Glioblastoma multiforme
GFP	Green fluorescent protein
GST	Glutathione S-transferase
GTP	Guanosine-5-triphosphate
Gy	Gray
h	hours
H2B	Histone 2B
HIF-1α	Hypoxia inducible factor 1, alpha subunit
HIPK	Homeodomain-interacting protein kinase
HNPCC	Hereditary nonpolyposis colorectal cancer
HPV	Human papillomavirus
IARC	International Agency for Research on Cancer
IDH1	Isocitrate dehydrogenase 1
IPF	Idiopathic pulmonary fibrosis
IPTG	Isopropyl β-D-1-thiogalactopyranoside
IR	Infrared (radiation)
JNK	Janus kinase
L1CAM	L1 cell adhesion molecule
LB	Lysogeny broth
LEF	Lymphoid enhancer-binding factor
LOH	Loss of heterozygosity
MAPK	Mitogen-activated protein kinase
MAPKK	Mitogen-activated protein kinase kinase
MDM2	Mouse double minute 2 homolog
MDS	Myelodysplastic syndrome
MEF2D	Myocyte enhancer factor 2D
MEK	see MAPKK
MGMT	O-6-methylguanine-DNA methyltransferase
miR	microRNA
mRNA	messenger DNA
MRT	Magnetic resonance tompgraphy

mTOR	Mechanistic target of rapamycin
Mut	mutation or mutated
NF- κB	Nuclear factor of kappa light polypeptide gene enhancer B-cells 1
NF1	Neurofibromatosis 1 or neurofibromin 1
NF2	Neurofibromatosis 2
NFKBIA	Nuclear factor of kappa light polypeptide gene enhancer in B-cells inhibitor, alpha
NLS	Nuclear localization signal
NP-40	Nonidet P40
NTP	Nucleoside triphosphate
PA	Pilocytic astrocytoma
PAGE	Polyacrylamide gel electrophoresis
PBS	Phosphate-buffered saline
PC2	Polycomb protein 2
PCAF	P300/CBP-associated factor
PEBP	Phosphatidylethanolamine binding protein
PEI	Polyethylenimine
PEST	peptide sequence rich in proline (P), glutamic acid (E), serine (S) and threonine (T)
PET	Positron emission tomography
PHLDB	Pleckstrin homology-like domain, family b
PI3KCA	Phosphatidylinositol-4,5-bisphosphate 3-kinase, catalytic subunit alpha
PIK3R1	Phosphoinositide-3-kinase, regulatory subunit 1 (alpha)
PIN	Peptidylprolyl cis/trans isomerase, NIMA-interacting
PIP2	Phosphatidylinositol (4,5)-bisphosphate
PIP3	Phosphatidylinositol (3,4,5)-trisphosphate
PKB	Protein kinase b
PKinase	Protein kinase
PML	Promyelocytic leukaemia (nuclear bodies)
PMSF	Phenylmethanesulfonyl fluoride
PTEN	Phosphatase and tensin homolog
PUMA	p53 upregulated modulator of apoptosis
PVDF	Polyvinylidene fluoride
qPCR	Real-time quantitative polymerase chain reaction
Raf	Rapidly accelerated fibrosarcoma (gene)
Ras	Rat sarcoma (gene)
RB1	Retinoblastoma 1
rpm	rounds per minute

RTEL	Regulator of telomere elongation helicase
RTK	Receptor tyrosine kinase
RUNX	Runt-related transcription factor
SCF^{Fbx3}	Skp, Cullin, F-box containing complex, F-box protein 3
SDS	Sodium dodecyl sulfate
shRNA	Short-hairpin RNA
Siah	Siah E3 ubiquitin protein ligase
SIM	SUMO-interacting motif
SMMHC	Smooth muscle myosin heavy chain
SNP	Single nucleotide polymorphism
SPECT	Single-photon emission computed tomography
ssDNA	Single-stranded DNA
STAT	Signal transducer and activator of transcription
SUMO	Small ubiquitin-like modifier 1
Sv	Sievert
TBS-T	Tris-buffered saline and tween
TCGA	The Cancer Genome Atlas
TEMED	N, N, N', N'-Tetramethylethylendiamine
TERT	Telomerase reverse transcriptase
TGF-β	Transforming growth factor, beta 1
TIMP3	Metallopeptidase inhibitor 3
TMZ	Temozolomide
TP53	Tumour protein p53
TSC	Tuberous sclerosis
UTR	untranslated region
UV	Ultraviolet (radiation)
V	Volt
VEGF	Vascular endothelial growth factor
WB	Western blot
WHO	World Health Organization
WIP	Wild-type p53-induced phosphatase
WSB	WD repeat and SOCS boy containing
wt	Wild-type
X-ray	X-radiation

Literature

1. Soussi, T. *Handbook of p53 mutation in cell lines*. 2007.
2. Koo T, C.I., Kim M, Lee JS, Oh E, Kim J, Yun CO, *Negative Regulation-Resistant p53 Variant Enhances Oncolytic Adenoviral Gene Therapy.* Hum Gene Ther, 2012. **23**(6): p. 609-22.
3. Bárbara Meléndez, A.G.a.-C., Yolanda Ruano, Yolanda Campos-Martín, Ángel Rodríguez de Lope, Elisa Pérez-Magán, Pilar Mur, Sofía Torres, Mar Lorente, Guillermo Velasco and Manuela Mollejo, *Copy Number Alterations in Glioma Cell Lines*. Glioma - Exploring Its Biology and Practical Relevance, ed. D.A. Ghosh. 2011.
4. Godbout R, M.J., Dobler KD, Andison R, Matsuo K, Allalunis-Turner MJ, Takebe H, Day RS 3rd, *Lack of expression of tumor-suppressor genes in human malignant glioma cell lines.* Oncogene, 1992. **7**(9): p. 1879-84.
5. Schwartzbaum JA, F.J., Aldape KD, Wrensch M, *Epidemiology and molecular pathology of glioma.* Nat Cln Pract Neurol., 2006. **2**(9): p. 494-503.
6. MF, G., *Classification and pathogenesis of brain tumors*. Brain Tumors. An Encyclopedic Approach, ed. C. Livingstone. 1995, Edinburgh.
7. Bennett AH, G.R., *Excision of a tumor from the brain.* Lancet, 1884. **2**: p. 1090-1091.
8. Cushing H, *The establishment of cerebral hernia as a decompressive measure for inacessible brain tumors.* Surg Gyn & Obstet, 1905. **1**: p. 297-314.
9. Taveras JM, H.G.J., Pool JL, *Should we treat glioblastoma multiforme?* Amer J Roentg, 1962. **87**: p. 473-479.
10. Bailey P, C.H., *A classification of the tumors of the glioma group on a histogenic basis with a correlated study of prognosis*. 1926, Philadelphia, Lippincott.
11. Scherer HJ, *Cerebral astrocytomas and their derivatives.* Amer J Cancer, 1940. **40**: p. 159-198.
12. Scherer HJ, *The forms of growth in gliomas and their practical significance.* Brain 1940. **63**: p. 1-35.
13. Tso CL, F.W., Day A, *Distinct transcription profiles of primary and secondary glioblastoma subgroups.* Cancer Res, 2006. **66**: p. 159-67.
14. Verhaak RG, K.A., Hoadley, Purdom E, Wang V, Qi Y, Matthew D, et al,, *An integrated genomic analysis identifies clinically relevant subtypes of glioblastoma characterized by abnormalities in PDGFRA, IDH1, EGFR and NF1.* Cancer Cell, 2010. **17**(1): p. 98.
15. Quinn T. Ostrom, L.B., Faith G. Davis, Isabelle Deltour, James L. Fisher, Chelsea Eastman Langer, Melike Pekmezci, Judith A. Schwartzbaum, et. al, *The epidemiology of glioma in adults: a "state of the science" review.* Neuro-Oncology, 2014. **16**(7): p. 896-913.
16. David N. Louis, H.O., Otmar D. Wiestler, Webster K. Cavenee, Peter C. Burger, Anne Jouvet, Bernd W. Scheithauer, Paul Kleihues, *The 2007 WHO*

Classification of Tumours of the Central Nervous System. Acta Neuropathol., 2007. **114**(2): p. 97-109.

17. Dubrow R, D.A., *Demographic variation in incidence of adult glioma by subtype, United States, 1992-2007.* BMC Cancer, 2011. **11**: p. 325.
18. Deltour I, A.A., Feychting M, Johansen C, Klaeboe L, Sankila R, Schüz J, *Mobile phone use and incidence of glioma in the Nordic countries 1979-2008: consistency check.* Epidemiology, 2012. **3**: p. 301-7.
19. Ostrom QT, G.H., Farah P, et al., *CBTRUS statistical report: primary brain and central nervous system tumors diagnosed in the United States in 2006 - 2010.* Neuro-Oncology, 2013. **15**(6): p. 1-56.
20. McKinley BP, M.A., Fenstermaker RA, Plunkett RJ, *The impact of age and sex on the incidence of glial tumors in New York state from 1976 to 1995.* J Neurosurg, 2000. **93**(6): p. 932-9.
21. Bondy ML, S.M., Malmer B, et. al, *Brain tumor epidemiology: consensus from the Brain Tumor Epidemiology Consortium.* Cancer Cell, 2008. **113**(7): p. 1953-68.
22. Sadetzki S, C.A., Freedman L, et al., *Long-term follow-up for brain tumor development after childhood exposure to ionizing radiation for tinea capitis.* Radiat Res., 2005. **163**(4): p. 424-432.
23. Prasad G, H.-K.D., *Radiation-induced gliomas.* Expert Rev Neurother, 2009. **9**(1511-17).
24. Pearce MS, S.J., Little MP, et al., *Radiation exposure from CT scans in childhood and subsequent risk of leukaemia and brain tumours: a retrospective cohort study.* Lancet, 2012. **380**(9840): p. 499-05.
25. Mathews JD, F.A., Brady Z, et al., *Cancer risk in 680,000 people exposed to computed tomography scans in childhood or adolescence: data linkage study of 11 million Australians.* BMJ, 2013. **346**.
26. Schoemaker MJ, S.A., Hepworth SJ, et al., *History of allergies and risk of glioma in adults.* Int J Cancer, 2006. **119**(9).
27. Turner MC, K.D., Armstrong BK, et al., *Allergy and brain tumors in the INTERPHONE study: pooled results from Australia, Canada, France, Israel, an New Zealand.* Cancer Causes Control, 2013. **24**(5): p. 949-60.
28. Wigertz A, L.S., Schwartzbaum J, et al., *Allergic conditions and brain tumor risk.* Am J Epidemiol., 2007. **166**(8): p. 941-50.
29. Linos E, R.T., Alonso A, et al., *Atopy and risk of brain tumors: a meta-analysis.* J Natl Cancer Inst., 2007. **99**(20): p. 1544-50.
30. Canniff J, D.A., Foreman NK, Weinberg A., *Cytotoxicity of glioblastoma cells mediated ex vivo by varicella-zoster virus-specific T cells.* J Neurovirol., 2011. **17**(5): p. 448-54.
31. Söderberg-Naucler C, I.J.J., *Cytomegalovirus in human brain tumors: Role in pathogenesis and potential treatment options.* World J Exp Med, 2015. **5**(1): p. 1-10.
32. Goodenberger ML, J.R., *Genetics of adult glioma.* Cancer Genet., 2012. **205**(12): p. 613-21.
33. Liu Y, Z.H., Zhou K, et al., *Tagging SNPs in non-homologous end-joining pathway genes and risk of glioma.* Carcinogenesis, 2007. **28**(9): p. 1906-13.

34. Baan R, G.Y., Lauby-Secretan B, et al., *Carcinogenicity of radiofrequency electromagnetic fields.* Lancet Oncol., 2011. **12**(7): p. 624-26.

35. Benson VS, P.K., Schuz J, et al., *Mobile phone use and risk of brain neoplasms and other cancers: prospective study.* Int J Epidemiol., 2013. **42**(3): p. 792-02.

36. Kim KE, K.K., Kim DC, Park JI, Han JY, *Cytogenetic characterizations of central nervous system tumors: the first comprehensive report from a single institution in Korea.* J Korean Med Sci, 2009. **24**(3): p. 453-60.

37. K Ichimura, D.P., S Kocialkowski, LM Bäcklund, R Chan, DT Jones, VP Collins, *IDH1 mutations are present in the majority of common adult gliomas but rare in primary glioblastomas.* Neuro Oncol., 2009. **11**(4): p. 341-7.

38. J Balss, J.M., W Mueller, A Korshunov, C Hartmann, A. von Deimling, *Analysis of the IDS1 codon 132 mutation of brain tumors.* Acta Neuropathol., 2008. **116**: p. 597-02.

39. A Deimling, A.K., C Hartmann, *The next generation of glioma biomarkers: MGMT methylation, BRAF fusions and IDH1 mutations.* Brain Pathol., 2011(1): p. 74-87.

40. Zhao S, L.Y., Xu W, Jiang W, Xiong Y et al, *Glioma-Derived Mutations in IDH1 Dominantly Inhibit IDH1 Catlytic Activity and Induce HIF-1α.* Science, 2009. **324**(5924): p. 261-265.

41. Dang L, W.D., Gross S, Bennett BD, Bittinger MA, et al, *Center-associated IDH1 mutations produce 2-hydroxygluterate.* Nature, 2009. **462**: p. 739-744.

42. S Turcan, D.R., A Goenka, TA Chan, et al, *IDH1 mutation is sufficient to establish the glioma hypermethylator phenotype.* Nature, 2012. **483**(7390): p. 479-83.

43. KD Aldape, K.B., A Furth, JC Buckner, C Giannini, PS Burger, BW Scheithauer, RB Jenkins, CD James, *Immunohistochemical detection of EGFRvIII in high malignancy grade astroyctomas and evaluation of prognostic significance.* J Neuropathol Exp Neurol., 2004. **63**: p. 700-7.

44. Q-W Fan, C.C., WC Gustafson, E Charron, P Zipper, RA Wong, et al, *EGFR phosphorylates tumor-derived EGFRvIII driving STAT3/5 and progression in glioblastoma.* Cancer Cell, 2013. **24**: p. 438-49.

45. M Huncharek, B.K., *Epidermal growth factor receptor gene amplification as a prognostic marker in glioblastoma multiforme: results of a meta-analysis.* Oncol Res, 2000. **12**(2): p. 107-12.

46. Chen JR, X.H., Yao Y, Qin ZY, *Prognostic value of epidermal growth factor receptor amplification and EGFRvIII in glioblastoma: meta-analysis.* Acta Neurol Scand, 2015.

47. Srividya MR, T.B., Shailaja BC, Arivazhagan A, Thennarasu K, et al, *Homozygous 10q23/PTEN deletion and its impact on outcome in glioblastoma: a prospective translational study on a uniformly treated cohort of adult patients.* Neuropathology, 2011. **31**: p. 376-383.

48. BJ Theeler, W.Y., GN Fuller, et al, *Moving toward molecular classification of diffuse gliomas in adults.* Neurology, 2012. **79**: p. 1917-26.

49. A Chakravarti, G.Z., Y Suzui, et al, *The prognostic significance of phoatidylinositol 3-kinase pathway activation in human gliomas.* J Clin Oncol, 2004. **22**: p. 1926-33.

50. TCGAN, *Comprehensive genomic characterization defines human glioblastoma genes and core pathways.* Nature, 2008. **455**: p. 1061-68.

51. M Bredel, D.S., AK Yadav, et al, *NFKBIA deletion in glioblastomas.* N Engl J Med., 2011. **364**(7): p. 627-37.

52. Z Zhao, X.Z., T Wu, T Yang, G Chen, X Xie, Y Wei, M Ye, Y Zhou, Z Du, *Identification of a NFKBIA polymorphism associated with lower NFKBIA protein levels and poor survival outcomes in patients with glioblastoma multiforme.* Int J Mol Med., 2014. **34**(5): p. 1233-40.

53. CB Knobbe, J.R., G Reifenberger, *Mutation analysis of the Ras pathway genes NRAS, HRAS, KRAS and BRAF in glioblastomas.* Acta Neuropathol., 2004. **108**: p. 467-70.

54. AD Recklies, C.W., H Ling, *The chitinase 3-like protein human cartilage glycoprotein 39 (HC-gp39) stimulates proliferation of human connective-tissue cells and activates both extracellular signal-regulated kinase- and protein kinase B-mediated signaling pathways.* Biochem J., 2002. **365**: p. 119-26.

55. H Ling, A.R., *The chitinase 3-like protein human cartilage glycoprotein 39 inhibits cellular responses to the inflammatory cytokines interleukin-1 and tumour necrosis factor-alpha.* Biochem J., 2004. **380**: p. 651-9.

56. G D'Orazi, B.C., T Bruno et al, *Homeodomain-interacting protein kinase-2 phosphorylates p53 at Ser46 and mediates apoptosis.* Nat Cell Biol, 2002. **4**: p. 11-19.

57. M Schiebe, P.O., W Hoffmann, R Meyermann, HP Rodemann, M Bamberg, *Analysis of MDM2 and p53 gene alterations in glioblastomas and its correlation with clinical factors.* J Neurooncol, 2000. **49**: p. 197-203.

58. D Hanahan, R.W., *Hallmarks of cancer: the next generation.* Cell, 2011. **144**: p. 646-74.

59. D Yin, S.O., N Kawamata, et al, *High-resolution genomic copy number profiling of glioblastoma multiforme by single nucleotide polymorphism DNA microarray.* Mol Cancer Res, 2009. **7**: p. 665-77.

60. DN, L., *The p53 gene and protein in human brain tumors.* J Neuropathol Exp Neurol., 1994. **53**(1): p. 11-21.

61. Kraus JA, G.N., Beck M, Krex D, Klockgether T, Schackert G, Schlegel U, *Molecular analysis of the PTEN, TP53 and CDKN2A tumor suppressor genes in long-term survivors of glioblastoma multiforme.* J Neurooncol, 2000. **48**(2): p. 89-94.

62. Puduvalli VK, K.A., Hess KR, Bondy ML, Fuller GN, Kouraklis GP, Levin VA, Bruner JM, *Patterns of expression of Rb and p16 in astrocytic gliomas, and correlation with survival.* Int J Oncol, 2000. **17**(5): p. 963-9.

63. Furnari FB, F.T., Bachoo RM, Mukasa A, Stommel JM, et al, *Malignant astrocytic glioma: genetics, biology, and paths to treatment.* Genes Dev., 2007. **21**(21): p. 2683-710.

64. Chan JA, K.A., Kosik KS, *MicroRNA-21 is an antiapoptotic factor in human glioblastoma cells.* Cancer Res, 2005. **65**(14): p. 6029-33.

65. Gaur AB, H.S., Colburn NH, Israel MA, *Downregulation of Pdcd4 by mir-21 facilitates glioblastoma proliferation in vivo.* Neuro Oncol., 2011. **13**(6): p. 580-90.

66. Kefas B, G.J., Comeau L, Li Y, Abounader R, Hawkinson M, Lee J, Fine H, Chiocca EA, Lawler S, Purow B, *microRNA-7 inhibits the epidermal growth factor receptor and the Akt pathway and is downregulated in glioblastoma.* Cancer Res, 2008. **68**(10): p. 3566-72.

67. Hayes J, T.H., Tumilson C, Droop A, Boissinot M, Highes TA, Westhead D, Alder JE, Shaw L, Short SC, Lawler SE, *Prediction of clinical outcome in glioblastoma using a biologically relevant nine-microRNA signature.* Mol Oncol, 2015. **9**(3): p. 704-14.

68. M Esteller, J.G.-F., E Andion, SN Goodman, OF Hidalgo, V Vanaclocha, SB Baylin, JG Herman, *Inactivation of the DNA-repair gene MGMT and the clinical response of gliomas to alkylating agents.* N Engl J Med., 2000. **343**(19): p. 1350-4.

69. R Martinez, M.E., *The DNA methylome of glioblastoma multiforme.* Neurobiol Dis., 2010. **39**(1): p. 40-6.

70. HS Friedman, T.K., H Calvert, *Temozolomide and treatment of malignant glioma.* Clin Cancer Res, 2000. **6**(7): p. 2585-97.

71. Tysnes BB, M.R., *Biological mechanisms of glioma invasion and potential therapeutic targets.* J Neurooncol, 2001. **53**(2): p. 129-47.

72. Lakhan SE, H.L., *Difficult diagnosis of brainstem glioblastoma multiforme in a woman: a case report and review of the literature.* J Med Case Rep., 2009. **3**: p. 87.

73. Sanli AM, T.E., Dolgun H, Sekerci Z, *Unusual manifestations of primary Glioblastoma Multiforme: A report of three cases.* Surg Neurol Int., 2010. **1**: p. 87.

74. Larjava S, M.R., Salminen T, Haapasalo H, Raitanen J, Jääskeläinen J, Auvinen A, *Incidence of gliomas by anatomic location.* Neuro Oncol., 2007. **3**: p. 319-325.

75. Matsuda M, O.K., Satomi K, Nakai K, Yamamoto T, Matsumura A *Exophytic Cerebellar Glioblastoma in the Cerebllopontine Angle: Case Report and Review of the Literature.* J neurol Surg Rep, 2014. **1**: p. e67-72.

76. Gessler F, F.M., Dutzmann S, Mittelbronn M, Hattingen E, Franz K, Seifert V, Senft C, *Combination of Intraoperative Magnetic Resonance Imaging and Intraoperative Fluorescence to Enhance the Resection fo Contrast Enhancing Gliomas.* Neurosurgery, 2015.

77. Laperriere N, Z.L., Cairncross G, *Radiotherapy for newly diagnosed malignant glioma in adults: a systematic review.* Radiother Oncol, 2002. **64**(3): p. 259-73.

78. Hart MG, G.R., Rogers G, Stein K, Grant R, *Temozolomide for high grade glioma.* Cochrane Database Syst Rev, 2013. **4**: p. CD007415.

79. Hegi ME, D.A., Gorlia T, et al, *MGMT gene silencing and benefit from temozolomide in glioblastoma.* N Engl J Med., 2005. **352**(10): p. 997-03.

80. Hart MG, G.R., Garside R, Rogers G, Somerville M, Stein K, *Chemotherapeutic wafers for High Grade Glioma.* Cochrane Database Syst Rev, 2008. **3**: p. CD007294.

81. Stupp R, H.M., Gorlia T, et al, *Cilengitide combined with standard treatment for patients with newly diagnosed glioblastoma with methylated MGMT promoter (CENTRIC EORTC 26071-22072 study): a multicentre, randomised, open-label, phase 3 tria.* Lancet Oncol, 2014. **15**(10): p. 1100-8.

82. Chinot OL, W.W., Mason W, Henriksson R, Saran F, et al, *Bevacizumab plus radiotherapy-temozolomide for newly diagnosed glioblastoma.* N Engl J Med., 2014. **370**(8): p. 709-22.

83. Gilbert MR, D.J., Armstron TS, et al, *A randomized trial of bevacizumab for newly diagnosed glioblastoma.* N Engl J Med., 2014. **370**(8): p. 699-708.

84. Sampson JH, H.A., Archer GE, et al, *Immunologic escape after prolonged progression-free survival with epidermal growth factor receptor variant III peptide vaccination in patients with newly diagnosed glioblastoma.* J Clin Oncol, 2010. **28**(31): p. 4722-9.

85. Sepulveda JM, Z.C., Hernandez-Lain A, et al, *Targeting EGFR in glioblastoma: Preclinical testing of dacomitinib.* J Clin Oncol, 2014.

86. M Jhanwar-Uniyal, M.L., M Friedmann, A Kwasnicki, R Murali, *Glioblastoma: Molecular Pathways, Stem Cells and Therapeutic Targets.* Cancers, 2015. **7**: p. 538-555.

87. Kim YH, C.C., Lee SJ, Conti MA, Kim Y., *Homeodomain-interacting protein kinases, a novel family of co-repressors for homeodomain transcription factors.* J Biol Chem., 1998. **273**(40): p. 25875-9.

88. Arai S, M.A., Du K, Yagi K, Okazaki Y, Kurokawa R, *Novel homeodomain-interacting protein kinase family member, HIPK4, phosphorylates human p53 at serine 9.* FEBS Lett., 2007. **581**(29): p. 5649-57.

89. Isono K, N.K., Li Y, Takada Y, Suzuki R, Katsuki M, Nakagawara A, Koseki H, *Overlapping roles for homeodomain-interacting protein kinases hipk1 and hipk2 in the mediation of cell growth in response to morphogenetic and genotoxic signals.* Mol Cell Biol., 2006. **26**(7): p. 2758-71.

90. Zhang J, P.V., Bonasera SJ, Holtzman J, Tang AT; Hellmuth J, Tang S, Janak PH, Ecott LH, Huang EJ, *Essential function of HIPK2 in TGFbeta-dependent survival of midbrain dopamine neurons.* Nat Neurosci, 2007. **10**(1): p. 77-86.

91. Wang Y, H.T., Runkel L, Haaf T, Schaller H, Debatin K, Hug H, *Isolation and characterization of cDNAs for the protein kinase HIPK2.* Biochim Biophys Acta, 2001. **1518**(1-2): p. 168-72.

92. Pierantoni GM, B.A., Pentimalli F, Fedele M, Iuliano R, Santoro M, Chiariotti L, Ballabio A, Fusco A, *The homeodomain-interacting protein kinase 2 gene is expressed late in embryogenesis and preferentially in retina, muscle and neural tissues.* Biochem Biophys Res Commun., 2002. **290**(3): p. 942-7.

93. Zou F, X.J., Fu H, Cao J, Mao H, Gong M, Cui G, Zhang Y, Shi W, Chen J, *Different functions of HIPK2 and CtBP2 in traumatic brain injury.* J Mol Neurosci, 2013. **49**(2): p. 395-408.

94. Valente D, B.G., Moncada A, Tornincasa M, Indelicato S, Piscuoglio S, Karamitopoulou ED, Bartolazzi A, Pierantoni GM, Fusco A, Soddu S, Rinaldo C, *HIPK2 deficiency causes chromosomal instability by cytokinesis failure and increases tumorigenicity.* Oncotarget, 2015.

95. Gresko E, R.A., Ritterhoff S, Vichalkovski A, del Sal G, Schmitz ML, *Autoregulatory control of the p53 response by caspase-mediated processing of HIPK2.* EMBO J, 2006. **25**(9): p. 1883-94.

96. Hofmann TG, M.A., Lichter P, Dröge W, Schmitz ML, *Human homeodomain-interacting protein kinase-2 (HIPK2) is a member of the DYRK family of protein kinases and maps to chromosome 7q32-q34.* Biochimie, 2000. **82**(12): p. 1123-7.

97. Möller A, S.H., Hofmann TG, Rueffer S, Klimczak E, Dröge W, Will H, Schmitz ML, *PML is required for homeodomain-interacting protein kinase 2 (HIPK2)-mediated p53 phosphorylation and cell cycle arrest but is dispensable for the formation of HIPK domains.* Cancer Res, 2003. **63**(15): p. 4310-4.

98. Eoscic A, M.A., Calzado MA, Renner F, Wimmer VC, Gresko E, Lüdi KS, Schmitz ML, *Phosphorylation-dependent control of Pc2 SUMO E3 ligase activity by its substrate protein HIPK2.* Mol Cell, 2006. **24**(1): p. 77-89.

99. de la Vega, F.K., Moreno R, Calzada MA, Geng H, Schmitz ML, *Control of nuclear HIPK2 localization and function by a SUMO interaction motif.* Biochim Biophys Acta, 2010. **1813**(2): p. 293-97.

100. Crone J, G.C., Schultheiss K, Moehlenbrink J, Krieghoff-Henning E, Hofmann TG, *Zyxin is a critical regulator of the apoptotic HIPK2-p53 signaling axis.* Cancer Res, 2011. **71**(6): p. 2350-9.

101. Sung KS, L.Y., Kim ET, Lee SR, Ahn JH, Choi CY, *Role of the SUMO-interacting motif in HIPK2 targeting to the PML nuclear bodies and regulation of p53.* Exp Cell Res, 2011. **317**(7): p. 1060-70.

102. Bitomski N, H.T., *Apoptosis and autophagy: Regulation of apoptosis by DNA damage signalling - roles of p53, p73 and HIPK2.* FEBS J, 2009. **276**(21): p. 6074-83.

103. Puca R, N.L., Givol D, D'Orazi G, *Regulation of p53 activity by HIPK2: molecular mechanisms and therapeutical implications in human cancer cells.* Oncogene, 2010. **5;29**(31): p. 4378-87.

104. Bitomsky N, C.E., Moritz C, Polonio-Vallon T, Sombroek D, Schultheiss K, Glas C, Greiner V, Herbel C, Mantovani F, del Sal G, Peri F, Hofmann TG, *Autophosphorylation and Pin1 binding coordinate DNA damaged-induced HIPK2 activation and cell death.* PNAS, 2013. **5**(110): p. E4203-12.

105. Polonio-Vallon T, K.D., Hofmann TG, *ShaPINg Cell Fate Upon DNA Damage: Role of Pin1 Isomerase in DNA Damage-Induced Cell Death and Repair.* Front Oncol., 2014. **16**(4): p. 148.

106. Zhang XP, L.F., Wang W, *Interplay between Mdm2 and HIPK2 in the DNA damage response.* J R Soc Interface, 2014. **11**(96).

107. Li Q, W.X., Wu X, Rui Y, Liu W, Wang J, Wang X, Liou YC, Ye Z, Lin SC, *Daxx cooperates with the Axin/HIPK2/p53 complex to induce cell death.* Cancer Res, 2007. **67**(1): p. 66-74.

108. Di Stefano V, S.S., Sacchi A, D'Orazi G, *HIPK2 contributes to PCAF-mediated p53 acetylation and selective transactivation of p21Waf1 after nonapoptotic DNA damage.* Oncogene, 2005. **24**(35): p. 5431-42.

109. Zhang Q, Y.Y., Hildebrand J, Frisch SM, Goodman RH, *Homeodomain interacting protein kinase 2 promotes apoptosis by downregulating the transcriptional corepressor CtBP.* Cell, 2003. **115**(2): p. 177-86.

110. Kanei-Ishii C, N.-T.J., Tanikawa J, Nomura T, Ishitani T, Kishida S, Kokura K, Kurahashi T, Ichikawa-Iwata E, Kim Y, Matsumoto K, Ishii S, *Wnt-1 signal induces phosphorylation and degradation of c-Myb protein via TAK1, HIPK2, and NLK.* Genes Dev., 2004. **18**(7): p. 816-29.

111. Hofmann TG, S.N., Schmitz ML, Will H, *HIPK2 regulates transforming growth factor-beta-induced c-Jun NH(2)-terminal kinase activation and apoptosis in human hepatoma cells.* Cancer Res, 2003. **63**(23): p. 8271-7.

112. Lazzari C, P.A., Siepi F, Rinaldo C, Galli F, Gentileschi M, Bartolazzi A, Costanzo A, Sacchi A, Guerrini L, Soddu S, *HIPK2 phosphorylates ΔNp63α and promotes its degradation in response to DNA damage.* Oncogene, 2011. **30**(48): p. 4802-13.

113. Lavra L, R.C., Ulivieri A, Luciani E, Fidanza P, Giacomelli L, Bellotti C, Ricci A, Trovato M, Soddu S, Bartolazzi A, Sciacchitano S, *The loss of the p53 activator*

HIPK2 is responsible for galectin-3 overexpression in well differentiated thyroid carcinomas. PLoS One, 2011. **6**(6).

114. Petroni M, V.V., Prodosmo A, Rinaldo C, et al, *MYCN sensitizes human neuroblastoma to apoptosis by HIPK2 activation through a DNA damage response.* Mol Cancer Res, 2011. **9**(1): p. 67-77.

115. Soubeyran I, M.I., Grigoletto A, Leste-Lasserre T, et al, *Tissue microarray cytometry reveals positive impact of homeodomain interacting protein kinase 2 in colon cancer survival irrespective of p53 function.* Am J Pathol, 2011. **178**(5): p. 1986-98.

116. Bon G, D.C.S., Folgiero V, Avetrani P, Lazzari C, D'Orazi G, et al, *Negative regulation of beta4 integrin transcription by homeodomain-interacting protein kinase 2 and p53 impairs tumor progression.* Cancer Res, 2009. **69**(14): p. 5978-86.

117. Tan M, G.H., Zeng Y, Tao L, Wang J, Jiang J, Xu D, Bao E, Qiu J, Liu Z, *Downregulation of homeodomain-interacting protein kinase-2 contributes to bladder cancer metastasis by regulating Wnt signaling.* J Cell Biochem., 2014. **115**(10): p. 1762-7.

118. Lin J, Z.Q., Lu Y, Xue W, Xu Y, Zhu Y, Hu X, *Downregulation of HIPK2 increases resistance of bladder cancer cell to cisplatin by regulating Wip1.* PLoS One, 2014. **9**(5).

119. Tong Y, L.Q., Xing TY, Zhang M, Zhang JJ, Xia Q, *HIF1 regulates WSB-1 expression to promote hypoxia-induced chemoresistance in hepatocellular carcinoma cells.* FEBS Lett., 2013. **587**(16): p. 2530-5.

120. Wei G, K.S., Ma GK, Saito S, Tang AA, Zhang J, Mao JH, Appella E, Balmain A, Huang EJ, *HIPK2 represses beta-catenin-mediated transcription, epidermal stem cell expansion, and skin tumorigenesis.* Proc Natl Acad Sci U S A., 2007. **104**(32): p. 13040-5.

121. Puca R, N.L., D'Orazi G, *Regulation of vascular endothelial growth factor expression by homeodomain-interacting protein kinase-2.* J Exp Clin Cancer Res., 2008. **27**: p. 22.

122. Muschik D, B.-W.I., Stockfleth E, Rösl F, Hofmann TG, Nindl I, *Cutaneous HPV23 E6 prevents p53 phosphorylation through interaction with HIPK2.* PLoS One, 2011. **6**(11).

123. Wee HJ, V.D., Bae SC, Ito Y, *PEBP2-beta/CBF-beta-dependent phosphorylation of RUNX1 and p300 by HIPK2: implications for leukemogenesis.* Blood, 2008. **112**(9): p. 3777-87.

124. Li XL, A.Y., Harada H, Shima Y, Yoshida H, Rokudai S, Aikawa Y, Kimura A, Kitabayashi I, *Mutations of the HIPK2 gene in acute myeloid leukemia and myelodysplastic syndrome impair AML1- and p53- mediated transcription.* Oncogene, 2007. **26**(51): p. 7231-9.

125. Mao JH, W.D., Kim IJ, Kang HC, Wei G, Climent J, Kumar A, Pelorosso FG, DelRosario R, Huang EJ, Balmain A, *Hipk2 cooperates with p53 to suppress y-ray radiation-induced mouse thymic lymphoma.* Oncogene, 2012. **31**(9): p. 1176-80.

126. H Deshmukh, T.Y., J Yu, *High-resolution, dual-platform aCGH analysis reveals frequent HIPK2 amplification and increased expression in pilocytic astrocytomas.* Oncogene, 2008. **27**(34): p. 4745-51.

127. Yu J, D.H., Gutmann RJ, Emnett RJ, Rodriguez FJ, Watson MA, Nagarajan R, Gutmann DH, *Alterations of BRAF and HIPK2 loci predominate in sporadic pilocytic astrocytoma.* Neurology, 2009. **73**(19): p. 1526-31.

128. Cheng Y, A.-B.M., Wang J, Wei G, Li J, Liang S, Lu X, *Correlation between homeodomain-interacting protein kinase 2 and apoptosis in cervical cancer.* Mol Med Rep, 2012. **5**(5): p. 1251-5.

129. Jin Y, R.K., Chuang PY, Fan Y, Zhong Y, Dai Y, Mazloom AR, Chen EY, D'Agati V, iong H, Ross MJ, Chen N, Ma'ayan A, He JC, *A systems approach identified HIPK2 as a key regulator of kidney fibrosis.* Nat Med., 2012. **18**(4): p. 580-8.

130. Chuang PY, M.M., He JC, *Molecular targets for treatment of kidney fibrosis.* J Mol Med (Berl). 2013. **91**(5): p. 549-559.

131. Ricci A, C.E., Ulivieri A, Lavra L, Sciacchitano S, Scozzi D, Mancini R, Ciliberto G, Bartolazzi A, Bruno P, Graziano P, Mariotta S, *Homeodomain-interacting protein kinase2 in human idiopathic pulmonary fibrosis.* J Cell Physiol., 2013. **228**(1): p. 235-41.

132. Stanga S, L.C., Govoni S, Uberti D, D'Orazi G, Racchi M, *Unfolded p53 in the pathogenesis of Alzheimer's disease: is HIPK2 the link?* Aging (Albany NY), 2010. **2**(9): p. 545-54.

133. Lanni C, N.L., Puca R, Stanga S, Uberti D, Memo M, Govoni S, D'Orazi G, Racchi M, *Homeodomain interacting protein kinase 2: a target for Alzheimer's beta amyloid leading to misfolded p53 and inappropriate cell survival.* PLoS One, 2010. **5**(3).

134. Choi DW, S.Y., Kim EA, Sung KS, Ahn JW, Park SJ, Lee SR, Choi CY, *Ubiquitination and degradation of homeodomain-interacting protein kinase 2 by WD40 repeat/SOCS box protein WSB-1.* J Biol Chem., 2008. **283**(8): p. 4682-9.

135. Winter M, S.D., Dauth I, Moehlenbrink J, Scheuermann K, Crone J, Hofmann TG, *Control of HIPK2 stability by ubiquitin ligase Siah-1 and checkpoint kinases ATM and ATR.* Nat Cell Biol, 2008. **10**(7): p. 812-24.

136. Shima Y, S.T., Chiba T, Irimura T, Pandolfi PP, Kitabayashi I, *PML activates transcription by protecting HIPK2 and p300 from SCFFbx3-mediated degradation.* Mol Cell Biol., 2008. **28**(23): p. 7126-38.

137. Calzado MA, d.I.V.L., Möller A, Bowtell DD, Schmitz ML, *An inducible autoregulatory loop between HIPK2 and Siah2 at the apex of the hypoxic response.* Nat Cell Biol, 2009. **11**(1): p. 85-91.

138. Nardinocchi L, P.R., Givol D, D'Orazi G, *HIPK2-a therapeutical target to be (re)activated for tumor suppression: role in p53 activation and HIF-1a inhibition.* Cell Cycle, 2010. **9**(7): p. 1270-5.

139. Choi DW, N.W., Kabir MH, Yi E, et al, *WIP1, a homeostatic regulator of the DNA damage response, is targeted by HIPK2 for phosphorylation and degradation.* Mol Cell, 2013. **51**(3): p. 374-85.

140. Kown MJ, M.S., Seo J, Kim DH, Sung CO, Lim MS, Cho J, Park HR, *HIPK2 expression in progression of cutaneous epithelial neoplasm.* Int J Dermatol, 2015. **54**(3): p. 347-54.

141. Al-Beiti MA, L.X., *Expression of HIPK2 in cervical cancer: correlation with clinicopathology and prognosis.* Aust N Z J Obstet Gynaecol, 2008. **48**(3): p. 329-36.

142. Puca R, N.L., Pistritto G, D'Orazi G, *Overexpression of HIPK2 circumvents the blockade of apoptosis in chemoresistant ovarian cancer cells.* Gynecol Oncol., 2008. **109**(3): p. 403-10.

143. Jacob K, A.S., Sollier C, Faury D, Sader E, Montpetit A, Serre D, Hauser P, Garami M, Bognar L, Hanzely Z, Montes JL, Atkinson J, Farmer JP, Bouffet E, Hawkins C, Tabori U, Jabado N, *Duplication of 7q34 is specific to juvenile pilocytic astrocytomas and a hallmark of cerebellar and optic pathway tumours.* Br J Cancer, 2009. **101**(4): p. 722-33.

144. Cameron W. Brennan, R.G.W.V., Aaron McKenna, Benito Campos, Houtan Noushmehr, Sofie R. Salama, Siyuan Zheng, Debyani Chakravarty, J. Zachary Sanborn, Samuel H. Berman, *The Somatic Genomic Landscape of Glioblastoma.* Cell, 2010. **155**(2): p. 462-477.

145. Barretina J, C.G., Stransky N, Venkatesan K, Margolin AA, Kim S, Wilson CJ, Lehár J, Kryukov GV, Sonkin D, Reddy A, Liu M, *The Cancer Cell Line Encyclopedia enables predictive modelling of anticancer drug sensitivity.* Nature, 2012. **28**(483): p. 603-7.

146. Network, C.G.A.R., *Comprehensive molecular characterization of clear cell renal cell carcinoma.* Nature, 2013. **499**(7456): p. 43-9.

147. Young Ho Kim, C.Y.C., Yongsok Kim, *Covalent modification of the homeodomain-interacting protein kinase 2 (HIPK2) by the ubiquitin-like protein SUMO-1.* PNAS, 1999. **96**(22): p. 12350-55.

148. Engelhardt OG, B.C., Orr A, Ullrich E, Haller O, Everett RD, *The homeodomain-interacting kinase PKM (HIPK2) modifies ND10 through both its kinase domain and a SUMO-1 interaction motif and alters the posttranslational modification of PML.* Exp Cell Res., 2003. **293**(1): p. 36-50.

149. Vera V. Saul, L.d.l.V., Maja Milanovic, Marcus Krüger, Thomas Braun, Karin Fritz-Wolf, Katja Becker, M. Lienhard Schmitz, *HIPK2 kinase activity depends on cis-autophosphorylation of its activation loop.* J Mol Cell Biol, 2012. **5**(1): p. 27-38.

150. Cinzia Rinaldo, F.S., Andrea Prodosmo, Silvia Soddu, *HIPKs: Jack of all trades in basic nuclear activities.* Biochim Biophys Acta, 2008. **1783**(11): p. 2124-29.

151. KIM YH, C.C., Kim Y., *Covalent modification of the homeodomain-interacting protein kinase 2 (HIPK2) by the ubiquitin-like protein SUMO-1.* PNAS, 1999. **26;96**(22): p. 12350-5.

152. Hofmann TG, J.E., Stollberg N, Hay RT, Will H., *Regulation of homeodomain-interacting protein kinase 2 (HIPK2) effector function through dynamic small ubiquitin-related modifier-1 (SUMO-1).* J Biol Chem., 2005. **280**(32): p. 29224-32.

153. Gresko E, M.A., Roscic A, Schmitz ML, *Covalent modification of human homeodomain interacting protein kinase 2 by SUMO-1 at lysins 25 affects its stability.* Biochem Biophys Res Commun., 2005. **329**(4): p. 1293-9.

154. Jones PA, L.P., *Cancer epigenetics comes of age.* Nat Genet, 1999. **21**(2): p. 163-7.

155. Scott AM, W.J., Old LJ, *Antibody therapy of cancer.* Nat Rev Cancer, 2012. **12**(4): p. 278-87.

156. Calzado MA, R.F., Roscic A, Schmitz ML, *HIPK2: a versatile switchboard regulating the transcription machinery and cell death.* Cell Cycle, 2007. **6**(2): p. 139-43.

157. Gurvinder Kaur, J.M.D., *Cell lines, valuable tools or useless artifacts.* Spermatogenesis, 2012. **2**(1): p. 1-5.

158. Sharmistha Pal, Y.B., Luke Macyszyn, Louise C. Showe, Donald M. O'Rourke, Ramana V. Davuluri, *Isoform-level gene signature improves prognostic stratification and accurately classifies glioblastoma subtypes.* Nucleic Acids Res., 2014. **42**(8).

159. Bar EE, L.A., Tihan T, Burger PC, Eberhart CG, *Frequent gains at chromosome 7q34 involving BRAF in pilocytic astrocytoma.* J Neuropathol Exp Neurol., 2008. **67**(9): p. 878-87.

160. Muller PA, V.K., *Mutant p53 in cancer: new functions and therapeutic opporunities.* Cancer Cell, 2014. **25**(3): p. 304-17.

161. Zerdoumi Y, A.-L.J., Bonaiti-Pellié C, Derambure C, Sesboué R, Renaux-Petel M, Frebourg T, Bougeard G, Flaman JM, *Drastic effect of germline TP53 missense mutations in Li-Fraumeni patients.* Hum Mutat, 2013. **34**(3): p. 453-61.

162. Wang Y, S.Y., Fuller MY, Jackson JG, Xiong S, Terzian T, Quintás-Cardama A, Bankson JA, El-Naggar AK, Lozano G, *Restoring expression of wild-type p53 suppresses tumor growth but does not cause tumor regression in mice with a p53 missense mutation.* J Clin Invest, 2011. **121**(3): p. 893-904.

163. Wang X, C.J., Liu JP, You C, Liu YH, Mao Q, *Gain of function of mutant TP53 in glioblastoma: prognosis and response to temozolomide.* 2014. **4**(1337-44).

164. Kemp CJ, S.S., Gurley KE, *p53 induction and apoptosis in response to radio- and chemotherapy in vivo is tumor-type-dependent.* Cancer Res, 2001. **61**(1): p. 327-32.

165. Reshma Vijayakumaran, K.H.T., Panimaya Jeffreena Miranda, Sue Haupt, Ygal Haupt, *Regulation of Mutant p53 Protein Expression.* Front Oncol, 2015(5): p. 284.

166. Gaiddon C, L.M., Ahn J, Zhang T, Prives C, *A subset of tumor-derived mutant forms of p53 down-regulate p63 und p73 through a direct interaction with the p53 core domain.* Mol Cell Biol, 2001. **21**(5): p. 1874-87.

167. Strano S, F.G., Costanzo A, Rizzo MG, Monti O, Baccarini A, Del Sal G, Levrero M, Sachhi A, Oren M, Blandino G, *Physical interaction with human tumor-derived p53 mutants inhibits p63 activities.* J Biol Chem, 2002. **277**(21): p. 18817-26.

168. Mancini F, P.L., Monteleone V, Lucà R, Fici L, Luca E, Urbani A, Xiong S, Soddu S, Masetti R, Lozano G, Pontecorvi A, Moretti F, *MDM4/HIPK2/p53 cytoplasmic assembly uncovers coordinated repression of molecules with anti-apoptotic activity during early DNA damage response.* Oncogene, 2016. **35**(2): p. 228-40.

169. Goldstein I, M.V., Olivier M, Oren M, Rotter V, Hainaut P, *Understanding wild-type and mutant p53 activities in human cancer: new landmarks on the way to targeted therapies.* Cancer Gene Therapy, 2011(18): p. 2-11.

170. Hofmann TG, G.C., Bitomsky N, *HIPK2: A tumour suppressor that controls DNA damage-induced cell fate and cytokinesis.* Bioessays, 2012. **35**(1): p. 55-64.

171. Lin J, Z.Q., Lu Y, Xue W, Xu Y, Zhu Y, Hu X, *Downregulation of HIPK2 increases resistance of bladder cancer cell to cisplatin by regulating Wip1.* PLoS One, 2014. **9**(5).

172. Iacovelli S, C.L., Lazzari C, Bracaglia G, Rinaldo C, Prodosmo A, Bartolazzi A, Sacchi A, Soddu S, *HIPK2 is involved in cell proliferation and its suppression*

promotes growth arrest independently of DNA damage. Cell Prolif., 2009. **42**(3): p. 373-84.

173. Le Cong, F.A.R., David Cox, Shuailiang Lin, Robert Barretto, Naomi Habib, Patrick D. Hsu, Xuebing Wu, Wenyan Jiang, Luciano A. Marraffini and Feng Zhang, *Multiplex Genome Engineering Using CRISPR/Cas Systems.* Science, 2013. **339**(6121): p. 819-823.

174. Saul VV, S.M., *Posttranslational modifications regulate HIPK2, a driver of proliferative diseases.* J Mol Med (Berl). 2013. **91**(9): p. 1051-8.

175. Bakhoum SF, S.C., *Chromosomal instability, aneuploidy, and cancer.* Front Oncol., 2014. **19**(4): p. 161.

176. de la Vega, F.K., Moreno R, Calzado MA, Geng H, Schmitz ML, *Control of nuclear HIPK2 localization and function by a SUMO interaction motif.* Biochim Biophys Acta, 2011. **1813**(2): p. 283-97.

177. de la Vega, H.J., Kremmer E, Milanovic M, Schmitz ML, *Homeodomain-interacting protein kinase 2-dependent repression of myogenic differentiation is relieved by its caspase-mediated cleavage.* Nucleic Acids Res, 2013. **41**(11): p. 5731-45.